

Preparation of Fully Miscible Nanocomposites

Dissertation

to be awarded the degree of Doctor rerum naturalium (Dr. rer. nat.) at the
Faculty of Biology, Chemistry and Earth Sciences,
University of Bayreuth

submitted by
Dipl.-Chem. Sascha Philipp Ehlert
from Hamburg
Bayreuth, 2014

Die vorliegende Arbeit wurde in der Zeit von 16. Dezember 2009 bis 15. Dezember 2010 an der Universität Hamburg am Institut für Physikalische Chemie und von 16. Dezember 2010 bis 30. September 2014 an der Universität Bayreuth am Lehrstuhl Physikalische Chemie I unter der Betreuung von Prof. Dr. Stephan Förster angefertigt.

Vollständiger Abdruck der von der Fakultät für Biologie, Chemie und Geowissenschaften der Universität Bayreuth genehmigten Dissertation zur Erlangung des akademischen Grades eines Doktors der Naturwissenschaften (Dr. rer. nat.).

Dissertation eingereicht am: 01.10.2014

Zulassung durch die Promotionskommission: 08.10.2014

Wissenschaftliches Kolloquium: 23.02.2015

Amtierender Dekan:

Prof. Dr. Rhett Kempe

Prüfungsausschuss:

Prof. Dr. Stephan Förster (Erstgutachter)

Prof. Dr. Andreas Fery (Zweitgutachter)

Prof. Dr. Birgit Weber (Vorsitz)

Prof. Dr. Hans-Werner Schmidt

The work described in this thesis was carried out at the Institute of Physical Chemistry at the University of Hamburg from 16. December 2009 until 15. December 2010 and from 16. December 2010 until 30. September 2014 at the Department of Physical Chemistry I at the University of Bayreuth under supervision of Prof. Dr. Stephan Förster.

This is a full reprint of the dissertation submitted to obtain the academic degree Doctor of Natural Sciences (Dr. rer. nat.) and approved by the Faculty of Biology, Chemistry and Geosciences of the University of Bayreuth.

Date of submission: 01.10.2014

Approved by committee: 08.10.2014

Date of scientific colloquium: 23.02.2015

Acting dean:

Prof. Dr. Rhetta Kempe

Doctoral Committee:

Prof. Dr. Stephan Förster (1st reviewer)

Prof. Dr. Andreas Fery (2nd reviewer)

Prof. Dr. Birgit Weber (Chairman)

Prof. Dr. Hans-Werner Schmidt

Contents

1	Overview	1
1.1	Outline	1
1.2	Content of Individual Parts	1
1.3	Individual Contributions	9
2	Introduction	13
2.1	Nanoparticles	13
2.2	Polymer-inorganic nanocomposite (PINC)	14
3	Theory	17
3.1	Nanoparticles	17
3.1.1	Surface effects	17
3.1.2	Size dependable quantum effects	18
3.1.3	Synthesis	22
3.1.4	Nucleation	22
3.1.5	Growth	25
3.1.6	Synthetic routes	27
3.1.7	Aggregation	30
3.1.8	Nanoparticle stabilization	33
3.1.9	Grafting methods	33
3.1.10	Properties/ Applications	39
3.2	Nanocomposites	39
3.2.1	Synthesis	40
3.2.2	Aggregation	42
3.2.3	Properties/ Applications	46
4	Facile large-scale synthetic route to monodisperse ZnO nanocrystals	59

5	Polymer Ligand Exchange to Control Stabilization and Compatibilization of Nanocrystals	69
6	A General Route to Optically Transparent, Highly Filled Polymer Nanocomposites	99
7	Summary	113
8	Zusammenfassung	115
9	Danksagung	117

1 Overview

1.1 Outline

The main subject of this work is the preparation of nanocomposites with surface modified nanoparticles. A great issue in nanocomposite preparation is the uncontrolled and therefore undesired aggregation of the nanoparticles in the polymer matrix. This work shows the process from a new synthesis of monodisperse, fluorescent and semiconducting ZnO nanoparticles over their surface modification with different polymers to fully miscible transparent nanocomposites with enhanced mechanical and optical properties. To show the versatility of the developed method surface modification is shown with various nanoparticles, which were synthesized according to literature (see table 1) and also with different polymers. The method gives a good control over the aggregation of nanoparticles, enabling the formation of nanoparticle doublets, short chains and networks. With this method the preparation of nanocomposites consisting of various nanoparticles in various polymers is possible and it gives good control over the nanoparticle distribution.

1.2 Content of Individual Parts

This thesis is composed of five main parts. The first part (**chapter 2**) is a short general introduction into nanoparticles and nanocomposites. The second part (**chapter 3**) is a review of the research in the fields of nanoparticle synthesis, nanoparticle modification, nanocomposite preparation and contains the associated theoretical background as well. The theory about nanoparticles span from their special properties compared to the bulk material, over their nucleation and growth, to the effects which determine their stability. The theory for the nanocomposites mostly addresses aggregation of nanoparticles and possibilities to prevent or control it.

Part three (**chapter 4**), the first publication, presents the development of a synthesis for large amounts of monodisperse, fluorescent, semiconductor ZnO nanoparticles based on the hydrolysis of zinc oleate in organic solvent.

Part four (**chapter 5**), the second publication, presents the surface mod-

1.2 Content of Individual Parts

ification of a broad variety of nanoparticles by a ligand exchange process, in which the original ligand is substituted by an end functionalized polymer ligand to form a brush-like polymer layer around the nanoparticles. This brush-like layer enhances the nanoparticle stability, allows due to the coordinative bond high grafting densities and a good control over aggregation. Every polymer with a coordinative end function should be suitable as ligand for this method.

In this work many different nanoparticles, which were synthesized according to the literature with some modifications presented in table 1 are used.

Table 1: Nanoparticle syntheses and modifications

Nanoparticle	Literature	Modification
Silver (Ag)	Yamamoto et al. ^[1]	• silver oleate as precursor
Gold (Au)	Yu et al. ^[2]	• squalene as solvent
Cadmium selenide (CdSe)	Yang et al. ^[3]	• cadmium oleate as precursor • cadmium : selen ratio 1 : 2 • no addition of oleic acid
Cadmium selenide core/shell/shell (CdSe/ZnSe/ZnS)	Kim and Lee ^[4]	• cadmium selenide by Yang ^[3] • zinc oleate as Zn precursor • bis(trimethylsilyl)-sulfid as S precursor
Lead sulfide (PbS)	Hines et al. ^[5]	• preformed lead oleate as precursor

Part five (**chapter 6**), the third publication, presents the incorporation of surface modified nanoparticles into a transparent homopolymer matrix to form transparent nanocomposites.

Large-scale synthetic route to monodisperse ZnO nanocrystals.

Part three, the publication "Facile large-scale synthetic route to monodisperse ZnO nanocrystals"^[6] introduces a new synthesis for ZnO nanoparticles. The robust and up-scalable synthesis leads to small, spherical, well-stabilized, narrow disperse, crystalline ZnO nanoparticles. These ZnO nanoparticles have great potential as photoluminescent semiconductors with a wide range of applications in solar energy conversion, photocatalysis, bio-labelling, UV-blockings, and electro-optical devices. Further they can be used as transparent fillers to prepare transparent nanocomposites with enhanced mechanical properties as shown in part 5 (chapter 6) of this work.

In the synthesis of ZnO nanoparticles Zn-oleate or the commercially available Zn-stearate are used as precursors, which are hydrolysed in polar organic solvents. The diameter of these nanoparticles are in the range of 3 - 5 nm and the yield of one batch is on a multi-gram scale. The use of oleate or stearate as precursor is due to their good stabilizing properties. Together with the hydrolytic route this leads to small ZnO nanoparticles in a well-controlled way. Figure 1 shows that ZnO nanoparticles obtained with the developed method are crystalline, monodisperse and fluorescent, as well as the up-scalability of the method. The nanoparticles can be precipitated, dried, and redispersed in common organic solvents without aggregation due to the good steric stabilization and hydrophobic coating. The robustness of the synthesis allows a range of reactants for the hydrolyzation such as NaOH, LiOH or KOH. The little influence of the temperature, the concentrations and the reaction time is due to the constant ratio of capping agent and precursor as a result of the *in-situ* formation of the capping agent.

1.2 Content of Individual Parts

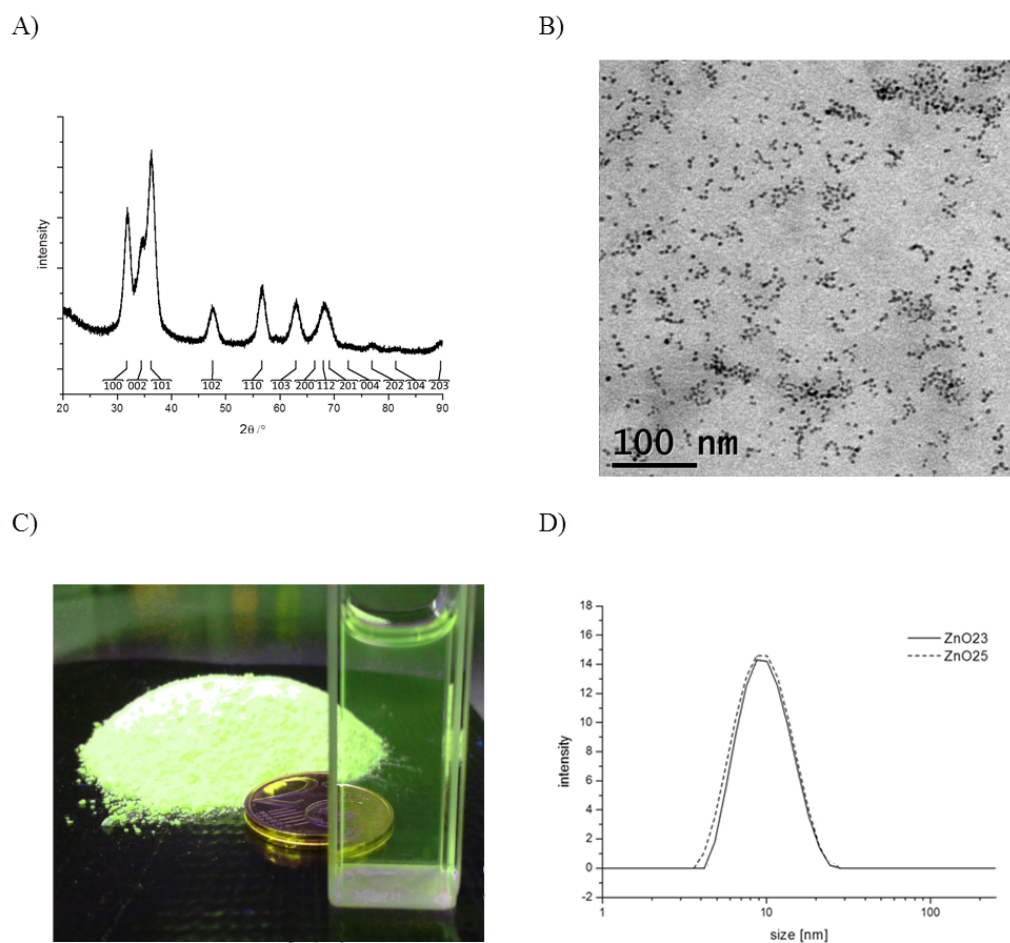


Figure 1: (A): XRD pattern of 5 nm ZnO nanoparticles showing the wurtzite hexagonal crystal structure. (B): TEM image of ZnO nanoparticles. (C): Image of 5 g of ZnO nanoparticles synthesized in one batch and a dilute solution of ZnO nanoparticles in THF under UV light showing a bright green fluorescence. (D): DLS measurements of 5 nm ZnO nanoparticles. The solid line shows the nanoparticles obtained with the standard synthesis, the dashed line the standard synthesis scaled up by a factor of 100.

Polymer Ligand Exchange of Nanocrystals.

Part four, the publication "Polymer Ligand Exchange to Control Stabilization and Compatibilization of Nanocrystals"^[7] introduces a versatile method to obtain polymer brush stabilized nanoparticles. The prevention of uncontrolled aggregation is very important for most applications of nanoparticles due to loss of their special properties upon aggregation. Stabilization by electro static repulsion is one of two stabilization concepts. However it only works in polar solvents and is sensitive to pH changes. Therefore most of the nanoparticles are stabilized by steric stabilization, which is achieved by surfactants. These surfactants are often introduced during synthesis and are mostly short alkyl chains. The stabilization provided by these surfactants is sometimes not sufficient enough and they have to be substituted subsequent to synthesis. Figure 2 A shows schematically the process of the exchange. The common methods to obtain a polymer brush layer on nanoparticle surfaces are the grafting-from or grafting-to methods by which the polymer chains are bond covalently to the surface.^[8] The process to achieve this has to be adjusted for every new nanoparticle/polymer combination and the covalent character of the bond prohibit an easy way to a controlled aggregation. The here presented exchange method can lead to grafting densities $> 1 \text{ nm}^{-2}$ for nearly any nanoparticle/polymer combination using only a few types of binding groups. The employed method consists of multiple precipitation-dissolving cycles of functionalized polymer (in excess) and nanoparticles. In these cycles the original ligand is depleted and the polymer can bind to the nanoparticles. With the developed method it is possible to stabilize various nanoparticles (e.g., Ag, Au, CdSe, ZnO or PbS) with a broad range of polymers (e.g., polystyrene (PS), poly(methyl methacrylate)(PMMA), polyisoprene (PI) or polyethylene (PE)), to control the inter-particle distance and the aggregation of the nanoparticles (Figure 2 C). Further it is possible to use commercially available copolymers to stabilize nanoparticles (Figure 2 B). The dense attachment of very short polymer ligands enables the preparation of ordered nanoparticle monolayers with an inter-particle distance of only 7.2 nm, that is corresponding to a potential magnetic storage density of 12.4 Tb/in². A lower grafting density leads to aggregation of the nanoparti-

cles to doublets, short chains or networks. This could be used, for example in photovoltaic applications to enhance the charge carrier transport by building a percolation network of semiconducting nanoparticles. The process is shown with different nanoparticles and different polymers to demonstrate the universality of this ligand exchange method.

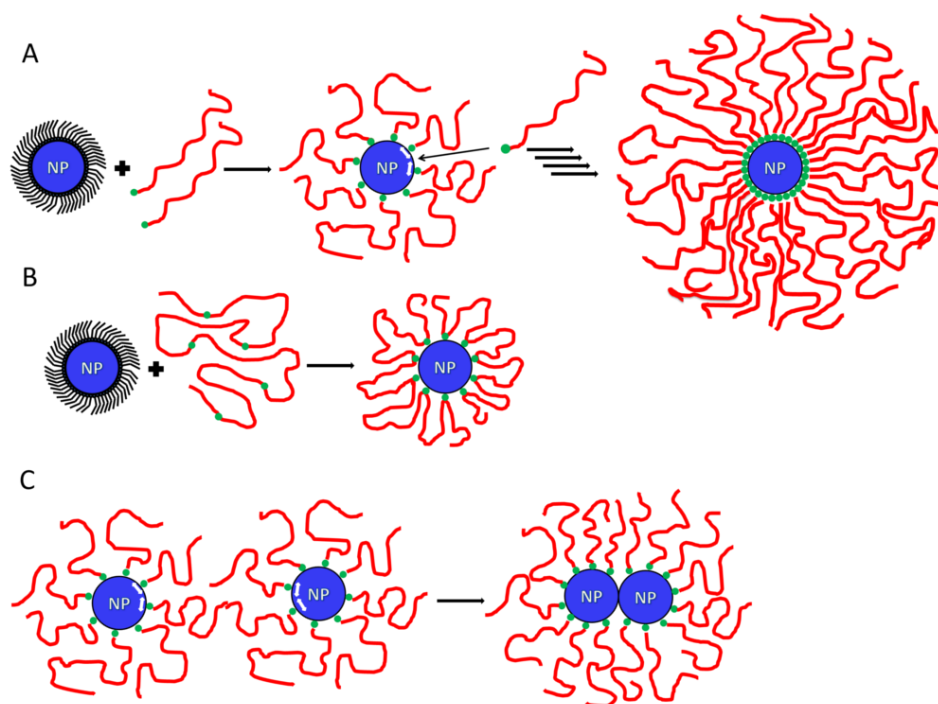


Figure 2: A scheme of (A): Nanoparticle coated with oleic acid (black), which is exchanged against a polymer (red) with a coordinating end-group (green). Because of the surface mobility of the end groups, bound polymer chains can relocate on the surface to facilitate attachment of further polymer chains to yield very high brush densities. (B): possibility to employ copolymers as polymer ligands to obtain dense polymer brushes. (C): Relocalization of surface-bound polymer to allow controlled agglomeration into nanoparticle doublets, and subsequently chains and networks.

Transparent Nanocomposites. Part five contains the publication "A General Route to Optically Transparent, Highly Filled Polymer Nanocomposites"^[9] illustrating a possible application of the in part four prepared nanoparticles. The prevention of aggregation is especially crucial for transparent nanocomposites because of the wavelength dependency of Rayleigh scattering. Rayleigh scattering causes turbidity in nanocomposites if the nanoparticles or their agglomerates reach a size about 40 nm or larger. The aggregation of nanoparticles in nanocomposites is entropically favoured since the matrix polymer loses conformational freedom on contact with the nanoparticle surface. The in part four introduced method provides nanoparticles with a polymer brush layer on the surface. The polymer brush layer mediates between the nanoparticles and the matrix polymer by minimizing the loss of conformational freedom, due to possible penetration of the brush layer by matrix polymer chains.

The applications for such nanocomposites are UV-photo-protective materials (ZnO, TiO₂), substitutes for organic fluorescent dyes (CdSe, CdTe) due to their higher photo stability and materials with extreme refractive indices (extreme high: PbS or extreme low: Au).^[10] Scratch resistant surface protective materials are another application for these nanocomposites. A ZnO-PMMA nanocomposite prepared in this work with a ZnO content of 10% is highly transparent, has a 300% enhanced elastic modulus and a four times higher scratch resistance than the neat PMMA.

Mixing the matrix polymer with the modified nanoparticles in a solvent leads to a homogeneous solution. From this solution transparent nanocomposite films can be prepared by simple solvent cast methods. Because of the universality of the exchange method (part four) it is possible to prepare a broad range of different nanocomposites. Figure 3 shows some of the in this work prepared transparent nanocomposites (B and C) and some corresponding UV-vis spectra (A). The weight fraction of the nanoparticles in the prepared nanocomposites is up to 45%.

1.2 Content of Individual Parts

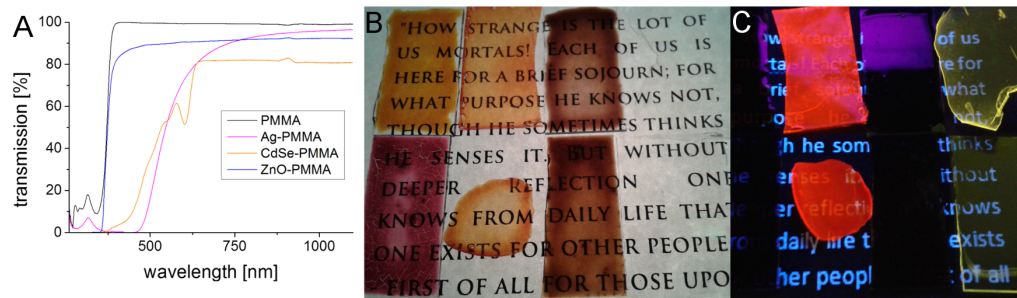


Figure 3: (A): UV-vis spectra of transparent nanocomposites with PMMA matrix, (B): optical image of solvent cast films of nanocomposites (top: Ag-PMMA 2wt%, CdSe-PMMA 10wt%, PbS-PI 10wt% and ZnO-PMMA 10wt%; bottom: Au-PS 2wt%, CdSe-PS 29wt%, Fe_2O_3 -P2VP 5wt% and ZnO-PS 45wt%) under day light and (C): UV-light.

1.3 Individual Contributions

Large-scale synthetic route to monodisperse ZnO nanocrystals

- I developed the synthesis, carried out the characterization and wrote the manuscript.
- T. Lunkenbein carried out the XRD measurements.
- J. Breu helped with discussions.
- S. Förster helped with discussions and corrected the manuscript.

Polymer Ligand Exchange of Nanocrystals

- I performed all syntheses, the characterization and wrote the manuscript.
- S. Mehdizadeh Taheri synthesized and processed the iron oxide nanoparticles.
- D. Pirner synthesized and modified the polyisoprene.
- M. Drechsler helped with discussions.
- H.-W. Schmidt helped with discussions.
- S. Förster helped with discussions, wrote parts of the manuscript and corrected the manuscript.

Transparent Nanocomposites

- I performed all syntheses, the characterization and wrote the manuscript.
- C. Stegelmeier synthesized the P2VP-iron oxide nanocomposite.
- D. Pirner synthesized and modified the polyisoprene.
- S. Förster helped with discussion, wrote parts of the manuscript and corrected the manuscript.

References

- [1] Yamamoto, M.; Kashiwagi, Y.; Nakamoto, M. Size-controlled synthesis of monodispersed silver nanoparticles capped by long-chain alkyl carboxylates from silver carboxylate and tertiary amine. *Langmuir* 2006,22,8581–8586.
- [2] Yu, H.; Chen, M.; Rice, P. M.; Wang, S. X.; White R. L. Sun, S. Dumbbell-like Bifunctional Au-Fe₃O₄ Nanoparticles *Nano Lett.* 2005,5,379–382.
- [3] Yang, Y. A.; Wu, H.; Williams, K. R.; Cao, Y. C. Synthesis of CdSe and CdTe nanocrystals without precursor injection. *Angew. Chem.* 2005,117,6870–6873.
- [4] Kim, J. I.; Lee, J.-K. Sub-kilogram-Scale One-Pot Synthesis of Highly Luminescent and Monodisperse Core/Shell Quantum Dots by the Successive Injection of Precursors. *Adv. Mater.* 2006,16,2077–2082.
- [5] Hines, M. A.; Scholes, G. D. Colloidal PbS nanocrystals with size-tunable near-infrared emission: Observation of post-synthesis self-narrowing of the particle size distribution. *Adv. Mater.* 2003,15,1844–1849.
- [6] Ehlert, S.; Lunkenbein, T.; Breu, J.; Förster, F. Facile large-scale synthetic route to monodisperse ZnO nanocrystals *Colloids Surf., A.* 2014,444,76–80.
- [7] Ehlert, S.; Mehdizadeh Taheri, S.; Pirner, D.; Drechsler, M.; Schmidt, H.- W.; Förster, S. Polymer Ligand Exchange to Control Stabilization and Compatibilization of Nanocrystals *ACS Nano* 2014,8,6114–6122.
- [8] Kango, S.; Kalia, S.; Celli, A.; Njuguna, J.; Habibi, Y.; Kumar, R. Surface modification of inorganic nanoparticles for development of organic-inorganic nanocomposites—A review. *Prog. Polym. Sci.* 2013,39,1232–1261.

- [9] Ehlert, S.; Stegelmeier, C.; Pirner, D.; Förster, S. A General Route to Optically Transparent, Highly Filled Polymer Nanocomposites *XXX* 2015,X,XX–XX.
- [10] Li, S.; Lin, M. M.; Toprak, M. S.; Kim, D. K.; Muhammed, M. Nanocomposites of polymer and inorganic nanoparticles for optical and magnetic applications. *Nano Reviews* 2010,1,5214.

2 Introduction

2.1 Nanoparticles

The term nano comes from the Greek word for dwarf "nanos". In the fields of nano-sciences, "nanoparticle" is a description for particles with at least one of its dimensions in the range of 1 to 100 nm. This includes disks, plates and sheets with one dimension in the nm range, rods and wires with two dimensions in the nm range and a broad range of particles with all three dimensions in the nm range such as spheres and cubes. The limits in this definition seem at first arbitrary, but in this range surface effects have a great influence on particle properties. This is due to the surface to volume ratio. The smaller the particle the more surface atoms and the less core atoms the particle contains. The surface atoms cause free coordination sites and are weaker bound, so they have a direct influence on the physical and chemical properties of the particle. This includes a higher chemical reactivity, a lower melting point, optical effects and many others.^[1, 2]

The synthesis and utilization of nanoparticles have a long history. One of the first applications for nanoparticles was the coloring of glass. The Lycurgus cup from the late roman period is a famous example. The glass for this cup contains colloidal gold nanoparticles, which made the glass appear red if the light shines through the glass and green when the light is reflected by the glass. Further applications for nanoparticles regarding their optical properties are transparent pigments, UV-absorber, photonic crystals and luminophores such as biomarkers in medicine or safety applications in copy protection. The electrical properties are also interesting for transparent conductive oxides such as indium tin oxide (ITO), as electrical devices like single-electron transistors or for energy conversion in hybrid solar cells. Magnetic materials such as iron, iron oxides or alloys like Fe-Pt have special properties as nanoparticles. If the diameter of these nanoparticles is smaller than the diameter of the magnetic domains, they show superparamagnetism. The nanoparticles are applied for magnetic data storage. The magnetization of every single nanoparticle in an ordered array can be used for this pur-

2.2 Polymer-inorganic nanocomposite (PINC)

pose, which leads to very high storage densities. The suspension of magnetic nanoparticles in a high viscous solvent leads to so called "Ferro fluids". These liquids are manipulable with an external magnetic field and are used for fast switching of valves. Medical applications of magnetic nanoparticles are the magneto thermal therapy and the magnetic resonance imaging. In thermal therapy the nanoparticles are encapsulated and labeled with anti-bodies, for the enrichment in the target tissue. After the enrichment has taken place an alternating magnetic field heats the tissue up to the point of a cytotoxic effect.

Another application for nanoparticles is the catalysis of chemical reactions. Because of the fact that catalysis takes place on the surface of the catalyst it is clear that nanoparticles are interesting for catalytic applications. Catalytic active nanoparticles are more effective in respect of material to catalysis ratio because of the larger surface. If the catalytic nanoparticles are also magnetic it is possible to remove the catalyst after the reaction very easily with a magnet. Most of these effects are size and form dependent. Therefore it is very important for most of the applications to have monodisperse and uniform nanoparticles. The development and/or improvement of such monodisperse and uniform nanoparticles was part of this work and will be directed to in chapter 4.^[1, 2]

2.2 Polymer-inorganic nanocomposite (PINC)

Another application of nanoparticles is the alteration of polymer properties in nanocomposites. These nanocomposites consist of a polymer matrix and nanoparticles as filler. To obtain PINCs there are two general physical and four chemical approaches. The first physical method is the melt mixing by which the PINCs are obtained simply by dispersing nanoparticles in a polymer melt and subsequent extrusion of the PINC. The other physical method is the film casting. The PINCs are obtained by dissolving nanoparticles in a solution of polymer in an organic solvent, coating a surface with the solution and subsequent evaporation of solvent. The first chemical method is the *in-*

situ polymerization. Nanoparticles are mixed with monomer which is finally polymerized, by emulsion polymerization for example. Complementary is the *in-situ* particle formation where the nanoparticles are directly synthesized in a polymer matrix, for example by a sol-gel process, where the nanoparticle precursor is loaded into a gel like polymer matrix and subsequently is hydrolyzed to form nanoparticles. Other approaches are the grafting-to and grafting-from methods by which polymer chains are attached directly to the nanoparticle. By the grafting-to method preformed polymer chains are attached to preformed nanoparticles *via* covalent bonds. By the grafting-from method nanoparticles are modified with short surface molecules containing polymerizable groups from which the polymer chains are polymerized.^[3]

The so obtained PINCs can show the best properties of both of its components. If colored nanoparticles are incorporated in transparent polymers, the resulting PINC should be likewise transparent and colored. The same holds for other optical effects such as UV-absorption and photoluminescence. Another application is the creation of materials with extreme refractive indices (RI). Normal RIs for polymers are in the range of 1 to 1.5. This can be changed with the incorporation of nanoparticles up to a RI of 3.2. PINCs with magnetic nanoparticles could be magnetic, or could be used as shielding against electromagnetic waves. By the use of silver nanoparticles it is possible to obtain antibacterial PINCs which could be used as surface improvement. In the field of energy conversion a lot of research is done on solar cells consisting of polymers and nanoparticles. A PINC of semiconducting nanoparticles and suitable polymers could be used to optimize energy conversion efficiency. Incorporation of nanoparticles into a polymer matrix also changes the mechanical properties of the polymer. This can be used to build very tough PINCs with additional functions such as scratch resistant surface coatings with high UV-absorption. All these effects are dependent on well-dispersed nanoparticles, since agglomeration of nanoparticles could prevent the desired effects, or worsen the properties of the matrix polymer. For example a transparent polymer could become nontransparent if the nanoparticle aggregates are larger than 40 to 100 nm. The synthesis and characterization of completely miscible nanoparticles and PINCs are part of this work and

REFERENCES

will be addressed in chapter 5 and 6.^[3]

References

- [1] Roduner, E. Size matters: why nanomaterials are different. *Chem. Soc. Rev.* 2006,35,583–592.
- [2] Goesmann, H. and Feldmann, C. Nanoparticulate Functional Materials. *Angew. Chem. Int. Ed.* 2010,49,1362–1395.
- [3] Li, S.; Lin, M. M.; Toprak, M. S.; Kim, D. K.; Muhammed, M. Nanocomposites of polymer and inorganic nanoparticles for optical and magnetic applications. *Nano Reviews* 2010,1,5214.

3 Theory

3.1 Nanoparticles

3.1.1 Surface effects

Because of the small size of nanoparticles the ratio of surface to core atoms is much higher than in the bulk material. This ratio is called dispersion F . For cubic particles the dispersion is given by equation 1 where n is the number of atoms along the edge.

$$F = \frac{6n^2 - 12n + 8}{n^3} \quad (1)$$

For larger particles the correction for the double counted edge atoms is negligible and F is given by equation 2 where N is the total number of atoms.

$$F \approx \frac{6}{N^{-\frac{1}{3}}} \quad (2)$$

In Figure 1 the plot for F versus n is shown. For $n = 2$ the dispersion is 1 because every atom is a surface atom. For spheres the development of the dispersion is similar. The surface of a sphere scales with the square of the radius r but the volume scales with r^3 .

The surface atoms have a lower coordination number than atoms in bulk. This means that the surface atoms form fewer bonds and are therefore less stable than the core atoms. In the cube shape the corner atoms are the least stable because they have the least neighbours. In the thermodynamic equilibrium the less stable corner and edge atoms are missing which finally leads to a sphere, the most stable geometry with the highest volume to surface ratio. An effect of this instability is the lower melting point of small particles. The difference in the melting point can be described by the Gibbs-Thomson equation 3.^[1]

$$\Delta T_m = T_{mb} \frac{2V_m \gamma_{sl}}{\Delta H_m r} \quad (3)$$

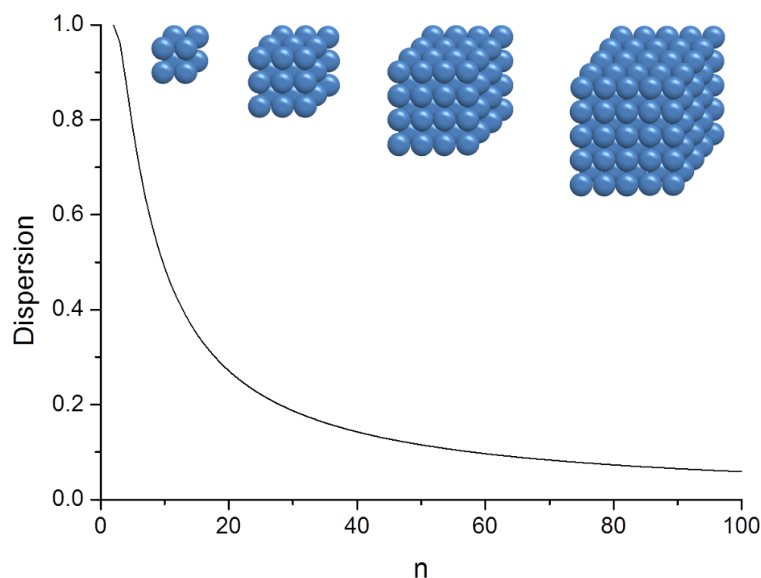


Figure 1: Plot of the dispersion F versus n and the schematic display of the corresponding particles with $n = 2$ to 5 .

With T_{mb} the melting point of the bulk, V_m the molar Volume of the liquid, γ_{sl} the interfacial tension, ΔH_m the latent heat of melting in bulk and r the radius of the particles. The melting point of gold in bulk is at a temperature of 1336 K in comparison to that the melting point of 2.5 nm gold particles was found to be 930 K.^[2] Another effect of the instability is the high reactivity of nanoparticles. Small metal nanoparticles such as chromium or iron are for example pyrophoric.^[3] As a result of the large surface nanoparticles have a higher catalytic activity than an equal amount of bulk material. For the catalysis of the Suzuki reaction used palladium nanoparticles have a turnover number of about 540000 if used in concentrations as low as 1 ppm of palladium.^[4]

3.1.2 Size dependable quantum effects

Some effects are also size dependent but have another scaling than the surface effects. These effects have a direct size dependency. The so called "quan-

tum confinement effect" can be found in semiconducting nanoparticles, for example cadmium selenide nanoparticles. These nanoparticles show size dependent luminescence in the range from 1.7 nm radius with a wavelength of about 450 nm (blue) to 5 nm radius and a wavelength of about 600 nm (red).^[5] To explain this dependency there are two theoretic models. The first is the "linear combination of atomic orbitals" (LCAO-theory)^[6] the second is the "Particle in a Box" model.^[7] In the "Particle in a Box" model the particles are described as very small bulk particles while the LCAO describes them as very big molecules.

The LCAO combines atomic orbitals with the same or a similar symmetry in molecules to molecule orbitals. For n atomic orbitals the LCAO leads to $0.5n$ bonding and $0.5n$ anti-bonding molecule orbitals. For a two atom molecule this means $n = 2$, so two atomic orbitals combine to one bonding orbital and one anti-bonding molecule orbital. The bonding orbital has a lower energy and the anti-bonding orbital has a higher energy as the atomic orbitals they are combined from. In the macroscopic material this leads to the valence band and the conduction band in which the distinct energy states of the molecule orbitals merge to a continuum. If the upper edge of the valence band and the lower edge of the conducting band have an overlap the material is a metal and can freely conduct electricity due to the unhindered transfer of electrons from the valence to the conducting band. If there is a gap between the bands this gap is called band gap (E_g). Dependent on the width of the gap the material is an insulator ($E_g > 4eV$) or a semi-conductor ($0eV < E_g < 4eV$). For semiconductors electrons can be transferred from the valence to the conducting band across the band gap by energy supply, for example thermic energy or radiation with light. Nanoparticles can be treated like large molecules. They have less molecule orbitals than the bulk material and therefore the density of states is reduced and the bands are splitting in discrete states. The smaller the particle is the less molecule orbitals it has and the lower is the density of states (Figure 2).^[6, 7]

If an electron gets excited by a photon of certain energy, the electron gets excited from the valence band to the conducting band. The relaxation of this electron leads to the emission of a photon with an energy equal to the

3.1 Nanoparticles

band gap (E_g). To emit a photon in the region of visible light the band gap has to be between 1.6 eV (red) and 3 eV (violet), which is in the range of the band gap of semiconductors.

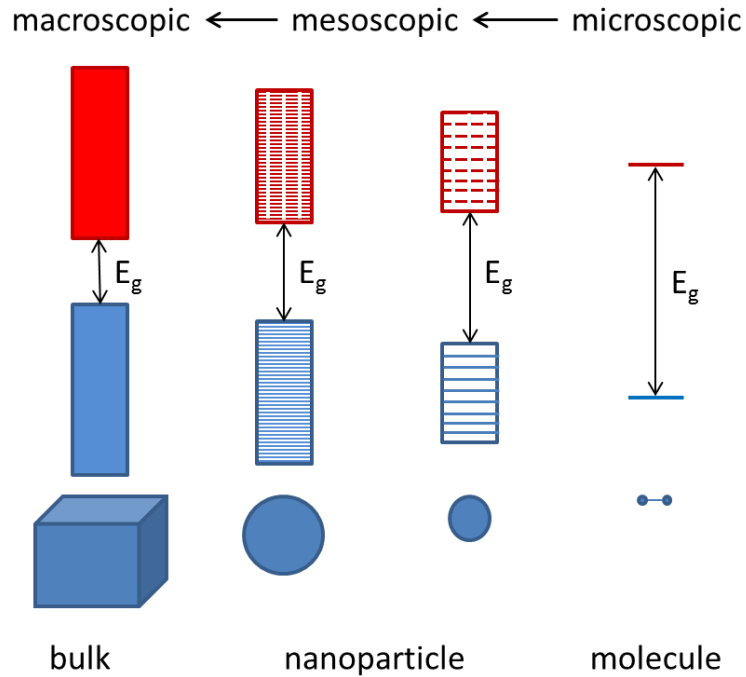


Figure 2: Scheme of the band gap E_g with size dependency from the bulk material to a two atom molecule. Horizontal lines indicate energy states.

The particle in a box model describes a particle in a box with infinitely high walls and a defined width in which the particle moves freely. In the case of nanoparticles the nanoparticle is the box and an electron-hole pair (exciton) is the particle. The electron and the hole have a certain distance from each other due to electrostatic attraction, the exciton-Bohr-radius. If the nanoparticle ("the box") gets smaller than the exciton-Bohr-radius, the exciton ("the particle") feels the restrictions of the wall. For a theoretical one dimensional potential well the energy levels are given by equation 4.

$$E = \frac{n^2 h^2}{8mL^2} \quad (4)$$

Where h is the Planck constant, m the mass of the particle and L the length of the well. The quantum number n is a positive integer. Due to the infinitely high potential the particle cannot leave the box and seen as a wave it must have L as an even multiple of half of its wavelength (Figure 3). Waves with wavelengths which are not in accordance with this extinguish itself upon reflection at the wall. This explains the restriction of the energy levels to the quantum number n .

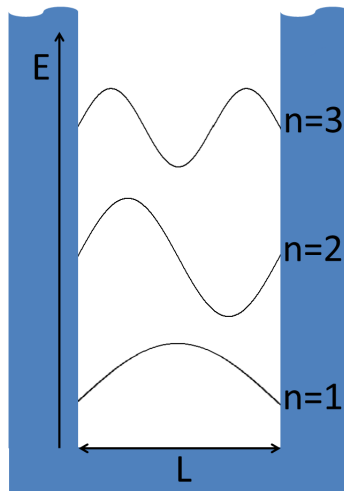


Figure 3: Scheme of the particle in a box model with the first three energy levels and the according wavelengths.

The change of the energy of the band gap E_g in dependency of the size for a spherical nanoparticle is given by the Brus equation 5.

$$\Delta E = \frac{h^2}{8R^2} * \left(\frac{1}{m_e} + \frac{1}{m_h} \right) - \frac{1.8e^2}{4\pi\epsilon\epsilon_0 R} \quad (5)$$

Where h is the Planck constant, R the particle radius, m_e the mass of the electron, m_h the mass of the hole, e the electron charge, ϵ the permittivity and ϵ_0 the vacuum permittivity. This shows that with decreasing size of the nanoparticle the band gap energy increases.^[7]

3.1.3 Synthesis

There are two main approaches for the synthesis of nanoparticles. The first one is the "top-down" method. This procedure uses mainly physical approaches to reduce the size of a material, such as milling^[8] or electron beam lithography^[9] for example. With most physical approaches it is possible to produce large quantities of nanoparticles. The control of the shape, the uniformity and a narrow particle size distribution is somehow hard to achieve with the physical approaches. Another drawback of the physical methods is the missing surface protection of the as-prepared nanoparticles which leads to aggregation in solution. The second procedure is the "bottom-up" method. This procedure uses mainly chemical approaches to build nanoparticles from molecular precursors. Most of these chemical reactions are batch reactions and therefore limited in respect of quantity of nanoparticles that can be obtained by them. In contrast to the physical approaches the chemical approaches are capable of controlling the shape, uniformity and size distribution due to the fine tunable reaction conditions. Under the right conditions it is even possible to produce nanorods and nanowires with a very high aspect ratio which is very difficult with physical methods. In addition to the control of the shape and size distribution it is also possible to adjust the solubility of the nanoparticles in different solvents *via* the use of different surfactants.^[10, 11]

3.1.4 Nucleation

As described earlier the properties of the nanoparticles are strongly dependent on their size. For the most applications it is desired to have monodisperse nanoparticles so the properties are well defined. To produce monodisperse nanoparticles the concept of "Burst nucleation" by LaMer from the 1940's^[12] was adopted. In this concept particles become monodisperse if the nucleation of all particles happens at the same time and they grow without further nucleation. This is because all nanoparticles have the same growth history. The method is also known as "the separation of nucleation and growth". LaMer employs the homogeneous nucleation process for the separation of growth and nucleation. In this process the nucleation happens in

solution without any seeds like dust, as it would be for heterogeneous nucleation. The spontaneous formation of nuclei in a homogeneous solution would induce a new phase therefore this nucleation has a high energy barrier. The burst of nucleation is divided into three parts (Figure 4). In the first part of the process the concentration of precursor in solution increases over the point of saturation (c_S) without nucleation due to the high energy barrier. This is called supersaturation and if the supersaturation reaches a critical level (c_{Sc}) it will overcome the energy barrier for nucleation. Like that in part two the nucleation occurs. The formation of nuclei will go on until the concentration of precursor decreases to the point of critical supersaturation. This will happen when the consumption of precursor for the formation of nuclei surpasses the precursor feed. This leads to part three where the supersaturation is again below the critical point and no further nuclei can form because of the energy barrier. Formed nuclei will grow until the concentration of precursor reaches the point of saturation in this part.

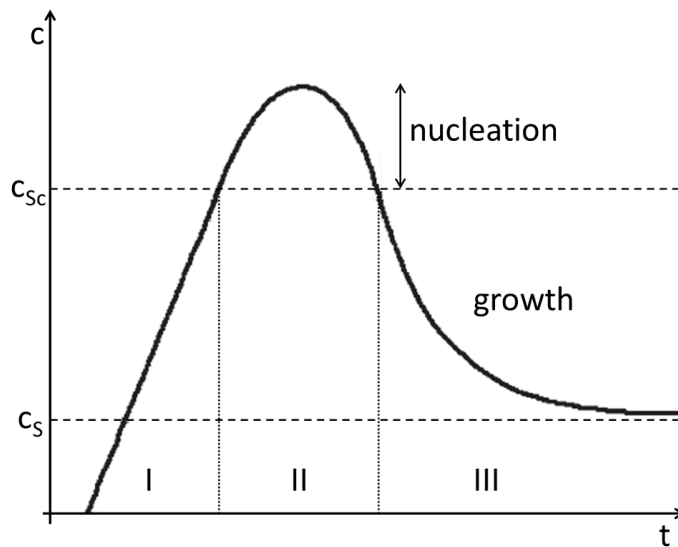


Figure 4: LaMer plot, the concentration as a function of time in the "burst nucleation" concept.

Because of their size the nuclei have a highly curved surface resulting in a very high surface energy. This surface energy is the reason why very small

3.1 Nanoparticles

nuclei dissolve again. The Gibbs free energy of the formation of a spherical particle is given in equation 6.^[13, 14]

$$\Delta G = 4\pi r^2 \gamma + \frac{4}{3}\pi r^3 \Delta G_\nu \quad (6)$$

Where r is the radius of the particle, γ is the surface free energy per unit area and always positive, ΔG_ν is the free energy change between the precursor in solution and unit volume of bulk crystal. ΔG_ν is negative as long as the concentration is above the saturation point. The value for r where ΔG is at a maximum is the smallest radius (r_c) of the nuclei that is stable and unlikely to dissolve again.^[15] A high supersaturation (S), as equation 7 shows, is necessary to have a small r_c so the forming nuclei do not dissolve again.

$$r_c = \frac{2\gamma V_m}{RT \ln S} \quad (7)$$

There are several methods for the separation of nucleation and growth. The two most common homogeneous methods are the "hot-injection"^[16] and the "heating-up"^[17] method. The "hot-injection" method was invented by Bawendi et.al. in 1993.^[18] They used it for the synthesis of monodisperse cadmium chalcogenide nanoparticles. This method creates the supersaturation by rapid injection of a precursor solution into a hot solution of surfactants. Due to the single injection of precursor the nucleation consumes the precursor fast and the decrease of the concentration is very steep. Therefore, the time frame for the nucleation is very short. In the other method the precursor, the surfactants and the reactants are mixed in a low temperature solution. This solution was subsequently heated to a certain temperature and the formation of nuclei occurs. As equation 7 shows the temperature is another factor which can reduce the critical radius of the nuclei. Both methods can produce monodisperse nanoparticles. The "heating-up" method has some advantages as the simplicity and the less problematic up scaling.

3.1.5 Growth

For monodisperse particles it is necessary that in the growth process no further nucleation occurs, which leads to particles with the same growth history. Another necessary condition for monodisperse particles is that all particles grow at the same rate. To this subject Reiss developed the first theoretical studies. His model is known as the "growth by diffusion" model.^[19] It states that the growth rate of a spherical particle is only dependent on the flux of precursor to the surface. If the inter-particle distance is sufficiently large the growth of every particle can be considered self-contained, since the diffusion layer around the particle is not affected by other particles. The correlation of the flux J and the growth rate $\frac{dr}{dt}$ is given in equation 8.

$$J = \frac{4\pi r^2}{V_m} \frac{dr}{dt} \quad (8)$$

$$J = 4\pi r^2 D \frac{dC}{dx} \quad (9)$$

With Fick's law (eq. 9) and under the assumption that J is constant for x the distance from the center, the integration of the concentration C from r to $r + \delta$ leads to equation 10. With D the diffusion coefficient, r the particle radius, t the time and the volume V_m .

$$J = 4\pi D \frac{r(r + \delta)}{\delta} [C(r + \delta) - C_s] \quad (10)$$

Where C_s is the precursor concentration at the surface of the particle. If δ gets large enough equation 10 reduces to equation 11 where $C(r + \delta)$ is C_b the concentration of the bulk solution.

$$J = 4\pi D (C_b - C_s) \quad (11)$$

If equation 11 is combined with equation 8 it leads to equation 12.

$$\frac{dr}{dt} = \frac{V_m D}{r} (C_b - C_s) \quad (12)$$

3.1 Nanoparticles

This equation shows an inversely proportional correlation of the growth rate and the radius, i.e. the growth of bigger particles is slower than that of smaller ones. This can be understood if one considers that the diffusion of the precursor increases with the square of the radius (eq. 8) but the amount of precursor the particle consists of increases with the third power of r . This deceleration of the growth with increasing particle radius has a focusing effect on the particle size.^[13] The big particles "wait" for the smaller ones. However this model is an oversimplification since it disregards the dissolution of surface units from the particles. The dissolution process is dependent on the chemical potential μ of the particle. The chemical potential is dependent on the surface free energy of area A . For spherical particles the change of the chemical potential with the radius r is given by equation 13.

$$\Delta\mu = \gamma \frac{dA}{dn} \quad (13)$$

Where dA is $8\pi r dr$ and dn is $4\pi r^2 \frac{dr}{V_m}$. Reduced this leads to the Gibbs-Thomson relation shown in equation 14.

$$\Delta\mu = \frac{2\gamma V_m}{r} \quad (14)$$

This equation shows that the chemical potential for very small particles is very large. This implies that small particles are more likely to dissolve again. The faster dissolution of small particles leads to a defocus of the size distribution of the particles. When the supersaturation is low Ostwald ripening occurs. Ostwald ripening is a combination of both effects. While the small particles dissolve the bigger particles grow on because they are fed with the material of the dissolved small particles. This leads to a broadening of the size distribution and an overall increase in particle radius.

3.1.6 Synthetic routes

There are several chemical reactions which can be utilized to produce nanoparticles. While, as mentioned earlier the physical methods can produce nanoparticles in large amounts and with high purity, the chemical methods give a good control over size and shape of the nanoparticles. Chemically derived nanoparticles are synthesized *via* colloidal solution chemistry. During the history of nanoparticle synthesis a broad range of different shapes and sizes of monodisperse nanoparticles were produced.^[20, 21] The next section is an introduction of the four most common synthetic routes for nanoparticles. These are the reduction of metal-salts (1), the thermal decomposition of precursors (2), the hydrolytic (3) and the non-hydrolytic sol-gel methods (4).

(1): The reduction of metal salts in aqueous solution by a reducing agent leads to the formation of metal nanoparticles under certain conditions. One of the first ever reported nanoparticle synthesis is the reduction of HAuCl_4 with phosphor by Faraday 1857.^[22] Other reducing agents for aqueous methods are sodium citrate^[23] or sodium borohydride.^[24] Most of the reducing methods are in aqueous solution. To perform the reduction of metal salts in organic solvents the reducing agent has to be soluble in the organic solvent such as superhydride, alcohols and alkyl amines. Bönemann et al.^[25] used tetraalkylammonium hydrotrialkylborate salts to produce metal nanoparticles. As metal salts many transition-metal salts (e.g., Co, Cu, Ru, Ir) and the noble metal salts (Ag, Au, Pd, Pt) are suitable to form nanoparticles.^[26, 27, 28, 29, 30] In most cases the reducing agent will be injected to the metal salt to start the nucleation for every particle at the same time. A drawback of the reduction methods is the sensitivity of the most reducing agents to water. This leads to a reduced reproducibility due to the uncertain amount of reducing agent.

(2): The decomposition of a precursor under high temperature is a very versatile method to produce monodisperse nanoparticles of various sizes and shapes with a high crystallinity due to the high temperature. Most of the precursors are organo-metallic compounds or metal-surfactant complexes such as dimethyl cadmium^[18] or a carboxylic acid metal salt like iron oleate.^[10] For the formation of metal chalcogenide nanoparticles other precursors can

3.1 Nanoparticles

be used, so called single source precursors (SSP). These SSPs already contain the metal-chalcogen bond like metal-xanthanates.^[31, 32] The decomposition reactions of the precursors are carried out in a hot surfactant solution. The surfactant solution consists of a high boiling organic solvent and a surfactant or the solvent is a surfactant. Bawendi et al. used the decomposition of dimethyl cadmium and a trioctylphosphine selenide respectively telluride complex in trioctylphosphine oxide (TOPO) at 260 to 300 °C to produce cadmium selenide or telluride nanoparticles.^[18] The prepared nanoparticles have a diameter between 1.5 and 11.5 nm dependent on the temperature and the growth time. The nanoparticles are monodisperse and uniform. The precursors are injected into the TOPO to separate the nucleation from the growth.

Another method is used by Hyeon et al. for the production of monodisperse iron oxide nanoparticles. The thermal decomposition of iron oleate in octadecene at 320 °C is a "heating-up" method. All reactants are dissolved in a high boiling organic solvent and are subsequently heated to the point of burst nucleation. This method can produce monodisperse iron oxide nanoparticles with diameters from 4 to 25 nm on a multiple gram scale. Further is it possible to produce cubic instead of spherical particles only by changing the amount of oleic acid in the reaction. Due to the very fine adjustability of these methods it is possible to achieve size distributions with $\sigma \leq 5\%$. The high temperature can be a problem because of side reactions with the atmosphere so it has to be carried out under protective atmosphere. The high temperature and the protective atmosphere cause these methods to be challenging and expensive.

(3),(4): For the formation of metal oxide nanoparticles there are two more procedures, the sol-gel methods. By these technique a sol is formed from a precursor solution, which subsequently reacts to form a porous inorganic network with a continuous liquid phase (gel). Most of the sol-gel nanoparticle syntheses are more like a sol-precipitation reaction than a classical sol-gel reaction. The two ways to perform the sol-gel synthesis are the hydrolytic^[33] and the non-hydrolytic^[11] way. The hydrolytic way involves hydroxyl-containing intermediates while the non-hydrolytic way avoids those

intermediates. Most of the sol-gel reactions are carried out in high boiling organic solvents, because the growth of the nanoparticles is better controllable and crystallinity at high temperatures is much higher. Water as oxygen source is not suitable in most cases because the reaction of water with most metal precursors is too fast to control the growth and it is also not suitable for high temperatures ($\sim 200^\circ\text{C}$) which are needed for a good crystallinity of the nanoparticles. A hydrolytic route is the reaction of an alcohol with a metal halide under the formation of an alkyl halide and a metal hydroxide which subsequently reacts to the metal oxide and water (Figure 5). To avoid the formation of hydroxyl groups and water there are two reaction routes. The first way is the reaction of a metal halide with a metal alkoxide under the formation of the metal oxide and an alkyl halide (Figure 6). The second way is the reaction of a metal alkoxide with a metal carboxylate which forms under an ester elimination reaction the metal oxide (Figure 7).^[34]

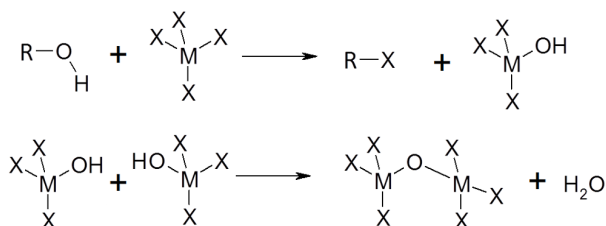


Figure 5: Reaction of an alcohol with a metal halide.

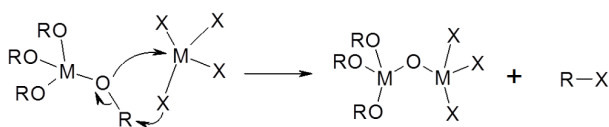


Figure 6: Reaction of a metal alkoxide with a metal halide

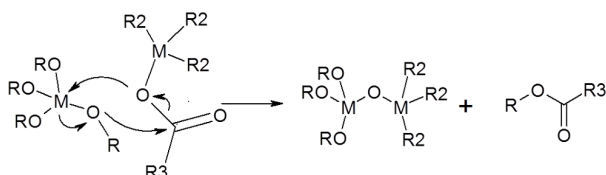


Figure 7: Reaction of a metal alkoxide with a metal carboxylate

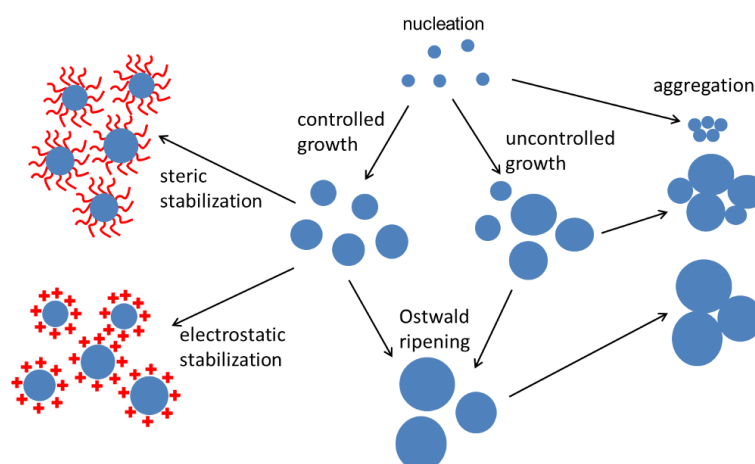


Figure 8: Scheme of the nanoparticle evolution.

With the sol-gel methods a broad range of highly crystalline metal oxide nanoparticles are accessible for example ZnO, TiO₂, MnO, CoO and even mixed oxides like MnFe₂O₄ or ITO.^[11] The uniformity and size distribution of the nanoparticles produced with sol-gel methods are not as good as with the other methods because of the more complex reactions. Some of the sol-gel reactions are surfactant free which sometimes leads to aggregation and even with surfactants the nanoparticles in the gel state are in close proximity to each other.

In summary the nanoparticle evolution involves the nucleation, the growth and the Ostwald ripening (Figure 8). That is not the final state of the nanoparticles. There are mainly two routes the evolution can continue. The aggregation, which often is an undesired event, or they can be stabilized either by electrostatic or by steric forces.

3.1.7 Aggregation

As mentioned earlier aggregation of nanoparticles is an undesired event because of the loss of the size dependent effects. The stability of nanoparticles

in solution is dependent on several factors. Nanoparticles with no surface modification can be described as a colloidal dispersion. For the description of colloidal dispersions Derjaguin, Landau, Verwey and Overbeek came up with a theory which combines the expected attractive and repulsive forces, the DLVO-theory.^[35, 36] The attractive forces are the van der Waals forces. These forces are due to a fluctuating electron distribution in the nanoparticles which cause a temporary dipole. The temporary dipole induces another temporary dipole in a neighbor nanoparticle and this leads to dipole-dipole interactions. For two particles with the radius r_1 and r_2 in a distance s from each other the potential energy of attraction V_a is given by equation 15. This is under the assumption that r_1 and r_2 are much bigger than the distance s .^[37]

$$V_a = \frac{Hr_1r_2}{6s(r_1 + r_2)} \quad (15)$$

With

$$H = \pi^2\rho_1\rho_2C$$

where ρ is the number of atoms or molecules per unit volume and C is a coefficient for the particle-particle pair interactions. The most important repulsive force between colloidal nanoparticles without a surface modification is the repulsion between their electric double layers. This double layer originates from the surface charges of the nanoparticle which attract oppositely charged ions from the solvent. This leads to a decreasing electrical potential with increasing distance from the particle surface. If two particles come close together the double layers come in contact and due to the same charge of the layers a repulsive force occurs. For two particles of the same radius and under the same assumptions as for the attractive interactions, the potential energy of repulsion V_r is given by equation 16.^[36, 37]

$$V_r = \frac{64\pi c_i RT r}{\chi^2} e^{-\chi s} \left[\frac{z^* F \Psi}{e \frac{2RT}{-1}} \right]^2 \quad (16)$$

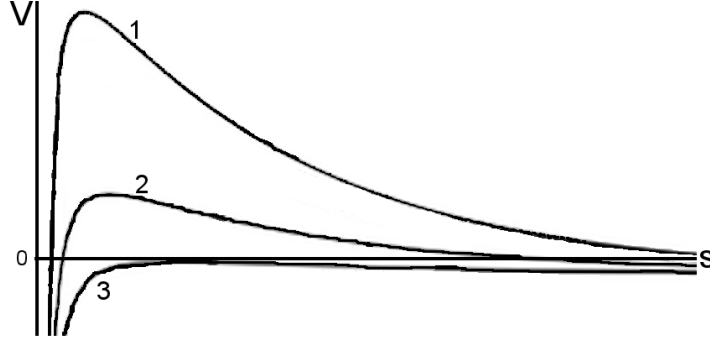


Figure 9: Potential energy curves for the approach of two identical spherical particles with a high energy barrier and relative stability (1), small energy barrier and low stability (2) and no energy barrier leads to fast aggregation (3).

Where z^* is the valency of the counter ions, F the Faraday constant, R the ideal gas constant, T the temperature, Ψ the Stern potential, s the distance between the two particles, r the radius of the particles, c_i the concentration of the counter ions and χ the reciprocal thickness of the double layer. The combination of the attractive and repulsive forces leads to equation 17.

$$V_{ra} = \frac{64\pi c_i R T r}{\chi^2} e^{-\chi s} \left[\frac{e \frac{z^* F \Psi}{2RT} - 1}{\frac{z^* F \Psi}{2RT} + 1} \right]^2 - \frac{H r_1 r_2}{6s(r_1 + r_2)} \quad (17)$$

Dependent on the ratio of the attractive forces to the repulsive forces there are different outcomes (Figure 9). If the repulsive forces are depleted, for example by increasing the ionic strength which results in a contraction of the double layer, the energy barrier decreases and the aggregation due to kinetic collision is more likely. If the repulsive forces are weak enough or the attractive forces strong enough the energy barrier disappears and the particles aggregate fast.

This applies to electrostatic stabilized nanoparticles. The electrostatic sta-

bilization has some draw backs. It does only work in non-polar solvents and is easily depleted by changes in the ionic strength or the pH.^[36, 37]

3.1.8 Nanoparticle stabilization

The electrostatic stabilization of nanoparticles has some restrictions. To stabilize nanoparticles in non-polar and/or organic solvents other methods must be utilized. The most common method is the steric stabilization. This method overcomes the van der Waals forces with a layer of molecules on the particle surface. The surfactants replace the double layer from the electrostatic stabilization. If two particles with surfactant molecules approach, the surfactant molecules come in contact with each other. This leads to a hindrance of conformational mobility and therefore to a loss of entropy. The product of this entropy loss is an osmotic repulsive force.^[36]

3.1.9 Grafting methods

There are many different ways to attach these surfactant molecules onto the nanoparticles. Some nanoparticle syntheses are carried out in a surfactant solution. In these cases the surfactant is a tool to control the growth and subsequently act as a stabilizer for the final nanoparticles. The initial surfactant is often a long chain alkyl -amine, -phosphine, -thiol or a carboxylic acid, like oleylamine, trioctylphosphine, dodecyl thiol or oleic acid. To attach other molecules on the surface one has to substitute the original ones or if they have a functional group one can couple it with the desired molecule by a chemical reaction. The next part will be an overview over the different methods to prepare such stabilized nanoparticles.

The first method is a chemical reaction with a silane coupling agent which can modify the surfaces of metal oxide nanoparticles. These silane coupling agents are mostly functional alkyl tri -methoxy or -ethoxy silanes. They react with the hydroxyl groups on the surface (Figure 10).^[38]

The alkyl groups can be of different length and can carry different functional groups. The most common coupling agents are 3-aminopropylethoxysilane (APTES), n-propyltriethoxysilane^[39, 40] and 3-methacryloxypropyltrimethoxy-

3.1 Nanoparticles

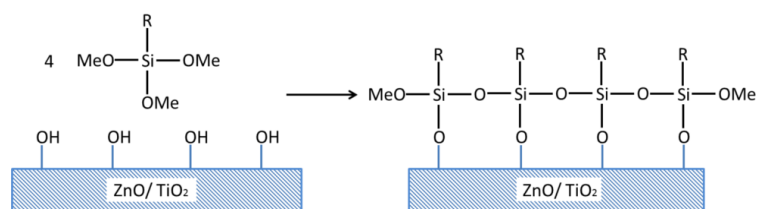


Figure 10: Scheme of the reaction of silane coupling agents with the surface hydroxyl groups of metal oxide nanoparticles.

silane (MPS).^[41] The alkyl group in these common agents is rather short but it still has a stabilizing ability and it has an impact on the solubility of the nanoparticles. The greatest advantage of this surface modification is the possibility to attach functional groups on the nanoparticle surface. These groups can be used in other chemical reactions to couple linker molecules, macro initiators or polymers to the nanoparticle.

Another possibility to use APTES is to coordinate the amine group onto nanoparticles and subsequently use the nanoparticle in a common Stöber synthesis as seeds. The growth of the silica shell from the trimethoxysilane groups on the nanoparticle surface is well controllable and can lead to very uniform core-shell particles as Liz-Marzán et al. show.^[42] The problem is these core-shell nanoparticles can still aggregate if the stabilization is not strong enough. However this method is good for the separation of the cores from each other due to the silica shell. The distance control of the gold cores through the silica shell is a very promising tool, for example to tune the plasmon interactions of the gold cores.^[43]

To attach macromolecules, like polymers, to the nanoparticle surface there are mainly two methods. Both of these procedures connect the nanoparticle and the polymer with a covalent chemical bond. The first one does this simply by coupling a preformed polymer to the nanoparticle, this method is called "grafting-to" method. There are various coupling reactions utilized for the grafting-to method. The prerequisites for the coupling are a functional group on the polymer as well as one at the nanoparticle surface. The most common polymer attachment form is the polymer brush layer by which the

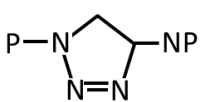
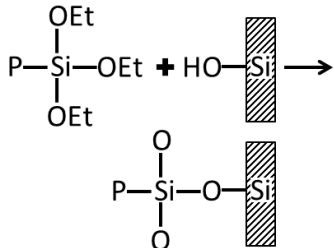
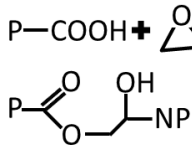
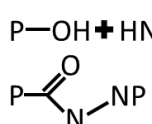
polymer is only attached with one end to the surface. Therefore the polymer must be end functionalized either directly by the synthesis or subsequently. The functionalities for the coupling are manifold and range from simple hydroxyl groups to trialkoxysilanes. The functionalities on the nanoparticle surface have an equally broad range. Some of the reactions utilized for the coupling are summarized in Table 2. There are different ways to bring the functionalities onto the surface of the nanoparticles. First is the aforementioned silanization with a functional alkyltrialkoxysilane. Another way is the usage of an alpha- omega- functionalized surfactant with a coordinating group on one side and the desired functionality on the other.

The drawbacks of this method are the low grafting density that can be reached and the necessity to develop new recipes for every polymer nanoparticle combination. The coupling reactions are mostly the same, while the exact conditions have to be adjusted to the different combinations. The grafting density, the amount of polymer chains per surface area, is crucial for the stability of the nanoparticles in solution. If the grafting density is too low the van der Waals forces may overcome the repulsive forces. This is due to the space that the attached polymer chain has, to avoid contact with the approaching nanoparticle and its surface polymers. If the grafting density is high enough the polymers are more brush like, extend further in to the solution and have less space to avoid contact.^[47]

The second method to attach polymers on the nanoparticle surface is the so called "grafting-from" method. By this procedure initiator molecules are attached to the nanoparticle surface from which the polymer can subsequently be polymerized. To bring the initiator to the nanoparticle surface the earlier mentioned silanization and the alpha-omega functional surfactants can be utilized. There are many different polymerization methods, the most common ones for grafting-from are controlled radical polymerizations. In 2002 Ohno et al.^[48] used a surface initiated living radical polymerization to produce polymethylmethacrylate (PMMA) grafted gold nanoparticles. For the surface initiated living radical polymerization the preformed gold nanoparticles are modified with a disulfide compound which contains two terminal, tertiary bromide alkyls as initiator groups. Copper bromide

3.1 Nanoparticles

Table 2: A summary of common coupling reactions used for nanoparticle modification.

Reaction	Functional groups / Bond	Examples / Literature
Click	$P-N_3 + \text{C}=\text{C}-NP \rightarrow$ 	polystyrene azide + strained double bond of C60 or SWCNT [44]
Silanization	$P-Si(OEt)_3 + HO-Si \rightarrow$ 	polystyrene triethoxysilane + silica surface ^[38, 39, 40, 41]
Epoxy/ Carboxylic acid	$P-COOH + \text{epoxy}-NP \rightarrow$ 	polystyrene carboxylic acid + epoxy silane surface ^[45]
Thiol/ Gold	$P-SH + Au \rightarrow P-S-Au$	Polystyrene thiol + gold nanoparticles [46]
Amide	$P-OH + HN-NP \xrightarrow{CDI}$ 	Peptide syntheses

is used as catalyst for the polymerization. The obtained PMMA grafted gold nanoparticles are well dispersed and the PMMA had a polydispersity index (PDI) of about 1.3. The grafting density is about 0.3 chains per nm^2 . Skaff and Emrick showed in 2004^[49] that the reversible addition fragmentation chain transfer (RAFT) polymerization is a suitable method for grafting-from. For the RAFT reaction the tri-n-octylphosphine oxide ligands on the cadmium selenide nanoparticles are exchanged by phosphine oxide ligands which contain a trithiocarbonate group. This trithiocarbonate group can be used as an initiator for the RAFT polymerization. Skaff and Emrick synthesized with this method cadmium selenide nanoparticles grafted with polystyrene, PMMA, poly-n-butylacrylate as well as the copolymers and the block-co-polymers of these. All the grafted polymers have a PDI of about 1.2. Li et al.^[50] used in 2006 the RAFT polymerization as well to graft polystyrene and PMMA onto silica nanoparticles. The silica nanoparticles are therefore modified with aminopropyltrimethoxysilane and afterwards with 4-cyanopentanoic acid dithiobenzoate which is coupled to the surface using the amine groups. The obtained polymers have a PDI of about 1.2. Marutani et al.^[51] used in 2004 silanization to attach 2-(4-chlorosulfonylphenyl)ethyltrichlorosilane (CTCS) to magnetite nanoparticles. CTCS is an initiator for atom transfer radical polymerization (ATRP) which is subsequently carried out with copper bromide as catalyst. The grafted PMMA had a PDI of about 1.2. Esteves et al.^[52] also used in 2007 the ATRP, to graft polybutylacrylate to cadmium sulfide nanoparticles. Like in the work of Skaff and Emrick a modified phosphine oxide was used to attach the initiator, 2-chloropropionyl chloride to the nanoparticles. As catalyst copper chloride was used and the polymer had a PDI of about 1.2. Another method is the in 2004 by Matsuno et al.^[53] utilized nitroxide-mediated radical polymerization (NMP). The preformed magnetite nanoparticles are modified with a phosphoric acid derivative which contains a (2,2,6,6-tetramethylpiperidin-1-yl)oxidanyl group. With this group Matsuno et al. polymerized polystyrene as well as poly-3-vinylpyridine onto the nanoparticles. The grafting density is about 0.15 chains per nm^2 and the PDI about 1.3. Further polymerization methods are used in 2002 by Carrot

et al.,^[54] they employed the surface-initiated ring-opening polymerization to graft polycaprolactone to silica and cadmium sulfide nanoparticles. The silica nanoparticles are modified *via* silanization to bring amine groups to the surface and the cadmium sulfide nanoparticles are modified with thioglycerol to bring hydroxyl groups to the surface. From these surface groups the caprolactone was polymerized with the aid of triethylaluminium. Another ring-opening method was used by Skaff et al. also in 2002.^[55] The ring-opening metathesis polymerization (ROMP) is ruthenium catalyzed and the catalyst is attached to the nanoparticles again *via* modified phosphine oxide. The so polymerized polycyclooctene had a PDI of about 2. Zhou et al.^[56] showed in 2002 that even the living anionic polymerization can be utilized to graft polymers onto nanoparticles. The preformed silica nanoparticles are modified by silanization with a 1,1 diphenylenethylene derivate. The polymerization of styrene was initialized with sec-butyl lithium and leads to polystyrene with a PDI of about 1.2.

Another stabilizing method for nanoparticles is to produce a polymer shell around the nanoparticles. Karg et al.^[57] showed in 2011 that butenylamine functionalized gold nanoparticles can be used in a precipitation polymerization to form a poly-N-isopropylacrylamide (PNIPAM) shell around them. This shell is consisting of cross-linked PNIPAM chains.

The last method to modify nanoparticle surfaces is the ligand exchange. This method was used in many of the above introduced methods to attach the required functional groups onto the nanoparticle surface. In principle it is just the substitution of the original ligand of the nanoparticle with a new one, by excess and/or by a superior coordination group. The ligand exchange can be utilized for other reasons than stabilizing, e.g. for the introduction of functional groups to nanoparticles, to induce a phase transfer from one solvent to another^[58] or it also can be used to cross-link nanoparticles with each other to form crystal-like structures. Skaff and Emrick^[59] introduced in 2003 the exchange of the original trioctylphosphine ligand with a para-substituted pyridine. The pyridine was used as coordinating group and the substitute was a polyethylenglycol with 14 repetition units. The usage of the ligand exchange method to produce polymer brush stabilized nanoparticles

was part of this work and will be addressed to in chapter 5.

3.1.10 Properties/ Applications

The in this work used nanoparticles are gold and silver metal nanoparticles as well as the semiconductor nanoparticles ZnO, PbS and CdSe. Gold and silver nanoparticles are of interest because of their plasmonic properties. They are also used to produce an electric conductive nanoparticle ink for inkjet printers. Another application for silver nanoparticles is their antimicrobial behaviour.^[60] ZnO is a semiconductor, it is colorless and an UV-absorber. It can be used in photovoltaic applications because of the semiconducting properties and the transparency of its nanocomposites.^[61] It was also used to produce a scratch resistant, transparent PMMA composite with the useful addition of the UV-absorption. Like ZnO, PbS is a semiconductor used in photovoltaic applications^[62] but, other than ZnO, PbS is coloured and therefore can be used to increase the absorbed amount of light. CdSe nanoparticles can be used similar to PbS nanoparticles in photovoltaic cells.^[63] In addition CdSe nanoparticles can emit light in the range of 400 to 630 nm. This can be used in medicine as a luminescent marker.^[64] CdSe nanoparticles with a polymer shell can be modified with molecules for tissue targeting and can, subsequently to the enrichment, be detected due to their luminescence. The luminescence can be tuned to enable simultaneous usage of more than one marker.

3.2 Nanocomposites

Composite materials are composed of two or more materials and have different physical and/or chemical properties compared to the individual materials. For nanocomposites at least one of the materials has to be in the size regime of 1 - 100 nm in at least one dimension. The main component is called matrix and is in many cases a continuous phase. The other components are called fillers. They are selected for their ability to modify the properties of the matrix in the desired way. The difference between nanocomposites and composites with filler materials in the size range of micrometers

is the matrix-filler interface. The filler materials in nanocomposites are in most cases nanoparticles, which have as mentioned above a very high surface to volume ratio and therefore a much larger interface at the same volume fraction. The larger interface is the reason that effects on the properties developed at much lower volume fractions. The most common combination is a polymer (e.g. polystyrene, PMMA) as matrix and inorganic nanoparticles (e.g. metal-, metal oxide-, semiconductor nanoparticles) as filler. The geometry of the filler and its orientation in the composite highly affects the composite properties. So can carbon nanotubes enhance the tensile strength of polymers.^[65] Montmorillonite nanoclays, which build plate-like structures, can enhance the gas barrier properties of polymers if they are orientated in the required way.^[66]

3.2.1 Synthesis

The goal of a nanocomposite synthesis is a controlled or at least a homogeneous distribution of the nanofiller in the polymer matrix and the possibility to give the nanocomposite the desired form. For the synthesis of these polymer inorganic nanocomposites there are physical and chemical methods. The first physical method is the melt mixing or melt compounding.^[67] By this method the nanoparticles are mixed with a polymer melt and are extruded afterwards. The advantage of this method is the great amount of nanocomposite that can be produced. In addition, the extrusion of polymers is a well-established technique. It is also possible to obtain nanocomposite fibers by melt compounding and subsequent melt spinning.^[68] The second physical method is the film casting method.^[69] For film casting a solution of polymer and nanoparticles is brought to a surface with subsequent evaporation of the solvent. This method is very simple to carry out, but it is only suitable for more or less thin composite films. If very thin films are needed the polymer nanoparticle solution can be spin coated to surfaces which leads to films with a thickness down to about 10 nm.^[70] For thicker sheets the evaporation of the solvent can be a problem due to bubble formation in the polymer matrix. This problem can be solved if the prepared sheets are treated in a

hot press. A third physical method is the intercalation of polymer chains between the layers of clay.^[71, 72] This method can lead to well-ordered multilayer nanocomposites with alternating polymer and clay layers. If the clay gets completely exfoliated the multilayer structure is lost and the clay sheets are dispersed in the polymer matrix.

The *in-situ* polymerization, the first of the two chemical methods to produce nanocomposites, is mainly a general term for many different techniques. All of the included methods have in common that the polymer matrix is formed around the nanofiller materials. The simplest method is to mix nanoparticles with the monomer and initiate the polymerization. The polymerization can be initiated with nearly every known initiation such as radical initiation,^[73, 74] UV-light initiation^[75] or even with gamma-ray initiation.^[76] A problem that can occur with this method is a low solubility of the nanoparticles in the monomer which quickly leads to aggregation and sedimentation of the nanoparticles. The final result of such sedimentation is a heterogeneous distribution of the nanoparticles. This problem can be solved with the above mentioned nanoparticle modifications and the therefore adjustable solubility of the nanoparticles. Another method is the above mentioned precipitation polymerization for nanoparticle modification. Under different conditions it is not only possible to synthesize a shell around the nanoparticles but a complete polymer matrix is formed around them.

The nanoparticle modification methods grafting-to and grafting-from also can be used to produce nanocomposites. That can either be done by change of the reaction conditions leading to longer polymer chains or by mixing the grafted nanoparticles with free polymer. The mixing can either be melt mixing or solvent mixing and is therefore a combination of the physical mixing methods and *in-situ* polymerization. If the grafted polymer is of the same type as the polymer matrix the distribution of the nanoparticles should be more homogeneous. The layer by layer deposition is another method to prepare highly homogeneous nanocomposites.^[77] The nanocomposites are prepared by alternating deposition of polymer and nanoparticles on a surface in a few nm thick layers. The second chemical method is the *in-situ* nanoparticle formation. It is similar to the first method a general term and describes

various methods. In all of these methods the nanoparticles are prepared in presence of the preformed polymer matrix. In general a nanoparticle precursor gets mixed with the polymer matrix and will subsequently form nanoparticles. With this method a homogenous dispersion of the nanoparticles in the polymer matrix is possible due to the fixation of the structure after the nanoparticle formation. The mixing of polymer and nanoparticle precursor can be achieved by a sol-gel process or with a microemulsion. An example is the reduction of a silver salt in a polyethyleneimine poly(acrylic acid) mixture by Dai and Bruening.^[78] The silver salt is therefore bound to the polyethyleneimine by the formation of complexes between the silver ions and the amine-moieties of the polyethyleneimine. The two polymers are deposited on a surface in alternating order with a subsequent reduction step. Another possibility is to combine both chemical pathways as Palkovits et al. demonstrated.^[79] The transparent SiO₂-PMMA composite was prepared by an *in-situ* nanoparticle synthesis in a reverse microemulsion with a subsequent polymerization of the microemulsion.

3.2.2 Aggregation

One problem of every nanocomposite synthesis is the aggregation of the nanoparticles in the polymer matrix. A possible solution for this problem is the above mentioned fixation of the nanoparticles during the composite synthesis. However this only works if the nanocomposite is in its final form. If the nanocomposite is meant to be treated in a way, mechanically or thermal, the nanoparticles become free to move again and aggregation may occur. In the Flory-Huggins solution theory the Gibbs free energy change of mixing is given by equation 18.^[80, 81]

$$\Delta G = \Delta H_m - T\Delta S_m \tag{18}$$

Where ΔH_m is the enthalpy change of mixing, T the absolute temperature and ΔS_m is the entropy change of mixing. If the Gibbs free energy change is negative the system is miscible, if it is not than the system will separate and

form two phases. In a normal system the entropy change by mixing two components (A and B) is relatively large. In a polymer-solvent system however, the entropy change is smaller due to the smaller conformational freedom of the polymer chains. Mixing two polymers with each other results in an even smaller entropy change. Nevertheless a positive change of the entropy favors the mixing of the system. The change of the enthalpy is dependent of the interactions of the two mixed components. If the interaction A-B is energetic more favourable than the interaction of A-A and B-B, the enthalpy change is negative. To determine if nanoparticles in a polymer matrix will be miscible or not is dependent on many more factors. Hooper and Schweizer^[82] have shown in a computational model that a hard sphere (nanoparticle) can be miscible with a polymer under certain circumstances. Prerequisite for the miscibility is an attractive force between the polymer chains and the sphere, e.g. a negative enthalpy change. The potential of mean force for the system hard sphere-polymer predicts four structural configurations for the system. The first is the entropic dominated situation where the spheres are aggregated because of the depletion which favors the segregation of the spheres (Figure 11A). This is due to the low attraction of the polymer to the spheres. The entropy loss of the polymer chains at the sphere surface is higher than the enthalpy change of polymer-sphere interaction. The second is the enthalpic dominated situation, where the polymer adsorbs to the sphere surface in a thin layer. The polymer-sphere interaction is very strong and attractive which leads to a small sphere-sphere distance due to polymer chains that are bonded to two spheres while the thin polymer layer separates the spheres (Figure 11B). The third situation is between these two extremes. The attraction between the polymer and the sphere is high enough to form a polymer layer around the sphere, which is thicker than in the second case. But the attraction is not high enough to overcome the entropy loss which is required to stretch and attach the polymer to another sphere. Therefore the sphere is surrounded by a polymer layer which is thermodynamically stable and stabilizes the sphere sterically in the polymer matrix (Figure 11C). The fourth situation is similar to the third with a little higher attraction between the polymer and the spheres. This leads to spheres with a polymer layer as

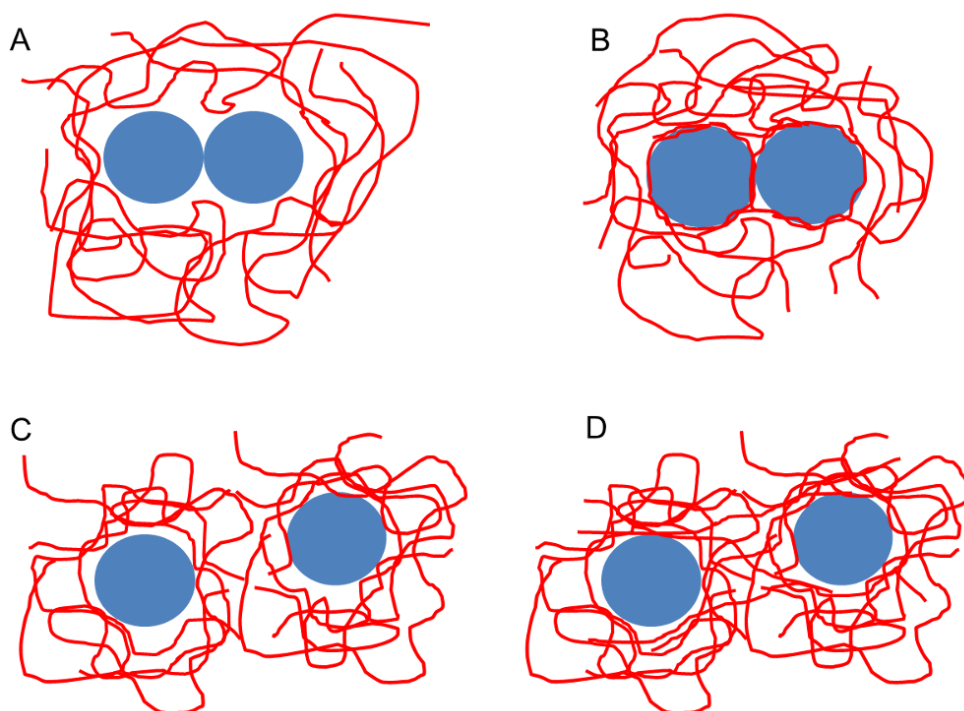


Figure 11: Scheme of the four situations predicted by Hooper and Schweizer. (A): Contact aggregation, (B): aggregation due to the bridging of polymer, (C): steric stabilization by a polymer shell and (D): the combination of the stabilizing shell with some bridging polymer chains.

thick as in the third case but some polymer chains connecting the spheres like in the second case (Figure 11D). This method of stabilizing nanocomposites is used in systems in which the requirements are met. As an example the synthesis of nanoparticles in the presence of polyvinylpyrrolidone (PVP) or the mixing of preformed nanoparticles with PVP.^[83]

For other nanoparticle-polymer combinations, which have not the required properties, other methods have to be employed. If there is no attractive interaction between the polymer and the nanoparticles ΔH_m is positive which leads to separation. To avoid this it is possible to coat the nanoparticle with a shell of the matrix polymer, as described above, so the ΔH_m for mixing polymers of the same type is 0. Because polymer chains are never indistinguishable the ΔS_m of mixing polymers is always positive but not very

large. From the Gibbs free energy change of mixing nanoparticles and polymer should be miscible if the nanoparticles are coated with a shell of the matrix polymer. However there are some other factors which have to be regarded, like the conformational entropy loss of the matrix polymer chains upon contact with the shell on the nanoparticles. If the layer of polymer around the nanoparticles is flat and therefore impenetrable for the matrix polymer chains, they are restricted in their conformational freedom and the entropy loss can overcome the entropy gain of the mixing (Figure 12A). To minimize the entropy loss due to the conformational restriction, the polymer layer around the nanoparticles has to be penetrable for the matrix polymer chains. This can be achieved by attaching the polymer on the nanoparticle in the form of a brush. To produce a brush like polymer layer on the surface the grafting density has to be high enough. If the grafting density (σ) is too small ($\sigma < \frac{1}{R_g^2}$ with R_g the radius of gyration) the polymer chains do not interact with adjacent chains. The polymer chains grafted to the surface would try to obtain the random walk conformation and therefore will form a coil on the surface, the "mushroom regime" (Figure 12B). This layer is too thin to provide good sterical stabilization and matrix polymer chains can reach the nanoparticle surface. If the grafting density increases the radius of gyration of the polymer chains begin to overlap and the polymer layer changes from the "mushroom regime" to a brush-like layer due to the packing constraints. If the grafting density is sufficiently high the polymer layer consists of stretched chains (Figure 12C).^[47, 84] This would lead to a penetrable polymer layer due to the curvature of the particle and the with the distance from the surface decreasing packing density. The matrix polymer now can penetrate the polymer layer which leads to more conformational freedom and the entropy loss will be minimized.^[85] The nanoparticles should be homogeneous and stable dispersed in the matrix polymer if the entropy loss due to the conformational restrictions is smaller than the entropy gain of mixing.

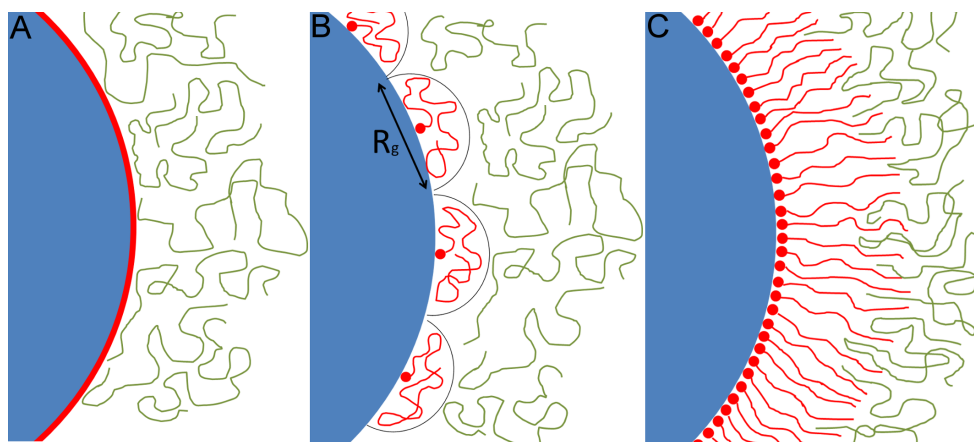


Figure 12: Scheme of the interaction of (A): matrix polymer (green) and a thin hard layer of polymer around a nanoparticle (red), (B): a polymer layer with low grafting density (mushroom-regime) and (C): a brush-like layer of polymer chains.

3.2.3 Properties/ Applications

The properties of polymers can be enhanced in a broad range. The first that came to one's mind are the mechanical properties. Also one of the early industrial applications is the mechanical enhanced nylon-6, which was used by Toyota in its cars.^[86] The clay/nylon-6 was a nanocomposite of montmorillonite (MMT) nanodisks in a matrix of nylon 6. The tensile- and flexural-strength are enhanced by 30% and 60% with a MMT amount of only 5 wt.-%. The elongation of the nylon-6 was also reduced from above 100% down to 7.3%. Similar results are shown for other composites like polybutylene terephthalate with carbon nanotubes.^[65, 86] With spherical nanoparticles the surface scratch resistance can be enhanced. In this work the elastic modulus of PMMA was increased by 300% with the incorporation of ZnO nanoparticles. The electrical and electro catalytic properties are another aim for nanocomposites. It is possible to tune the conductivity of nanocomposites by change of the nanoparticle type, the nanoparticle shape and the nanoparticle content. Ahmad et al.^[87] used SiO₂- and TiO₂- PMMA composites to tune the conductivity and prepare polymer electrolytes. Macanás et al.^[88] utilized copper platinum core-shell nanoparticles in a polymer matrix to tune

the conductivity and the electro catalytic activity. The thermal conductivity can also be increased as Agarwal et al.^[89] showed in 2008 with a polycarbonate carbon nanotube composite. The thermal conductivity is particularly increased when the carbon fibers are aligned vertically. The optical properties of nanocomposites are of great interest. For example the UV-light absorbing ability of ZnO or TiO₂ nanoparticles can be used to protect polymer components from UV-degradation. A ZnO content as low as 0.017 wt.-% is sufficient to block about 99% of the UV-light.^[90] If the nanoparticles are distributed homogeneously in the polymer matrix and are smaller than about 40nm the resulting nanocomposite should be transparent if the matrix polymer is transparent. These effects can be combined with surface hardening to yield a UV-resistant, tough and transparent surface protection. It is also possible to obtain a transparent and colored polymer component due to the absorption of visible light from the nanoparticles. This is known especially for gold nanoparticles. The color of a polyvinyl alcohol gold nanocomposite is dependent on the gold nanoparticle size. It ranges from pink (16 nm nanoparticles) over purple (43 nm) to blue (79 nm).^[91] The complementary effect, the photoluminescence is very promising for the construction of new display devices or in lighting. The light emission of high quality quantum dots (QD) is known to be tunable from 400 to 1400 nm, has 20 times more intensity compared to organic dyes with only one-third of the emission linewidth and is 100 times more stable.^[92] The properties of nanocomposites with iron, iron oxide or other magnetic nanoparticles are of interest for applications in the fields of electromagnetic (EM) shielding, absorption or for data storage. The electromagnetic interference shielding is important for modern electronic devices because of the increasing usage of EM emitters in everyday life. Guo et al.^[93] showed a reduction of EM wave intensity of almost 5 db by an iron oxide-silica core-shell epoxy resin composite. The absorption of EM waves is largely used for military applications as a coating for stealth aircrafts and boats.^[94] The magnetic data storage is dependent on the possibility to build arrays of magnetic nanoparticles with a defined inter-particle distance and a high quality arrangement with very few defects. This can be realized with an iron oxide polymer nanocomposite shown in chapter 5. Another property

REFERENCES

that can be altered is the refractive index (RI). For most polymers the RI is around 1.3 to 1.7. The RI of inorganic materials is in the range of above 3 for PbS and far below 1 for gold. This leads to a tunable RI for nanocomposites because the RI depends linearly on the nanoparticle content.^[95, 96] This makes transparent nanocomposites interesting materials for optical waveguides in telecommunication or in photovoltaic applications as well as for lenses or optical filters.

References

- [1] Roduner, E. Size matters: why nanomaterials are different. *Chem. Soc. Rev.* 2006,35,583–592.
- [2] Koga, K.; Ikeshoji, T.; Sugawara, K. Size- and temperature-dependent structural transitions in gold nanoparticles. *Phys. Rev. Lett.* 2004,92,115507.
- [3] Son, S. U.; Jang, Y.; Yoon, K. Y.; An, C.; Hwang, Y.; Park, J.-G.; Noh, H.-J.; Kim, J.-Y.; Park, J.-H.; Hyeon, T. Synthesis of monodisperse chromium nanoparticles from the thermolysis of Fischer carbene complex. *Chem. Commun.* 2005,1,86–88.
- [4] Diallo, A.K.; Ornelas, C.; Salmon, L.; Aranzaes, J. R.; Astruc, D. "Homeopathic" Catalytic Activity and Atom-Leaching Mechanism in Miyaura–Suzuki Reactions under Ambient Conditions with Precise Dendrimer-Stabilized Pd Nanoparticles. *Angew. Chem. Int. Ed.* 2007,46,8644–8648.
- [5] Talapin, D. V. *Experimental and theoretical studies on the formation of highly luminescent II-VI, III-V and core-shell semiconductor nanocrystals*. PhD thesis, Universität Hamburg, 2002.
- [6] Lippens, P. E.; Lannoo, M. Calculation of the band gap for small CdS and ZnS crystallites. *Phys. Rev. B* 1989,39,10935–10942.

-
- [7] Brus, L. E. A simple model for the ionization potential, electron affinity, and aqueous redox potentials of small semiconductor crystallites. *J. Chem. Phys.* 1983,79,5566–5571.
- [8] Newbery, A. P.; Han, B. Q.; Lavernia, E. J.; Suryanarayana, C.; Christodoulou, J. A. Mechanical alloying and severe plastic deformation. *Mater. Process. Handb.* 2007,13-1.
- [9] Hicks, E. M.; Zou, S.; Schatz, G. C.; Spears, K. G.; van Duyne, R. P. Controlling plasmon line shapes through diffractive coupling in linear arrays of cylindrical nanoparticles fabricated by electron beam lithography. *Nano Lett.* 2005,5,1065–1070.
- [10] Park, J.; Joo, J.; Kwon, S. G.; Jang, Y.; Hyeon, T. Synthesis of monodisperse spherical nanocrystals. *Angew. Chem. Int. Ed.* 2007,46,4630–4660.
- [11] Bilecka, I.; Niederberger, M. New developments in the nonaqueous and/or non-hydrolytic sol-gel synthesis of inorganic nanoparticles. *Electrochim. Acta* 2010,55,7717–7725.
- [12] LaMer, V. K.; Dinegar, R. H. Theory, production and mechanism of formation of monodispersed hydrosols. *J. Am. Chem. Soc.* 1950,72,4847–4854.
- [13] Peng, X.; Wickham, J.; Alivisatos, A. P. Kinetics of II-VI and III-V colloidal semiconductor nanocrystal growth: "focusing" of size distributions. *J. Am. Chem. Soc.* 1998,120,5343–5344.
- [14] Mullin, J. W. *Crystallization, 3rd ed.* Oxford University Press, 1997.
- [15] Vossmeier, T.; Katsikas, L.; Giersig, M.; Popovic, I. G.; Diesner, K.; Chemseddine, A.; Eychmüller, A.; Weller, H. CdS nanoclusters: Synthesis, characterization, size dependent oscillator strength, temperature shift of the excitonic transition energy, and reversible absorbance shift. *J. Phys. Chem.* 1994,98,7665–7673.

REFERENCES

- [16] Talapin, D. V.; Rogach, A. L.; Kornowski, A.; Haase, M.; Weller, H. Highly luminescent monodisperse CdSe and CdSe/ZnS nanocrystals synthesized in a hexadecylamine-trioctylphosphine oxide-trioctylphosphine mixture. *Nano Lett.* 2001,1,207–211.
- [17] Park, J.; An, K.; Hwang, Y.; Park, J.G.; Noh, H. J.; Kim, J. Y.; Park, J. H.; Hwang, N. M.; Hyeon, T. Ultra-large-scale syntheses of monodisperse nanocrystals. *Nat. Mater.* 2004,3,891–895.
- [18] Murray, C. B.; Norris, D. J.; Bawendi, M. G. Synthesis and characterization of nearly monodisperse CdE (E = sulfur, selenium, tellurium) semiconductor nanocrystallites. *J. Am. Chem. Soc.* 1993,115,8706–8715.
- [19] Reiss, H. The growth of uniform colloidal dispersions. *J. Chem. Phys.* 1951,19,482–487.
- [20] Grzelczak, M.; Pérez-Juste, J.; Mulvaney, P.; Liz-Marzán, L. M. Shape control in gold nanoparticle synthesis. *Chem. Soc. Rev.* 2008,37,1783–1791.
- [21] Kwon, G. S.; Hyeon, T. Colloidal chemical synthesis and formation kinetics of uniformly sized nanocrystals of metal, oxides, and chalcogenides. *Acc. Chem. Res.* 2008,41,1696–1709.
- [22] Faraday, M. The bakerian lecture: Experimental relations of gold (and other metals) to light. *Philos. Trans. R. Soc. London* 1857,147,145–181.
- [23] Enustun, B. V.; Turkevich, J. Coagulation of colloidal gold. *J. Am. Chem. Soc.* 1963,85,3317–3328.
- [24] Brust, M.; Walker, M.; Bethell, D.; Schiffrin, D. J.; Whyman, R. Synthesis of thiol-derivatised gold nanoparticles in a two-phase liquid-liquid system. *J. Chem. Soc., Chem. Commun.* 1994,7,801–802.
- [25] Bönnemann, H.; Brijoux, W.; Brinkmann, R.; Dinjus, E.; Jaussen, T.; Korall, B. Formation of colloidal transition metals in organic phases and their application in catalysis. *Angew. Chem. Int. Ed. Engl.* 1991,30,1312–1314.

-
- [26] Moumen, N.; Pileni, M. P. New syntheses of cobalt ferrite particles in the range 2-5 nm: comparison of the magnetic properties of the nanosized particles in dispersed fluid or in powder form. *Chem. Mater.* 1996,8,1128–1134.
- [27] Pileni, M. P.; Ninham, B. W.; Gulik-Krzywicki, T.; Tanori, J.; Lisiecki, I.; Filankembo, A. Direct relationship between shape and size of template and synthesis of copper metal particles. *Adv. Mater.* 1999,11,1358–1362.
- [28] Maillard, M.; Giorgio, S.; Pileni, M. P. Silver nanodisks. *Adv. Mater.* 2002,14,1084–1086.
- [29] Sun, Y.; Xia, Y. Shape-controlled synthesis of gold and silver nanoparticles. *Science* 2002,298,2176–2179.
- [30] Bonet, F.; Delmas, V.; Grugeon, S.; Herrera Urbina, R.; Silvert, P.-Y.; Tekaiia-Elhsissen, K. Synthesis of monodisperse Au, Pt, Pd, Ru and Ir nanoparticles in ethylene glycol. *Nanostruct. Mater.* 1999,11,1277–1284.
- [31] Duan, T.; Lou, W.; Wang, X.; Xue, Q. Size-controlled synthesis of orderly organized cube-shaped lead sulfide nanocrystals via a solvothermal single-source precursor method. *Colloid. Surface. A* 2007,310,86–93.
- [32] Lee, S.-M.; Jun, Y.-W.; Cho, S.-N.; Cheon, J. Single-crystalline star-shaped nanocrystals and their evolution: Programming the geometry of nano-building blocks. *J. Am. Chem. Soc.* 2002,124,11244–11245.
- [33] Iida, H.; Takayanagi, K.; Nakanishi, T.; Osaka, T. Synthesis of Fe₃O₄ nanoparticles with various sizes and magnetic properties by controlled hydrolysis. *J. Colloid Interf. Sci.* 2007,314,274–280.
- [34] Vioux, A. Nonhydrolytic sol-gel routes to oxides. *Chem. Mater.* 1997,9,2292–2299.
- [35] Atkins, P. W.; de Paula, J. *Physikalische Chemie, vierte Edition*. Wiley-VCH Verlag GmbH & Co. KGaA, 2006.

REFERENCES

- [36] Barnes, G. T.; Gentle, I. R. *interfacial science: an introduction 2nd ed.* Oxford University Press Inc., 2011.
- [37] Brezesinski, G.; Mögel, H.-J. *Grenzflächen und Kolloide.* Spektrum Akademischer Verlag GmbH, 1993.
- [38] Zhao, J.; Milanova, M.; Warmoeskerken, M. M. C. G.; Dutschk, V. Surface modification of TiO₂ nanoparticles with silane coupling agents. *Colloid. Surface. A* 2012,413,273–279.
- [39] Ukaji, E.; Furusawa, T.; Sato, M.; Suzuki, N. The effect of surface modification with silane coupling agent on suppressing the photo-catalytic activity of fine TiO₂ particles as inorganic UV filter. *Appl. Surf. Sci.* 2007,254,563–569.
- [40] Tang, E.; Liu, H.; Zheng, E.; Cheng, G. Fabrication of zinc oxide/poly(styrene) grafted nanocomposite latex and its dispersion. *Eur. Polym. J.* 2007,43,4210–4218.
- [41] Guo, Y. K.; Wang, M. Y.; Zhang, H. Q.; Liu, G. D.; Zhang, L. Q.; Qu, X. W. The surface modification of nanosilica, preparation of nanosilica/acrylic core-shell composite latex, and its application in toughening PVC matrix. *J. Appl. Polym. Sci.* 2008,107,2671–2680.
- [42] Liz-Marzán, L.; Giersig, M.; Mulvaney, P. Synthesis of nanosized gold-silica core-shell particles. *Langmuir* 1996,12,4329–4335.
- [43] Karg, M.; Hellweg, T.; Mulvaney, P. Self-assembly of tunable nanocrystal superlattices using poly-(NIPAM) spacers. *Adv. Funct. Mater.* 2011,21,4668–4676.
- [44] Qin, S.; Qin, D.; Ford, W. T.; Resasco, D. E.; Herrera, J. E. Functionalization of single-walled carbon nanotubes with polystyrene *via* grafting to and grafting from methods. *Macromolecules* 2004,37,752–757.
- [45] Luzinov, I.; Julthongpiput, D.; Malz, H.; Pionteck, J.; Tsukruk, V. V. Polystyrene layers grafted to epoxy-modified silicon surfaces. *Macromolecules* 2000,33,1043–1048.

-
- [46] Corbierre, M. K.; Cameron, N. S.; Sutton, M.; Laaziri, K.; Lennox, R. B. Gold nanoparticle/polymer nanocomposites: dispersion of nanoparticles as a function of capping agent molecular weight and grafting density. *Langmuir* 2005,21,6063–6072.
- [47] de Gennes, P. G. Conformations of polymers attached to an interface. *Macromolecules* 1980,13,1069–1075.
- [48] Ohno, K.; Koh, K.-M.; Tsujii, Y.; Fukuda, T. Synthesis of gold nanoparticles coated with well-defined, high-density polymer brushes by surface-initiated living radical polymerization. *Macromolecules* 2002,35,8989–8993.
- [49] Skaff, H.; Emrick, T. Reversible addition fragmentation chain transfer (RAFT) polymerization from unprotected cadmium selenide nanoparticles. *Angew. Chem. Int. Ed.* 2004,43,5383–5386.
- [50] Li, C.; Han, J.; Ryu, C. Y.; Benicewicz, B. C. A versatile method to prepare RAFT agent anchored substrates and the preparation of PMMA grafted nanoparticles. *Macromolecules* 2006,39,3175–3183.
- [51] Marutani, E.; Yamamoto, S.; Ninjbadgar, T.; Tsujii, Y.; Fukuda, T.; Takano, M. Surface-initiated atom transfer radical polymerization of methyl methacrylate on magnetite nanoparticles. *Polymer* 2004,45,2231–2235.
- [52] Esteves, A. C. C.; Bombalski, L.; Trindade, T.; Matyjaszewski, K.; Barros-Timmons, A. Polymer grafting from CdS quantum dots *via* AGET ATRP in miniemulsion. *Small* 2007,3,1230–1236.
- [53] Matsuno, R.; Yamamoto, K.; Otsuka, H.; Takahara, A. Polystyrene- and poly(3-vinylpyridine)-grafted magnetite nanoparticles prepared through surface-initiated nitoxide-mediated radical polymerization. *Macromolecules* 2004,37,2203–2209.

REFERENCES

- [54] Carrot, G.; Rutot-Houzé, D.; Pottier, A.; Degée, P.; Hilborn, J.; Dubois, P. Surface-initiated ring-opening polymerization: A versatile method for nanoparticle ordering. *Macromolecules* 2002,35,8400–8404.
- [55] Skaff, H.; Ilker, M. F.; Coughlin, E. B.; Emrick, T. Preparation of cadmium selenide-polyolefin composites from functional phosphine oxides and ruthenium-based metathesis. *J. Am. Chem. Soc.* 2002,124,5729–5733.
- [56] Zhou, Q.; Wang, S.; Fan, X.; Advincula, R. Living anionic surface-initiated polymerization (LASIP) of a polymer on silica nanoparticles. *Langmuir* 2002,18,3324–3331.
- [57] Karg, M.; Jaber, S.; Hellweg, T.; Mulvaney, P. Surface plasmon spectroscopy of gold-poly-N-isopropylacrylamide core-shell particles. *Langmuir* 2010,27,820–827.
- [58] Karg, M.; Schelero, N.; Oppel, C.; Gradzielski, M.; Hellweg, T.; von Klitzing, R. Versatile phase transfer of gold nanoparticles from aqueous media to different organic media. *Chem. Eur. J.* 2011,17,4648–4654.
- [59] Skaff, H.; Emrick, T. The use of 4-substituted pyridines to afford amphiphilic, pegylated cadmium selenide nanoparticles. *Chem. Commun.* 2003,1,52–53.
- [60] Kim, J. S.; Kuk, E.; Yu, K. N.; Kim, J. H.; Park, S. J.; Lee, H. J.; Kim, S. H.; Park, Y. K. Antimicrobial effects of silver nanoparticles. *Nanomedicine: Nanotechnology, Biology and Medicine* 2007,3,95–101.
- [61] Beek, W. J. E.; Wienk, M. M.; Janssen, R. A. J. Efficient hybrid solar cells from zinc oxide nanoparticles and conjugated polymer. *Adv. Mater.* 2004,16,1009–1013.
- [62] Günes, S.; Fritz, K. P.; Neugebauer, H.; Sariciftci, N. S.; Kumar, S.; Scholes, G. D. Hybrid solar cells using PbS nanoparticles. *Sol. Energ. Mat. Sol. C.* 2007,91,420–423.

-
- [63] Robel, I.; Subramanian, V.; Kuno, M.; Kamat, P. V. Quantum dot solar cells. Harvesting light energy with CdSe nanocrystals molecularly linked to mesoscopic TiO₂ films. *J. Am. Chem. Soc.* 2006,128,2385–2393.
- [64] Rizvi, S. B.; Ghaderi, S.; Keshtgar, M.; Seifalian, A. M. Semiconductor quantum dots as fluorescent probes for in vitro and in vivo bio-molecular and cellular imaging. *Nano Rev.* 2010,1,5161–5176.
- [65] Njuguna, J.; Pielichowski, K. Polymer nanocomposites for aerospace applications: Fabrication. *Adv. Eng. Mater.* 2004,6,193–203.
- [66] Ebina, T.; Mizukami, F. Flexible transparent clay films with heat-resistant and high gas-barrier properties. *Adv. Mater.* 2007,19,2450–2453.
- [67] Hao, C.; Zhao, Y.; He, A.; Zhang, X.; Wang, D.; Ma, Q. Investigation on the melt spinning fibers of PP/ organoclay nanocomposites prepared by *in-situ* polymerization. *J. Appl. Polym. Sci.* 2010,116,1384–1391.
- [68] Erdem, N.; Cireli, A. A.; Erdogan, U. H. Flame retardancy behaviors and structural properties of polypropylene/ nano-SiO₂ composite textile filaments. *J. Appl. Polym. Sci.* 2009,111,2085–2091.
- [69] Chae, D. W.; Kim, B. C. Characterization on polystyrene/ zinc oxide nanocomposites prepared from solution mixing. *Polym. Adv. Technol.* 2006,16,846–850.
- [70] Hall, D. B.; Underhill, P.; Torkelson, J. M. Spin coating of thin and ultrathin polymer films. *Polym. Eng. Sci.* 1998,38,2039–2045, 1998.
- [71] Mehrotra, V.; Giannelis, E. P. Conducting molecular multilayers: intercalation of conjugated polymers in layered media. *Mater. Res. Soc. Symp. Proc.* 1990,171,39–44.
- [72] Vaia, R. A.; Giannelis, E. P. Polymer melt intercalation in organically-modified layered silicates: model predictions and experiment. *Macromolecules* 1997,30,8000–8009.

REFERENCES

- [73] Xie, X.-L.; Liu, Q.-X.; Li, R. K.-Y.; Zhou, X.-P.; Zhang, Q.-X.; Yu, Z.-Z.; Mai, Y.-W. Rheological and mechanical properties of PVC/CaCO₃ nanocomposites prepared by in situ polymerization. *Polymer* 2004,45,6665–6673.
- [74] Cheng, Y.; Lü, C.; Lin, Z.; Liu, Y.; Guan, C.; Lü, H.; Yang, B. Preparation and properties of transparent bulk polymer nanocomposites with high nanophase contents. *J. Mater. Chem.* 2008,18,4062–4068.
- [75] Clayton, L. M.; Sikder, A. K.; Kumar, A.; Cinke, M.; Meyyappan, M.; Gerasimov, T. G.; Harmon, J. P. Transparent poly(methyl methacrylate)/ single-walled carbon nanotube (PMMA/ SWNT) composite films with increased dielectric constants. *Adv. Funct. Mater.* 2005,15,101–106.
- [76] Lü, C.; Cheng, Y.; Liu, Y.; Liu, F.; Yang, B. A facile route to ZnS-polymer nanocomposite optical materials with high nanophase content via gamma-ray irradiation initiated bulk polymerization. *Adv. Mater.* 2006,18,1188–1192.
- [77] Podsiadlo, P.; Kaushik, A. K.; Arruda, E. M.; Waas, A. M.; Shim, B. S.; Xu, J. Ultrastrong and stiff layered polymer nanocomposites. *Science* 2007,318,80–83.
- [78] Dai, J.; Bruening, M. L. Catalytic nanoparticles formed by reduction of metal ions in multilayered polyelectrolyte films. *Nano Lett.* 2002,2,497–501.
- [79] Palkovits, R.; Althues, H.; Rumpelcker, A.; Tesche, B.; Dreier, A.; Holle, U.; Fink, G.; Cheng, C. H.; Shantz, D. F.; Kaskel, S. Polymerization of w/o microemulsions for the preparation of transparent SiO₂/PMMA nanocomposites. *Langmuir* 2005,21,6048–6053.
- [80] Flory, P. J. Thermodynamics of high polymer solutions. *J. Chem. Phys.* 1942,10,51–61.
- [81] Huggins, M. L. Some properties of long-chain compounds. *J. Phys. Chem.* 1942,46,151–158.

-
- [82] Hooper, J. B.; Schweizer, K. S. Theory of phase separation in polymer nanocomposites. *Macromolecules* 2006,39,5133–5142.
- [83] Lu, Y.; Yang, W.; Yin, M. Facile synthesis of fluorescent silica-doped polyvinylpyrrolidone composites: From cross-linked composite film to core-shell nanoparticles. *Ind. Eng. Chem. Res.* 2014,53,2872–2877.
- [84] Dukes, D.; Li, Y.; Lewis, S.; Benicewicz, B.; Schadler, L.; Kumar, S. K. Conformational Transitions of Spherical Polymer Brushes: Synthesis, Characterization, and Theory. *Macromolecules* 2010,43,1564–1570.
- [85] Milner, S. T. Polymer brushes. *Science* 1991,251,905–914.
- [86] Okada, A.; Usuki, A. Twenty years of polymer-clay nanocomposites. *Macromol. Mater. Eng.* 2006,291,1449–1476.
- [87] Ahmad, S.; Agnihotry, S. A.; Ahmad, S. Nanocomposite polymer electrolytes by in situ polymerization of methyl methacrylate: For electrochemical applications. *J. Appl. Polym. Sci.* 2008,107,3042–3048.
- [88] Macanás, J.; Parrondo, J.; Munoz, M.; Alegret, S.; Mijangos, F.; Muraviev, D. N. Preparation and characterisation of metal-polymer nanocomposite membranes for electrochemical applications. *Phys. Stat. Sol. A* 2007,204,1699–1705.
- [89] Agarwal, S.; Khan, M. M. K.; Gupta, R. K. Thermal conductivity of polymer nanocomposites made with carbon nanofibers. *Polym. Eng. Sci.* 2008,48,2474–2481.
- [90] Li, S.; Toprak, M. S.; Jo, Y. S.; Dobson, J.; Kim, D. K.; Muhammed, M. Bulk synthesis of transparent and homogenous polymeric hybrid materials with ZnO quantum dots and PMMA. *Adv. Mater.* 2007,19,4347–4352.
- [91] Heffels, W.; Friedrich, J.; Darribère, C.; Teisen, J.; Interewicz, K.; Bastiaansen, C. Polymers and metals: nanocomposites and complex salts with metallic chain structure. *Recent Res. Devel. Macromol. Res.* 1997,2,143–156.

REFERENCES

- [92] Chan, W. C. W.; Nie, S. Quantum dot bioconjugates for ultrasensitive nonisotopic detection. *Science* 1998,281,2016–2018.
- [93] Guo, X. H.; Deng, Y. H.; Gu, D.; Che, R. C.; Zhao, D. Y. Synthesis and microwave absorption of uniform hematite nanoparticles and their core-shell mesoporous silica nanocomposites. *J. Mater. Chem.* 2009,19,6706–6712.
- [94] Chen, Y. J.; Gao, P.; Zhu, C. L.; Wang, R. X.; Wang, L. J.; Cao, M. S. Synthesis, magnetic and electromagnetic wave absorption properties of porous Fe₃O₄/Fe/SiO₂ core/shell nanorods. *J. Appl. Phys.* 2009,106,054303–054304.
- [95] Zimmermann, L.; Weibel, M.; Caseri, W.; Suter, U. W.; Walter, P. Polymer nanocomposites with "ultralow" refractive index. *Polym. Adv. Technol.* 1993,4,1–7.
- [96] Weibel, M.; Caseri, W.; Suter, U. W.; Kiess, H.; Wehrli, E. Preparation of polymer nanocomposites with "ultrahigh" refractive index. *Polym. Adv. Technol.* 1991,2,75–80.

4 Facile large-scale synthetic route to monodisperse ZnO nanocrystals

Sascha Ehlert,^{*} Thomas Lunkenbein,[#] Josef Brey,[#] and Stephan Förster^{*}

^{*} Physical Chemistry I, University of Bayreuth, Germany,

[#] Inorganic Chemistry I, University of Bayreuth, Germany

Published in: Colloids and Surfaces A: Physicochem. and Eng. Aspects
444 (2014) 76-80

Keywords: zinc oxide, nanoparticles, large-scale synthesis

Abstract

We report an efficient, robust and up-scalable synthetic route to small, spherical, well-stabilized, narrow disperse, crystalline ZnO nanoparticles. The synthesis utilizes Zn-oleate or Zn-stearate as precursors, which are hydrolyzed in polar organic solvents to obtain ZnO nanoparticles in diameters in the range of 3 – 5 nm on multi-gram scales. The synthesis exploits the use of oleates and stearates as good precursors and stabilizing agents together with the hydrolysis route to obtain small ZnO nanoparticles in a well-controlled way. The nanoparticles show the characteristic bright green fluorescence emission, and can be precipitated, dried, and redispersed in common organic solvents without aggregation. Because of their good steric stabilization and hydrophobic coating, these nanoparticles are very suitable for applications in polymer nanocomposites for UV-absorption and opto-electronic applications.

Introduction

Zinc oxide nanoparticles have great potential as photoluminescent semiconductors with a wide range of applications in solar energy conversion, photocatalysis, bio-labeling, UV-blockings, and electro-optical devices.^[1] Many of these applications depend on a reproducible synthesis of luminescent ZnO nanoparticles on larger scales without aggregation. The latter point is par-

ticularly important, since aggregation is a major factor prohibiting their use particular in biomedical and opto-electronic applications.

Synthetic routes to ZnO nanoparticles involve either the thermolysis of zinc complexes in high boiling solvents, or the hydrolysis of zinc complexes in alcohols.^[1, 2] An example for the hydrolytic decomposition is the still most commonly used route developed by Spanhel and Anderson.^[3] In their classical procedure zinc acetate is dissolved in ethanol, heated, and then reacted with LiOH at room temperature. The primary product are a green-emitting ZnO nanoparticles with weakly stabilizing acetate surface groups. The purification of the ZnO nanoparticles requires precipitation and drying, which usually leads to nanoparticle aggregation, noticeable by a change of the emission from green to yellow. Drying of the precipitate often produces powders of aggregated particles with weak yellow emission. The classical procedure has been investigated in detail with regard to variations in temperature, water content, acetate concentration, and washing conditions and optimized to obtain more narrow size distributions.^[4] Recent modifications involved microwave- and ultra-sound assisted methods, the latter allowing facile doping of ZnO nanoparticles to vary their optical properties.^[6, 7] Improvements concerning nanoparticle stability have been reported by Guo et al. who used a zinc acetate/NaOH route in the presence of poly(vinyl pyrrolidone) (PVP) as a stabilizing agent to prevent nanoparticle agglomeration.^[5]

Recent investigations of the thermal decomposition route yielded ZnO nanoparticles with narrow size distribution by dissolution and subsequent thermolysis of a zinc carboxylates (cyclohexanbutyrate, acetate) in DMSO or DMF, albeit with only weak stabilization of the nanoparticle against aggregation.^[8] Motivated by successes of using oleates in hot-injection route to nanoparticles,^[10] Li et al. investigated the thermolysis of zinc oleate in high-boiling solvents (octadecene, octylether) and reported the formation of uniform-sized hexagonal crystalline ZnO nanoparticles with sizes of 10 nm and larger.^[9]

This indicates that zinc-oleate complexes are very suitable precursor materials for the synthesis of ZnO nanoparticles, because they can be readily prepared and provide excellent stabilizing properties for the nanoparticles. However, to yield very small, monodisperse crystalline nanoparticles, the hy-

drolysis route seems much more suitable. Since oleates are inexpensive precursor materials, which could possibly even be substituted by the still less expensive commercially available stearates, there might be the potential to synthesize narrow disperse, well stabilized and redispersable ZnO nanoparticles in multi-gram quantities suitable for applications particularly in polymer nanocomposites and opto-electronics.

Experimental Section

Materials

All chemicals were used as received, which include zinc chloride (ZnCl_2 , Grüssing GmbH, 98%), sodium oleate (TCI Europe, >97.0%), tetrahydrofuran (THF, Sigma-Aldrich, 99,9%), tetrabutylammonium hydroxide (TBAH, Alfa Aesar, 1M in methanol), LiOH (Applichem, p.A.), potassium hydroxide (KOH, Sigma-Aldrich, 90%), sodium hydroxide (NaOH, Merck, p.A.) and zinc stearate (Sigma-Aldrich, technical)

Synthesis

The following procedure yields spherical ZnO nanocrystals with a typical diameter of 3-5 nm. The zinc-oleate precursor was prepared by reacting ZnCl_2 and sodium-oleate. To a solution of 12.16 g (40 mmol) sodium-oleate in 75 mL water a solution of 2.73 g (20 mmol) ZnCl_2 in 75 mL water was added. The resulting precipitate was filtered, washed with water, dried and dissolved in THF. In the subsequent nanoparticle synthesis 0.5 g (0.8 mmol) of zinc oleate was dissolved in 15 mL THF. To this solution 0.8 mL (0.8 mmol) of the TBAH solution was added. The resulting mixture was heated to 50 °C overnight. After cooling to room temperature an excess of ethanol was added and the white precipitate was collected by centrifugation at 3250 g. The precipitate was redispersible in different organic solvents including THF, chloroform and toluene. To remove remaining traces of reactants another precipitation and centrifugation step is advisable. As zinc precursor, the oleate can be replaced by the commercially available stearate. The TBAH can be replaced by different hydroxides such as LiOH, NaOH or KOH with a slight loss of the

uniformity. If the TBAH was replaced by the alkali hydroxides, 30 minutes of sonification were necessary for complete dissolution prior to the heating. The synthesis could be scaled up to an initial amount of zinc oleate of 40 g (63.7 mmol), resulting in 4.75 g yield of oleic acid stabilized 3 nm nanocrystals.

Characterization

The ZnO nanocrystals were characterized by transmission electron microscopy (TEM), powder X-ray diffraction (XRD), UV/Vis absorption, photoluminescence and dynamic light scattering (DLS). TEM images were obtained on a Zeiss 922 Omega microscope. X-ray diffraction patterns were obtained with a XPERT-PRO, (PANalytical B.V.) equipped with an X'Celerator Scientific RTMS detector. The UV/Vis spectra were measured using an Agilent 8453 and for the photoluminescence spectra a Jasco FP 6500. For the DLS measurements a Malvern Zetasizer Nano SZ were used.

Results and Discussion

For the synthesis of the nanoparticles, zinc oleate is prepared by mixing an aqueous solution of ZnCl_2 with sodium oleate, from which the zinc oleate precipitates. The ZnO nanoparticles are then synthesized from a zinc oleate solution in THF by hydrolysis with tetrabutylammonium hydroxide (TBAH). The obtained ZnO nanoparticles are well stabilized by the oleate ligands, such that they can be precipitated in ethanol or methanol, dried, and redispersed in common organic solvents (THF, toluene, chloroform). The synthesis can be easily upscaled. For the present work and for applications in polymer nanocomposites amounts of ca. 5 g per batch were routinely synthesized (Figure 1).

The synthesis can be further simplified by using commercially available zinc stearate as a precursor material, and LiOH, NaOH, or KOH as hydrolytic agents. These precursor materials yield slightly more polydisperse, but also well stabilized ZnO nanoparticles. The size, quality and properties of the nanoparticle depend only very minor on variations in temperature, concentration and stoichiometry of precursors and ligands. Thus it is a very ro-

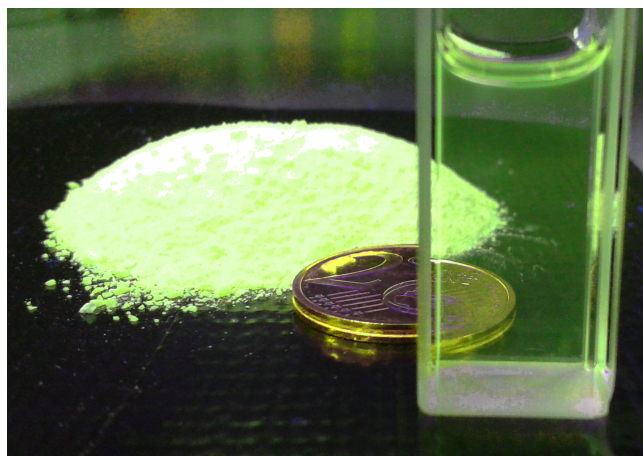


Figure 1: Optical image of ca. 5 g of ZnO nanoparticles synthesized in one batch together with a dilute solution (1mg/ml) of ZnO nanoparticles dissolved in THF under UV light. The bright green fluorescence can well be observed.

bust synthetic procedure to yield 3-5 nm size ZnO nanoparticles. The crystallinity of the obtained ZnO nanoparticles was investigated by TEM and X ray diffraction (XRD). The interplanar spacing of 0.3 nm as obtained from the TEM-image in Fig. 2B is in good agreement with the published value of 0.325 nm. The powder pattern (Figure 2A) shows the typical size-broadened reflections from wurtzite-type ZnO.

The optical properties of the ZnO nanoparticles were investigated by UV/Vis- and fluorescence spectroscopy. The UV/Vis spectrum in Figure 2C shows an absorption edge onset at 360 nm for the ZnO nanocrystals, which corresponds well to a diameter of 5.0 nm,^[11] and which is close to the absorption threshold for macrocrystalline ZnO.^[12] The emission spectrum shows a weak UV emission at 380 nm corresponding to the exciton fluorescence and the characteristic strong green-yellow ZnO emission at 550 nm, which is due to trapped anion surface states.^[12] The size distribution of the ZnO nanoparticles was determined by dynamic light scattering in THF as a solvent, and is shown in Figure 2D. The measured hydrodynamic diameter of 9.0 nm is in good agreement with 5 nm diameter ZnO nanocrystals having a layer of oleic acid of approximately 2 nm thickness.^[13] The measured relative polydispersity

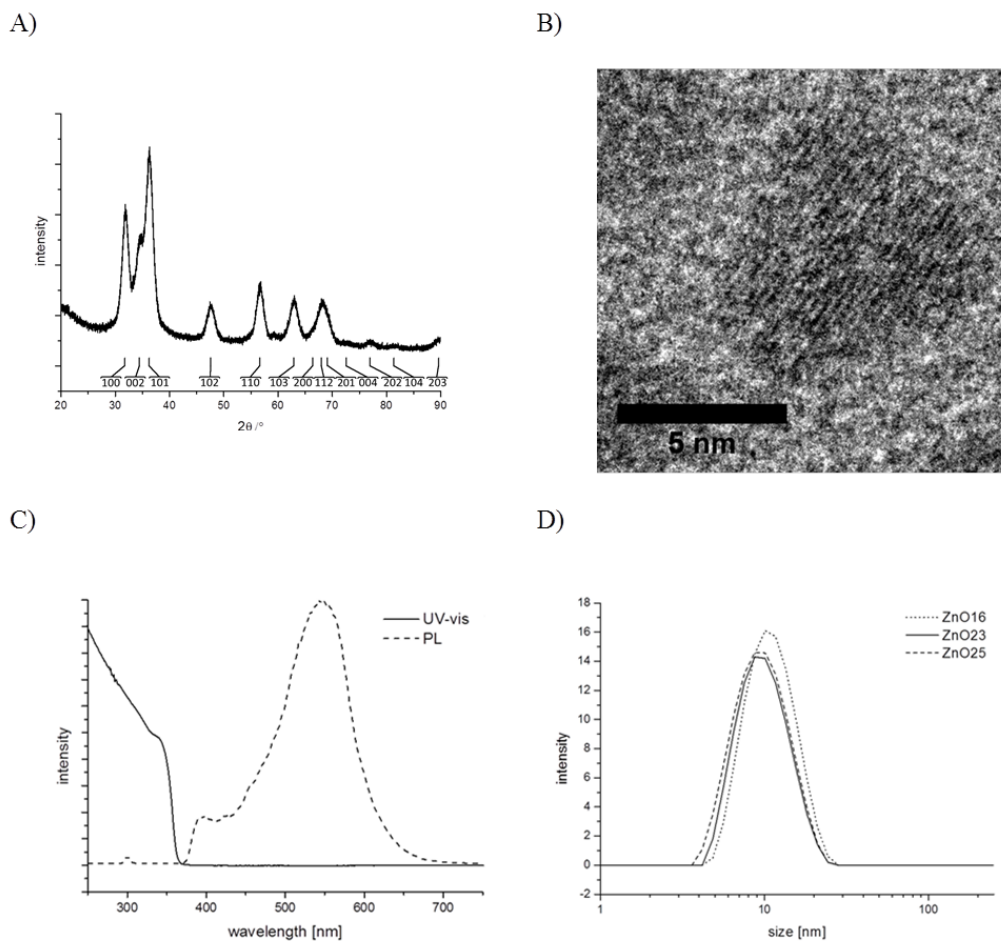


Figure 2: (A) Typical XRD pattern of 5 nm ZnO nanocrystals. The vertical lines indicate the expected positions for the ZnO wurtzite hexagonal crystal structure. (B) TEM image of 5 nm ZnO nanocrystals. (C) UV/Vis-absorption and photoluminescence spectrum of 5 nm ZnO nanocrystals. (D) DLS measurements of 5 nm ZnO nanocrystals. The solid line shows the size distribution of the nanocrystals obtained according to the standard synthesis described below, the dashed line after the standard synthesis scaled up by a factor of 100, and the dotted line according to a synthesis with three times the amount of hydroxide.

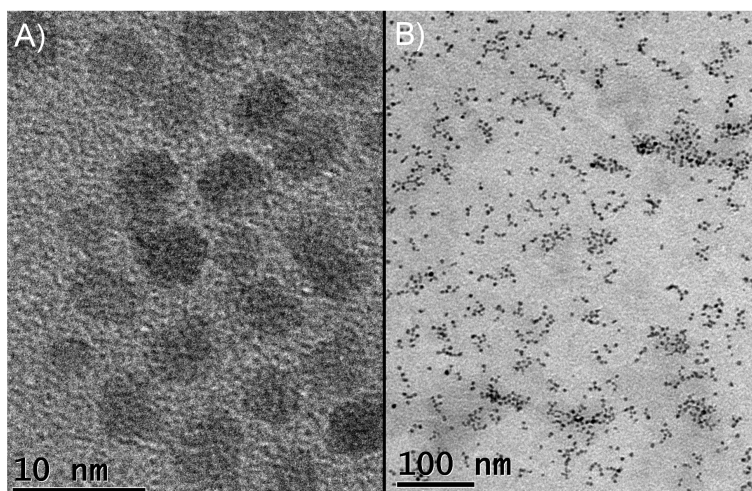


Figure 3: TEM images of 5 nm ZnO nanoparticles at high (A) and low (B) magnification.

is 0.09. The size and shape of the nanoparticles was further characterized by transmission electron microscopy. As shown in Figure 3, the obtained nanoparticles are nearly spherical in shape, and have a narrow size distribution. The oleic acid layer is not visible because of its low contrast.

If the TBAH was replaced by another hydroxide (LiOH, NaOH or KOH) the TEM images show that the obtained ZnO nanocrystals were slightly more polydisperse (Figure 4). For temperatures between 30 and 66C, concentrations between equimolar and three times excess of hydroxide as well as ageing times from 12 to 94 hours there are little or no effects on particle sizes and polydispersity. The small influence of external factors like temperature, hydroxide excess and ageing time is due to the fact the ratio of precursor and capping agent is always constant. This is the case because the capping agent is always produced in proportion to the Zn-precursor during degradation of the oleate complex. Since the final size of the nanoparticles is solely determined by this ratio, as shown by the work of Searson^[14], there is hardly any influence of other experimental factors.

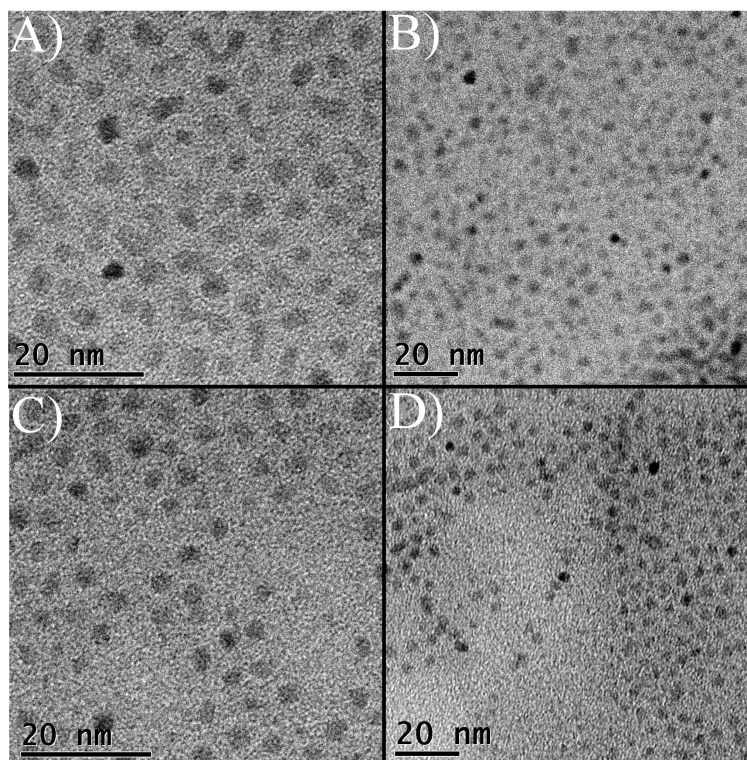


Figure 4: TEM images of ZnO nanocrystals between 3 and 5 nm hydrolyzed by LiOH (A); NaOH (B); KOH (C); ZnO nanocrystals with zinc stearate as precursor and TBAH as hydroxide (D)

Conclusions

By using zinc oleate or zinc stearate as precursors, hydrolysis yields well-stabilized, crystalline, fluorescent, narrow disperse zinc oxide nanoparticles in the size range of 3-5 nm on scales of several grams per batch. The obtained nanoparticles can be precipitated, dried, and redispersed in common organic solvents without aggregation. Because of their good steric stabilization and hydrophobic coating, these nanoparticles are very suitable for applications in polymer nanocomposites for UV-absorption and opto-electronic applications.

Acknowledgements

We thank Markus Drechsler for help with transmission electron microscopy. Financial support for the DFG within the SFB 840, TP B9, is gratefully

acknowledged.

References

- [1] S.-H. Choi, E.-G. Kim, J. Park, J. K. An, N. Lee, S.C. Kim, T. Hyeon, *J. Phys. Chem. B* 109, (2005), 14792.
- [2] L. Chen, J. Xu, J.D. Holmes, M.A. Morris, *J. Phys. Chem. C* 114, (2010), 2003.
- [3] L. Spanhel, M.A. Anderson, *J. Am. Chem. Soc.* 113, (1991), 2826.
- [4] E.A. Meulenkamp, *J. Phys. Chem. B* 102, (1998), 5566.
- [5] L. Guo, S. Yang, C. Yang, P. Yu, J. Wang, W. Ge, G.K.L. Wong, *Appl. Phys. Lett.* 74, (1999), 2939.
- [6] I. Bilecka, P. Elser, M. Niederberger, *ACS Nano* 3, (2009), 467.
- [7] H.-M. Xiong, D.G. Shchukin, H. Möhwald, Y. Xu, Y.-Y. Xia, *Angew. Chem.* 48, (2009), 2727.
- [8] G. Rodriguez-Gattorno, P. Santiago-Jacinto, L. Rendon-Vazquez, J. Nemeth, I. Dekany, D. Diaz, *J. Phys. Chem. B* 107, (2003), 12597.
- [9] C.-S. Li, Y.-N. Li, Y.-L. Wu, B.S. Ong, R.O. Loutfy, *Sci. China Ser. E - Tech. Sci.* 51, (2008), 2075.
- [10] J. Park, J. Joo, S.G. Kwon, Y. Jang, T. Hyeon, *Angew. Chem. Int. Ed.* 46, (2007), 4630.
- [11] D. Sun, H.-J. Sue, N. Miyatake, *J. Phys. Chem. C* 112, (2008), 16002.
- [12] U. Koch, A. Fojtik, H. Weller, A. Henglein, *Chem. Phys. Lett.* 122, (1985), 507.
- [13] C. Schliehe, B. H. Juarez, M. Pelletier, S. Jander, D. Greshnykh, M. Nagel, A. Mayer, S. Foerster, A. Koronowski, C. Klinke, H. Weller, *Science* 329, (2010), 550.

REFERENCES

- [14] E. M. Wong, P. G. Hoertz, C. J. Liang, B.-M. Shi, G. J. Meyer, P. C. Searson, *Langmuir* 17, (2001), 8362.

5 Polymer Ligand Exchange to Control Stabilization and Compatibilization of Nanocrystals

Sascha Ehlert,[†] Sara Mehdizadeh Taheri,[†] Daniela Pirner,[†] Markus Drechsler,[§] Hans Werner Schmidt,^{‡§} Stephan Förster^{*†§}

[†] Physical Chemistry I, University of Bayreuth, Germany

[‡] Macromolecular Chemistry I, University of Bayreuth, Germany

[§] Bayreuther Institut für Makromolekülforschung and Bayreuther Zentrum für Kolloide Grenzflächen, University of Bayreuth, Germany

Published in: ACS Nano 8 (2014) 6114-6122

Keywords

nanocomposites, nanoparticles

Abstract

We demonstrate polymer ligand exchange to be an efficient method to control steric stabilization and compatibilization of nanocrystals. A rational design of polymer binding groups and ligand exchange conditions allows to attach polymer brushes with grafting densities $> 1 \text{ nm}^{-2}$ to inorganic nanocrystals for nearly any nanocrystal/polymer combination using only a few types of binding groups. We demonstrate the potential of the method as an alternative to established grafting-from and grafting-to routes in considerably increasing the stabilization of inorganic nanocrystals in solution, to prepare completely miscible polymer nanocomposites with a controllable distance between nanoparticles, and to induce and control aggregation into percolation networks in polymeric matrices for a variety of different nanocrystal/polymer combinations. A dense attachment of very short polymer ligands is possible enabling to prepare ordered nanoparticle monolayers with a distance or pitch of only 7.2 nm, corresponding to a potential magnetic storage density of 12.4 Tb/in². Not only end-functionalized homopolymers, but also commercially available copolymers with functional comonomers can be used for

stable ligand exchange, demonstrating the versatility and broad potential of the method.

Introduction

Nanocrystals and polymer nanocomposites are of immense interest in fundamental research as well as in a large variety of industrial applications. As an example, semiconductor nanocrystals (quantum dots) are used in medical applications as fluorescent tags,^[1, 2] as LEDs^[1, 2] or tunable lasers^[1, 2] in optical applications, or for energy conversion in photovoltaic cells.^[6, 7, 8] Magnetic nanocrystals find applications as contrast agents in magnetic resonance imaging,^[9] or metal nanoparticles in catalytic applications.^[10] The stability of nanocrystals in solution is crucial to prevent agglomeration with loss of functionality. The combination of nanocrystals and a polymer matrix leads to nanocomposites. These composites could have enhanced mechanical,^[11] optical^[12] or electrical^[13] properties, but uncontrolled agglomeration often prevents the enhancement and even deteriorates many useful properties. Therefore it is of great importance to avoid or, even better to control the agglomeration of nanocrystals.

The most common way to efficiently stabilize nanocrystals against agglomeration is to cover them with a polymeric brush. Such sterically stabilized particles are known to form stable colloidal solutions^[14] or, if the polymer brush is compatible with a polymer matrix, to form well dispersed nanocomposites.^[15] There are two established approaches to form a polymer brush on a surface. The first approach is the grafting-from method. By this method the polymer is grown from initiator groups which have been covalently linked to the nanocrystal surface^[16] to obtain a covalently bound polymer layer. The polymer density depends on the grafting density of the initiator groups. The grafting-from method allows a variety of different polymerization types such as radical, anionic and cationic polymerization. Because of the covalent bond of the polymer a grafting density of 0.4 nm^{-2} is sufficient to stabilize nanocrystals.^[17] A drawback of this method is the need to develop a new initiator coupling reaction scheme for each new nanocrystal-polymer com-

ination. Further, there is no straightforward way to control nanocrystal agglomeration, if this would be desired.

The second approach is the grafting-to method. This method has the advantage that polymers could be presynthesized with established polymerization procedures for a state-of-the-art control of composition, architecture, and polydispersity. The preformed polymer will be covalently bound to the nanocrystals by a chemical reaction between a functional end group of the polymer and a functional group at the nanocrystal surface.^[18] Again, a drawback is the need to establish new functional group linking schemes for each new nanocrystal-polymer combination. In addition, a control of agglomeration cannot easily be achieved, and due to steric repulsion of the attached polymer chains, high grafting densities are hard to reach.

A concept to work around establishing new covalent linker chemistries is to coat nanocrystals with a shell of silica, for which covalent attachment schemes for initiators and covalent binding groups have been well established.^[19, 20, 21] However, this requires to develop and optimize new nanocrystal-silica core/shell-growth procedures, which is not a trivial task. Therefore a versatile method that would allow stable, high-density polymer attachment for a large variety of nanocrystal-polymer combinations would be highly desirable.

A possible approach could be based on the exchange of nanocrystal surface ligands. State-of-the-art methods to prepare inorganic nanocrystals^[22] yield nanoparticles that are stabilized by alkyl phosphines, amines or carboxylic acids. These groups have proven to be most efficient in controlling nanocrystal growth during synthesis, and to provide stability of the final particles in solution. The exchange of these surface ligands with polymers could be an attractive route for a flexible and versatile polymer attachment. So far, the exchange of coordinating surfactants has been only reported for short organic molecules^[23] and thiol-functionalized polymers.^[24, 25] The exchange with short organic molecules is mostly used to attach new functional groups to the nanocrystal surface or to transfer the nanocrystals into another solvent.^[26, 27, 28] The exchange with thiol groups is specifically used for gold nanocrystals because of the high affinity of gold to thiols, providing bonding that is nearly as strong as a covalent bond.

Here, we outline a polymer ligand exchange method which is broadly applicable to stabilize a large variety of different nanocrystal-polymer combinations. It is based on coordinative surface binding, which is successfully used in nanocrystal synthesis. We demonstrate the versatility of this ligand exchange method for the preparation of a variety of different polymer brush stabilized nanocrystals and show the potential for solution stabilization, nanocomposite compatibility, nanoparticle distance control to sub-10 nm pitch structures, and the controlled agglomeration to form percolation networks.

Results and Discussion

Thermodynamic considerations.

The coordinative ligand exchange can be thermodynamically described by a reaction $NP-L1+L2 \rightleftharpoons NP-L2+L1$, where $NP-L1$ are the nanocrystals (NP) coated with the original low-molecular weight ligand $L1$, and $NP-L2$ are the nanocrystals coated with the desired polymer ligand $L2$. From the law of mass action it follows that the concentration of the desired polymer-coated ligand is given by

$$[NP-L2] = K \frac{[NP-L1][L2]}{[L1]} \quad (1)$$

where K is the equilibrium binding constant. In order to achieve a high yield of $NP-L2$, one has to choose ligands with a large binding constant K , work with a large excess of polymer ligand $L2$, and remove the originally bound low-molecular weight ligand $L1$.

Ligands with suitable binding constants for ligand exchange procedures can be identified in a rational way by using Pearsons hard/soft acid/base (HSAB) principle. Most of the metals or metal ions in nanocrystals can be characterized as soft acids (Cd^{2+} , Ag^0 , Au^0) or as borderline acids (Fe^{2+} , Pb^{2+} , Zn^{2+}). Oxidic nanoparticles (ZnO , Fe_2O_3) can be considered as hard bases. Accordingly, the metals would best be coordinated by soft bases such as thiols, phosphines or phosphonates, or borderline bases such as pyridine. Hard

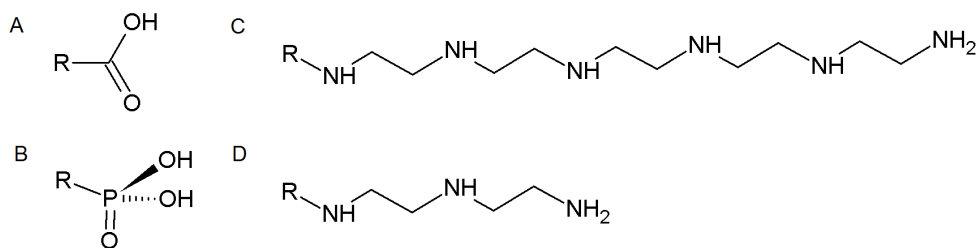


Figure 1: Suitable coordinating groups for polymer ligand exchange: (A) carboxylic acid (-COOH), (B) phosphonic acid (-PO(OH)₂), (C) pentaethylenhexamine (-PEHA), and (D) diethylenetriamine (-DETA). R represents the polymer chain, which in the present study comprises polystyrene (PS), poly(methyl methacrylate) (PMMA), and polyisoprene (PI).

bases would be best stabilized by hard acids, such as carboxylic acids. For a given ligand, the binding strength could be further increased by using multidentate ligands.

Not surprisingly, the above choice of ligands corresponds to the set of ligands which are used in the currently most efficient synthetic procedures of nanocrystals, e.g. by hot injection routes, where alkyl oleates (e.g. oleic acid), phosphines (e.g. trioctyl phosphine (TOP)), phosphonates (e.g. trioctylphosphine oxide (TOPO)) are commonly used to stabilize nanoparticles during synthesis.^[22]

An important issue when using polymeric ligands is to not use the ligands having the highest binding strength, but somewhat more moderate binding. A certain reversibility of surface coordination and decoordination is needed to obtain dense brush layers for sufficient steric stabilization of the nanocrystals in solution or compatibilization in polymer nanocomposites. This reversibility allows polymer chains to relocalize on the nanoparticle surface to facilitate attachment of further polymer chains to increase the brush density. The importance of chain relocalization on nanocrystal surfaces has been recently shown by HRTEM, and has a pronounced effect on the colloidal stability and aggregation.^[29]

In line with these considerations we observe that optimal for polymer ligand exchange procedures are (1) combinations of PbS-, Fe₃O₄-, ZnO- (borderline

acids Pb^{2+} , Fe^{2+} , Zn^{2+}) and CdSe-, Ag-nanoparticles (soft acids Cd^{2+} , Ag^0) with multidentate amines (hard bases) such as diethylenetriamine (DETA) or pentaethylenhexamine (PEHA), or (2) Fe_3O_4 -, ZnO-nanoparticles (hard bases) with the hard acid RCOOH . PEHA can nearly be considered a general purpose ligand, since it also very well stabilizes oxidic, hard base nanocrystals such as ZnO and Fe_3O_4 where it coordinates to the metal centers. The structure of the respective polymer ligands are shown in Figure 1. Polymers used as examples in the present work include polystyrene (PS), polyisoprene (PI), and poly(methyl methacrylate) (PMMA) in combination with the coordinating groups $-\text{COOH}$, $-\text{PEHA}$, or $-\text{DETA}$ to act as polymeric ligands $L2$. Many other polymers such as polyethylene (PE), poly-3-hexylthiophene (P3HT), and poly(ethylene oxide) will work as well.^[30] In principle, nearly every polymer which could be functionalized with one of the coordinating groups above should be suitable for the ligand exchange procedure. The same holds for the choice of nanocrystals, where in this work Ag-, Au-, CdSe-, PbS-, Fe_3O_4 -, and ZnO-nanoparticles are investigated.

The nanocrystals used in the present study were originally coated with oleic acid, since they were synthesized by thermal decomposition of their oleate complexes, an established state-of-the art procedure to prepare highly crystalline monodisperse nanocrystals in large quantities.^[22] For the ligand exchange procedures described below, the oleic acid $L1$ -coated nanocrystals were dissolved in a common solvent (THF) together with a large excess of the polymeric ligand $L2$. Generally we find that just mixing the components in dilute solution is insufficient to achieve complete polymer ligand exchange. We attribute this to the good steric stabilization provided by oleic acid ($L1$), which was chosen to bind sufficiently strong to limit the growth and stabilize the nanocrystals during their synthesis. Thus, in the sense of Equation (1) the concentrations $[\text{NP} - L1]$ and $[L2]$ must be considerably increased to achieve complete ligand exchange. We find that this can be accomplished by precipitating the nanoparticles and polymeric ligands *via* the addition of a common nonsolvent (ethanol) to bring nanoparticles (NP) and polymer ligands ($L2$) in direct contact thereby considerably increasing the local polymer segment density. This step is in the following termed quantitative precipita-

tion. As oleic acid ($L1$) is soluble in ethanol, this will simultaneously deplete ligand $L1$ from the mixture which further promotes ligand exchange. In a second step, the precipitate, a mixture of $NP - L2$, free polymeric ligand $L2$, and remaining amounts of oleic acid ($L1$), is redissolved in THF. To subsequently remove excess free polymeric ligand and remaining oleic acid, the $NP - L2$ nanoparticles undergo a selective precipitation by the stepwise addition of small amounts of the nonsolvent ethanol. The selective precipitation of $NP - L2$ in the presence of free polymeric ligand $L2$ is possible due to the low entropy of mixing of high molecular weight polymers. The entropy of mixing of polymers in solution is proportional to $1/N$, where N is the degree of polymerization. In our context, polymer-coated nanoparticles can be considered as very high molecular weight polymers with a much lower solubility compared to the free polymer chains. Thus they precipitate at much less nonsolvent content compared to the free polymer. This principle is the basis of established procedures for polymer fractionation. Depending on the desired purity of the $NP - L2$, each of the quantitative and selective precipitation can be repeated. The progress in removing ligands $L1$ and excess $L2$ can be monitored by thermo gravimetric analysis (TGA). The stability against aggregation in solution can be assessed by dynamic light scattering (DLS), and in the dry state by transmission electron microscopy (TEM).

Ligand exchange monitoring. As a first example for the ligand exchange procedure we describe the preparation of polystyrene (PS) brush coated CdSe nanocrystals with PS-PEHA as a polymer ligand ($L2$) starting from oleic acid coated nanocrystals. Grafting-from or grafting-to procedures to coat CdSe nanocrystals with polystyrene have been published, but are synthetically challenging^[26, 31] The polymer ligand exchange can conveniently be followed by thermo gravimetric analysis. The TGA-curves in Fig. 2 (A) show that already after the first quantitative precipitation the amount of oleic acid in the mixture has reduced to below 3wt% as deduced from the small decrease of the relative mass from 1.00 at 250 °C to 0.97 at 350 °C. The drop of the relative mass between 380 °C and 480 °C is due to the thermal degradation of the polystyrene chains. This is supported by reference measurements of

pure oleic-acid coated nanocrystals and pure polystyrene in the Supporting Information (Figure 8). As seen in Figure 2 (A), the solid nanoparticle content is 8% after the first quantitative precipitation, increasing to 13wt% after the second and to 14wt% after the third quantitative precipitation due to the removal of free unbound polystyrene chains. The excess of free polymer chains is considerably further reduced by selective precipitation, where the solid content increases to 22wt% and 28wt%, finally nearly saturating at 30wt%, indicating an almost complete removal of free polymer ligand.

With the mean diameter and the bulk density of the nanocrystals, the molecular weight of the polymer, and the ratio of polymer to nanocrystals from the TGA measurement a grafting density of 1.2 nm^{-2} can be calculated for the CdSe-polystyrene particles shown in Figure 2. This grafting density is much higher than the grafting densities reported for the covalent grafting-to and grafting-from methods.^[17] These high grafting densities can be explained with the mobility of the polymer chains on the particle surface due to the reversible coordinating and decoordination of the ligands, as illustrated in Figure3.

The obtained polymer-brush coated nanoparticles are well stabilized in solution and in bulk. The measured particle size distributions of oleic acid- and polystyrene-coated CdSe-nanoparticles dispersed in solution (Figure 2 (B)) show the increase of the hydrodynamic radius expected for the attachment of a spherical polymer brush, and no signs of agglomeration. TEM-images (Figure 2 (C,D)) show the increase of the interparticle distance after attachment of the polymer chains.

Increased solution stability. Also metal nanocrystals can be polymer brush-coated with polymers *via* the ligand exchange procedure. We investigated silver nanocrystals which are relevant for many applications where their unique plasmonic properties or their antibacterial properties are exploited. A specific issue for small (5 nm) silver nanoparticles is the lack of long-term stability in solution^[32] as shown in Figure 4. After 2 weeks in THF solution the nanocrystals have become polydisperse due to aggregation and

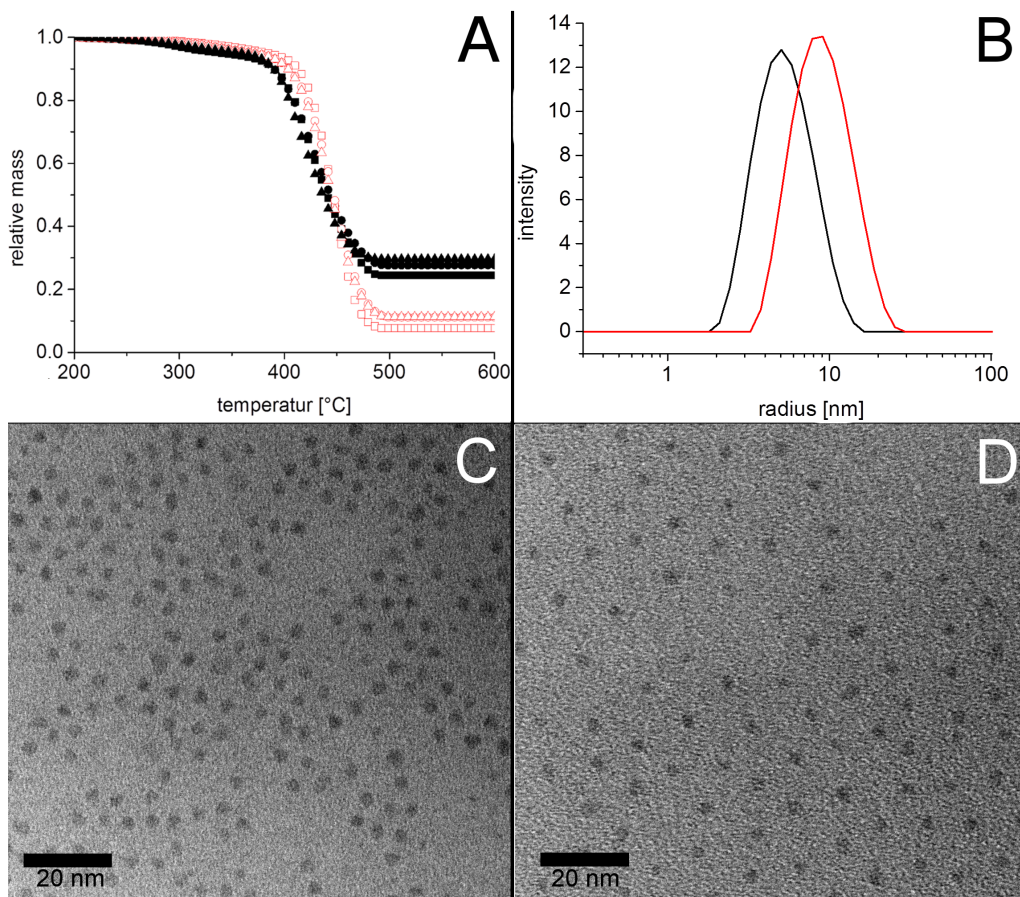


Figure 2: (A) TGA measurements of the ligand exchange steps (red = quantitative steps; black = selective steps; squares = step 1; circles = step 2; triangles = step 3). (B) Particle size distribution measured by DLS measurements in THF of 3 nm CdSe nanocrystals stabilized with oleic acid (black) and after ligand exchange with polystyrene-PEHA 2700 g/mol (red). TEM images of the CdSe nanocrystals with oleic acid (C) and with polystyrene-PEHA 2700 g/mol (D). The increased interparticle distance after coating with polystyrene is a clear indication of stable polymer brush binding.

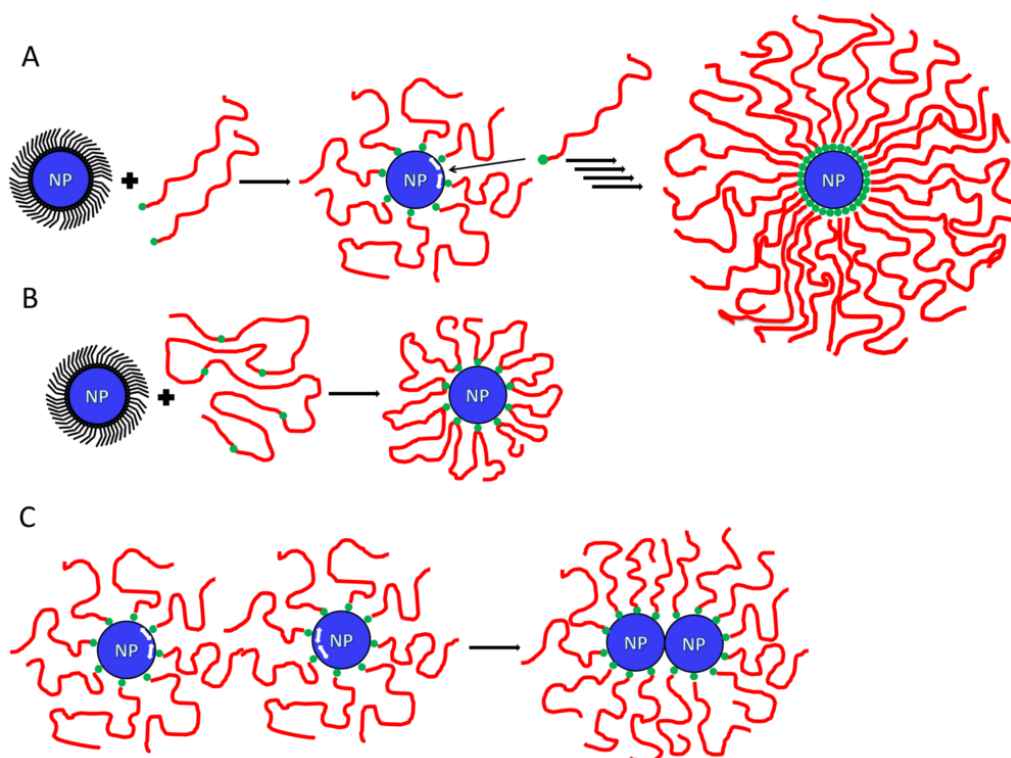


Figure 3: A scheme of (A): Nanocrystal coated with oleic acid (black), which is exchanged against a polymer (red) with a coordinating end-group (green). Because of the surface mobility of the end groups, bound polymer chains can relocate on the surface to facilitate attachment of further polymer chains to yield very high brush densities. (B) The possibility to employ copolymers as polymer ligands to obtain dense polymer brushes. (C): Relocalization of surface-bound polymer to allow controlled agglomeration into nanoparticle dimers, and subsequently chains and networks.

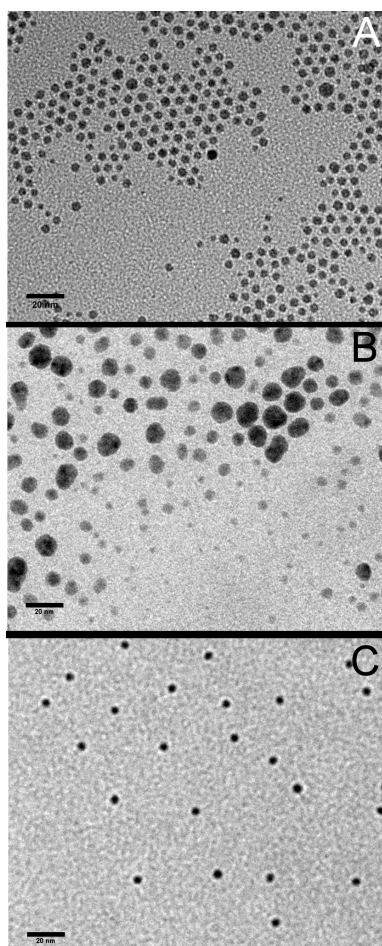


Figure 4: TEM images of silver nanocrystals (A) after synthesis with oleic acid as surfactant, (B) after 2 weeks in THF with oleic acid as surfactant and (C) after 2 weeks with a polystyrene (PS-DETA) brush in THF solution, prepared by the ligand exchange method (scale bars are 20nm).

fusion into larger nanoparticles. We found that the ligand exchange with PS(16k)-DETA yielded silver nanocrystals coated with a dense polystyrene brush which considerably improved steric stabilization. Even after several months there was no noticeable change of the size distribution of the silver nanocrystals.

Nanoparticle distance control. For many applications it is important to control the distance between nanocrystals on surfaces or in bulk, e.g. in magnetic storage layers to achieve high storage densities, or in the active matrix of hybrid solar cells to adjust the nanoparticle distance to the exciton diffusion length. Because of the high grafting density achievable by the ligand exchange method the polymer brushes are dense and homogeneous, resulting in a well-defined and controllable interparticle distance. The distance can be varied *via* the molecular weight of the polymer ligands. Figure 5 shows the example of iron oxide nanocrystals which were coated with PS-DETA and PS-PEHA with different molecular weights. For iron oxide nanoparticles also a covalent grafting-to/grafting-from method has been developed, which, however, is quite involved.^[33] As shown in Figure 5, we demonstrate that by adjusting the PS molecular weight, the center-to-center distances between the nanocrystals can not only be increased, but also decreased compared to the distance resulting from the original oleic acid layer. The smaller distance is remarkable, since it demonstrates the possibility to prepare polymer-stabilized nanocrystal assemblies with a distance or pitch smaller than 10 nm, in our case 7.2 nm, corresponding to a potential magnetic storage density of 12.4 Tb/inch², which is very high, and not possible with current state-of-the-art block copolymer templating procedures.^[34] This control over the distance is a very useful tool for the generation of nanocrystal superlattices.^[35]

As an example for a further nanocrystal-polymer combination we show in Figure 6(A) polyisoprene-coated PbS-nanocrystals obtained by ligand exchange with PI-PEHA. Polyisoprene is a viscous liquid, but the PI-coated nanocrystals are solid, indicating strong reinforcement of the nanocomposite due to the nanocrystals.

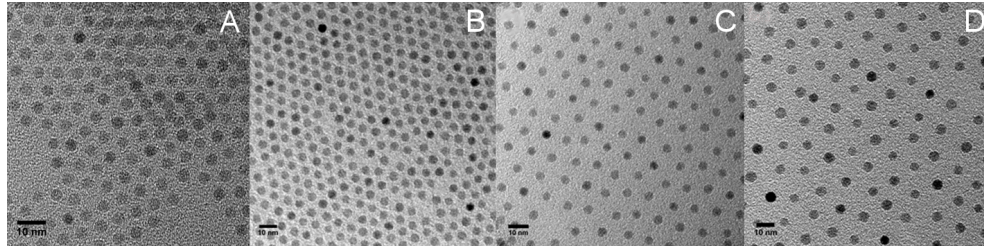


Figure 5: TEM images of 5nm Fe₃O₄ nanocrystals coated with (A) oleic acid, and polystyrene ligands of different molecular weights, i.e. (B) 1000 g/mol, (C) 3450 g/mol, and (D) 8450 g/mol (scale bars are 10 nm). We note the interparticle distance in (B) is smaller than that of oleic acid, with a distance below 10 nm (7.2 nm) which is relevant for magnetic storage layers.

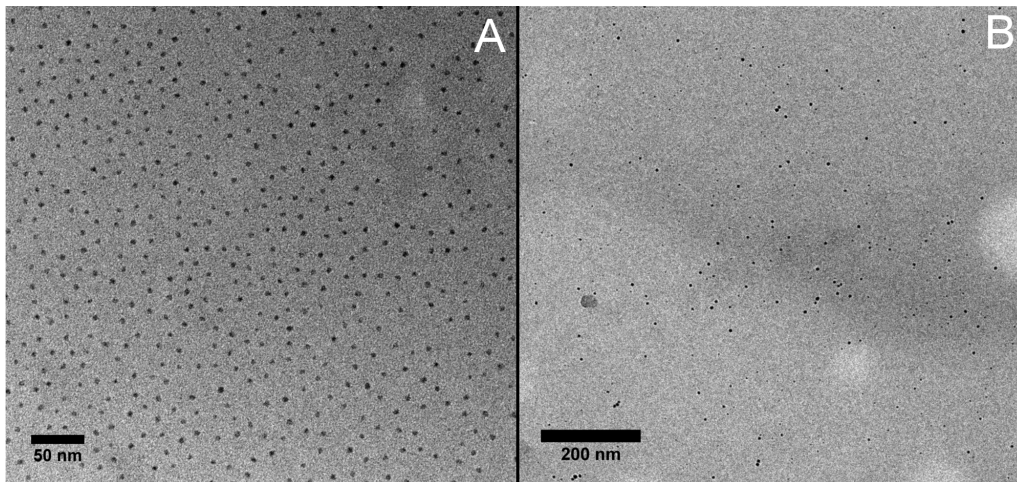


Figure 6: TEM images of 7nm PbS nanocrystals coated with polyisoprene (PI-PEHA) 15000 g/mol (A) and 15nm Ag-nanocrystals coated with PMMA-co-polymethacrylic acid (Aldrich, Mw 34000 g/mol, 1.6% methacrylic acid) in a PMMA matrix (2wt%) (B)

Extension to copolymer ligands. So far we used end-functionalized homopolymers as polymeric ligands for the ligand exchange procedure. However, also copolymers can be used as ligands, which considerably broadens the variability of available polymeric ligands and provides a route for up-scaling, since many functional copolymers are commercially available. Figure 3 (B) shows how copolymers can similarly coordinate to the nanocrystal surface *via* functional comonomers to form flower-like, dense polymer brushes. Here the brush thickness depends on the molar fraction of binding groups. In Figure 6(B) we show the example of Ag-nanocrystals coated with poly(methyl methacrylate) (PMMA) by ligand exchange with a commercially available PMMA-co-polymethacrylic acid copolymer (Aldrich, Mw 34000 g/mol, 1.6% methacrylic acid), incorporated into a PMMA-homopolymer. Also in this case, high ligand densities for sufficient stabilization in solution and compatibilization with PMMA-matrices can be achieved. Using these copolymers we could prepare up to 20 g of PMMA-coated ZnO-nanoparticles for reinforcement and surface hardening for PMMA-ZnO-nanocomposites on the kg-scale.

Controlled nanocrystal aggregation. For nanocomposites it is often desired to not have singly dispersed nanocrystals, but to rather have aggregated nanocrystal assemblies to increase e.g. electrical or thermal conductivity. Examples are hybrid solar cells where the semiconductor nanocrystals should form a percolation network to provide sufficient electrical conductivity. Here, nanocrystals with coordinatively bound polymers - attached *via* ligand exchange - open a route for a controlled aggregation into percolation networks. The stabilization of the nanocrystals depends on the binding strength of the ligand and the density of the polymer brush. By using a ligand with lower binding strength and/or reducing the excess of polymer ligand $[L2]$ in the ligand exchange procedure, the stability of the polymer-coated nanocrystals against aggregation can be reduced in a controlled fashion. Upon aggregation, polymer ligands can relocalize on the nanoparticle surface (see Figure 3(C)) to stabilize extended string-like assemblies that form cross-links and thus efficiently percolate into a continuous network.^[29, 36] Such a controlled aggregation would not be possible with covalently-bound polymers. With the

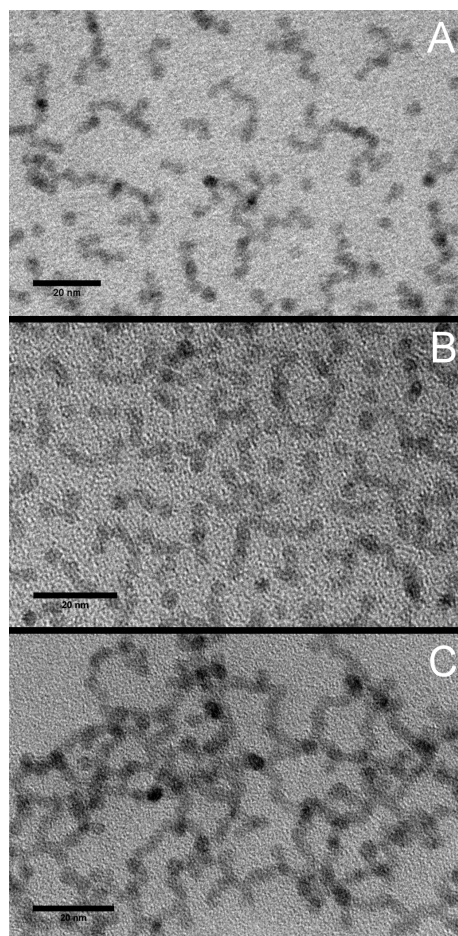


Figure 7: TEM images of 4nm CdSe nanocrystals with a polystyrene brush forming (A) single crystals and short multiplet chains; (B) short chains and networks; (C) a percolating branched network (scale bars are 20nm).

example of polystyrene-stabilized CdSe-nanocrystals we show that by variation of the ligand excess in the ligand exchange procedure it is possible to tune the stability and aggregation of the nanocrystals from a stable, singly dispersed, well-separated state (Figure 2) to slightly aggregated, string-like multiplet assemblies (Fig. 7(A,B)), and eventually to a continuous percolation network, as shown in Figure 7(C). This can be favorably employed e.g. in active matrices of solar cells, where in a first step well-stabilized nanocrystals can be incorporated at high volume fractions with good homogeneous dispersion and no clustering, and then aggregated into a dense percolation network by e.g. thermal destabilization in the polymer matrix.

Conclusions

We show that polymer ligand exchange is a very versatile method to coat nanocrystals densely with a spherical polymer brush, shown for a variety of nanocrystal/polymer combinations including PS-PEHA@CdSe, PS-DETA@Ag, PS-PEHA@Fe₃O₄, PI PEHA@PbS, and PMMA-co-PMAc@ZnO, for which otherwise suitable linker chemistries involving covalent attachment of initiators for grafting-from or functional groups for grafting-to would have to be developed. A rational design of the coordinating groups for polymer ligand exchange is possible and a set of a few different ligands is sufficient to apply this procedure to nearly every nanocrystal/polymer combination. We show the excellent solution stability of the polymer-coated nanocrystal, the possibility to adjust interparticle distances, the possibility to aggregate the particles in a controlled way into percolation networks, and the use of commercially available copolymers to broaden the scope of the method.

Materials and Methods

Chemicals. Cyclohexane (Aldrich) and tetrahydrofuran (THF, Aldrich) were purified by distillation from a sodium-potassium alloy and from the benzophenone-potassium adduct. Isoprene (Aldrich) was purified successively by distillation from CaH₂ (Aldrich) and di-n-butyl magnesium (Aldrich).

Ethylene oxide (AirLiquide) was purified by distillation from CaH_2 and *n*-butyl lithium (Aldrich). All other chemicals were used as received, which include sodium oleate (TCI Europe, >97.0%), *sec*-butyl lithium (1.4 M in cyclohexane; Aldrich), tetrahydrofuran (THF, Sigma-Aldrich, 99,9%), cadmium acetate dihydrate (Sigma-Aldrich, 98%), octadecene (Sigma-Aldrich, tech.), methanol (AppliChem, tech.), silver nitrate (Sigma-Aldrich, $\geq 99\%$), triethylamine (Sigma-Aldrich, $\geq 99\%$), acetone (AppliChem, tech.), iron chloride hexahydrate (Sigma-Aldrich, >98%), hexane (Sigma-Aldrich, 95%), oleic acid (Alfa Aesar, 90%), *sec* butyl lithium (Sigma-Aldrich, 1,4M in cyclohexane), ethylene oxide (Sigma-Aldrich, 99,5%), 1,1' carbonyldiimidazole (CDI, Sigma-Aldrich, reagent grade), chloroform (Aldrich, anhydrous, amylene stabilized), pentaethylenehexamine (PEHA, Sigma-Aldrich, tech.)

Nanocrystal synthesis. Cadmium selenide nanocrystals were synthesized by the method of Cao^[37] *via* the thermal decomposition of cadmium oleate. Silver nanocrystals were synthesized after Nakamoto^[32] *via* the reduction of silver oleate. Iron oxide nanocrystals were synthesized after Hyeon^[38] *via* thermal decomposition of iron oleate. The lead sulfide nanocrystals were synthesized as reported by Hines.^[39] Zinc oxide nanocrystals were synthesized by hydrolysis of zinc oleate in organic solvent as reported by our group.^[40] Detailed procedures are described in the Supporting Information.

Polymer ligand synthesis. Polystyrene (PS) was synthesized by living anionic polymerization with *sec* butyl lithium as initiator at $-70\text{ }^\circ\text{C}$ in THF. The polymerization was terminated either with ethylene oxide to obtain a hydroxyl end group or with CO_2 to obtain a carboxylic acid end group. The hydroxyl end group was subsequently activated by CDI and reacted with PEHA or DETA to create a multivalent amine function. Polyisoprene (PI) was synthesized by living anionic polymerization in cyclohexane. The polymerization was initiated with *sec*-butyl lithium at $30\text{ }^\circ\text{C}$ and terminated with ethylene oxide to obtain hydroxyl terminated PI. The hydroxyl end group was subsequently activated by CDI and reacted with PEHA or DETA to create a multivalent amine function. Detailed procedures are described in

the Supporting Information.

Ligand exchange. The ligand exchange consists of two phases. In the first phase the nanocrystals in solution were mixed with an excess of the polymer followed by three cycles of quantitative precipitation, centrifugation and dissolving. The excess of polymer was removed in the second phase composed of three cycles of selective precipitation, centrifugation and dissolving. In a typical exchange 100 mg of 3 nm CdSe nanocrystals were dissolved in 5 ml THF. To the nanocrystal solution 1 g of polystyrene ligand (PS-X) in 10 ml THF was added. After the two solutions were completely mixed 50 ml of ethanol was added for quantitative precipitation. The precipitate was separated by centrifugation at 3250 g. The supernatant was discarded and the precipitate was dissolved in 10 ml of THF. This procedure was repeated two times. Subsequently ethanol was added slowly until precipitation occurs. The precipitate was separated by centrifugation at 3250 g. After centrifugation the supernatant was checked for remaining nanocrystals by fluorescence or color. If there were remaining nanocrystals more ethanol was added and the precipitate was separated again. This was repeated until no nanocrystals remain in the supernatant. The supernatant was discarded and the precipitate was dissolved in 10 ml of THF. This procedure was repeated two times.

Characterization. The nanocrystals were characterized by transmission electron microscopy (TEM) and dynamic light scattering (DLS). The coated nanocrystals were characterized by TEM, DLS and thermo gravimetric analysis (TGA). TEM images were obtained on a Zeiss 922 Omega microscope. For the DLS measurements a Malvern Zetasizer Nano SZ were used. The TGA measurements were performed with a Mettler Toledo TGA1 with alumina pans, under nitrogen flow and a heating rate of 20K/min.

Associated Content

Supporting Information. Synthesis information, additional TEM images of ligand exchange examples. This material is available free of charge *via* the Internet at <http://pubs.acs.org>.

Author Information

Corresponding Author stephan.foerster@uni-bayreuth.de

Acknowledgments

Financial support for S.E. and D.P. by the German Science Foundation (collaborative research center SFB840, project TPB09 and SPP 1369) is gratefully acknowledged.

References

- [1] Pathak, S.; Choi, S. K.; Arnheim, N.; Thompson, M. E. Hydroxylated quantum dots as luminescent probes for in situ hybridization. *J. Am. Chem. Soc.* 2001,123,4103–4104.
- [2] Mattoussi, H.; Mauro, J. M.; Goldman, E. R.; Green, T. M.; Anderson, G. P.; Sundar, V. C.; Bawendi, M. G. Bioconjugation of highly luminescent colloidal CdSe–ZnS quantum dots with an engineered two-domain recombinant protein. *Phys. Status Solidi B* 2001,224,277–283.
- [3] Lee, J.; Sundar, V. C.; Heine, J. R.; Bawendi, M. G.; Jensen, K. F. Full color emission from II–VI semiconductor quantum dot–polymer composites. *Adv. Mater.* 2000,12,1102–1105.
- [4] Klimov, V. I.; Mikhailovsky, A. A.; Xu, S.; Malko, A.; Hollingsworth, J. A.; Leatherdale, C. A.; Eisler, H. J.; Bawendi, M. G. Optical gain and stimulated emission in nanocrystal quantum dots. *Science* 2000,290,314–317.
- [5] Eisler, H. J.; Sundar, V. C.; Bawendi, M. G.; Walsh, M.; Smith, H. I.; Klimov, V. Color-selective semiconductor nanocrystal laser. *Appl. Phys. Lett.* 2002,80,4614–4616.

REFERENCES

- [6] Tachibana, Y.; Nazeeruddin, M.K.; Gratzel, M.; Klug, D. R.; Durrant, J. R. Electron injection kinetics for the nanocrystalline TiO₂ films sensitised with the dye (Bu₄N)₂Ru(dcbpyH)₂(NCS)₂. *Chem. Phys.* 2002,285,127–132.
- [7] Stathatos, S.; Lianos, P.; Zakeeruddin, S. M.; Liaks, P.; Gratzel, M. A quasi-solid-state dye-sensitized solar cell based on a sol-gel nanocomposite electrolyte containing ionic liquid. *Chem. Mater.* 2003,15,1825–1829.
- [8] Huynh, W. U.; Dittmer, J. J.; Alivisatos, A. P. Hybrid nanorod-polymer solar cells. *Science* 2002,295,2425–2427.
- [9] Masotti, A.; Pitta, A.; Ortaggi, G.; Corti, M.; Innocenti, C.; Lascialfari, A. Synthesis and characterization of polyethylenimine-based iron oxide composites as novel contrast agents for MRI. *Magn. Reson. Mater. Phys., Biol. Med.* 2009,22,77–87.
- [10] Wang, D. S.; Wang, Y. H.; Li, X. Y.; Luo, Q. Z.; An, J.; Yue, H. X. Sunlight photocatalytic activity of polypyrrole-TiO₂ nanocomposites prepared by in situ method. *Catal. Commun.* 2008,9,1162–1166.
- [11] van Zyl, W. E.; García, M.; Schrauwen, B. A. G.; Kooi, B. J.; De Hosson, J. Th. M.; Verweij, H. Hybrid polyamide/silica nanocomposites: Synthesis and mechanical testing. *Macromol. Mater. Eng.* 2002,287,106–110.
- [12] Hung, C.-H.; Whang, W.-T. Effect of surface stabilization of nanoparticles on luminescent characteristics in ZnO/poly(hydroxyethyl methacrylate) nanohybrid films. *J. Mater. Chem.* 2005,15,267–274, 2005.
- [13] Singha, S.; Thomas, M. J. Dielectric properties of epoxy nanocomposites. *IEEE Trans. Dielectr. Electr. Insul.* 2008,15,12–23.
- [14] Napper, D. H. *Polymeric Stabilization of Colloidal Dispersions*. Academic Press Incorporated, 1983.

-
- [15] Fischer, S.; Salcher, A.; Kornowski, A.; Weller, H.; Foerster, S. Completely miscible nanocomposites. . *Angew. Chem. Int. Ed.* 2011,50,7811–7814.
- [16] Tsubokawa, N.; Kogure, A.; Sone, Y. Grafting of polyesters from ultra-fine inorganic particles: Copolymerization of epoxides with cyclic acid anhydrides initiated by COOK groups introduced onto the surface. *J. Polym. Sci., Part A: Polym. Chem.* 1990,28,1923–1933.
- [17] Ohno, K.; Koh, K.; Tsujii, Y.; Fukuda, T. Fabrication of ordered arrays of gold nanoparticles coated with high-density polymer brushes. *Angew. Chem. Int. Ed.* 2003,42,2751–2754.
- [18] Mansky, P.; Liu, Y.; Huang, E.; Russell, T. P.; Hawker, C. Controlling polymer-surface interactions with random copolymer brushes. *Science* 1997,275,1458–1460.
- [19] Li, G.; Zeng, D. L.; Wang, L.; Zong, B.; Neoh, K. G.; Kang, E. T. Hairy hybrid nanoparticles of magnetic core, fluorescent silica shell, and functional polymer brushes. *Macromolecules* 2009,42,8561–8565.
- [20] He, W.; Cheng, L.; Zhang, L.; Jiang, X.; Liu, Z.; Cheng, Z.; Zhu, X. Bifunctional nanoparticles with magnetism and NIR fluorescence: Controlled synthesis from combination of AGET ATRP and ‘Click’ reaction. *Nanotechnology* 2014,25,045602.
- [21] Awada, H.; Medlej, H.; Blanc, S.; Delville, M.-H.; Hiorns, R. C.; Bousquet, A.; Dagron-Lartigau, C.; Billon, L. Versatile functional poly(3-hexylthiophene) for hybrid particles synthesis by the grafting onto technique: Core@shell ZnO nanorods. *J. Polym. Sci., Part A: Polym. Chem.* 2014,52,30–38.
- [22] Park, J.; Joo, J.; Kwon, S. G.; Jang, Y.; Hyeon, T. Synthesis of monodisperse spherical nanocrystals. *Angew. Chem. Int. Ed.* 2007,46,4630–4660.

REFERENCES

- [23] Karg, M.; Schelero, N.; Oppel, C.; Gradzielski, M.; Hellweg, T.; v. Klitzing, R. Versatile phase transfer of gold nanoparticles from aqueous media to different organic media. *Chem. Eur. J.* 2011,17,4648–4654.
- [24] Pletsch, H.; Peng, L.; Mitschang, F.; Schaper, A.; Hellwig, M.; Nette, D.; Seubert, A.; Greiner, A.; Agarwal, S. Ultrasound-mediated synthesis of high-molecular weight polystyrene-grafted silver nanoparticles by facile ligand exchange reactions in suspension. *Small* 2014,10,201–208.
- [25] Corbierre, M. K.; Cameron, N. S.; Sutton, M.; Laaziri, K.; Lennox, R. B. Gold nanoparticle/polymer nanocomposites: Dispersion of nanoparticles as a function of capping agent molecular weight and grafting density. *Langmuir* 2005,21,6063–6072.
- [26] Skaff, H.; Emrick, T. Reversible addition fragmentation chain transfer (RAFT) polymerization from unprotected cadmium selenide nanoparticles. *Angew. Chem. Int. Ed.* 2004,43,5383–5386.
- [27] Zhang, T.; Ge, J.; Hu, Y.; Yin, Y. A general approach for transferring hydrophobic nanocrystals into water. *Nano Lett.* 2007,7,3202–3207.
- [28] Celika, D.; Krueger, M.; Veit, C.; Schleiermacher, H. F.; Zimmermann, B.; Allarde, S.; Dumsche, I.; Scherf, U.; Rauscher, F.; Niyamakom, P. Performance enhancement of CdSe nanorod-polymer based hybrid solar cells utilizing a novel combination of post-synthetic nanoparticle surface treatments. *Sol. Energy Mater. Sol. Cells.* 2012,98,433–440.
- [29] Nikolic, M. S.; Olsson, C.; Salcher, A.; Kornowski, A.; Rank, A.; Schubert, R.; Froemsdorf, A.; Weller, H.; Foerster, S. Micelle and vesicle formation of amphiphilic nanoparticles. *Angew. Chem. Int. Ed.* 2009,48,2752–2754.
- [30] T. Honold. Nanoparticle polymer hybrids for sandwich solar cells. Master's thesis, University of Bayreuth, Germany, 2013.

-
- [31] Esteves, A. C. C.; Bombalski, L.; Trindade, T.; Matyjaszewski, K.; Barros-Timmons, A. Polymer grafting from CdS quantum dots *via* AGET ATRP in miniemulsion. *Small* 2007,3,1230–1236.
- [32] Yamamoto, M.; Kashiwagi, Y.; Nakamoto, M. Size-controlled synthesis of monodispersed silver nanoparticles capped by long-chain alkyl carboxylates from silver carboxylate and tertiary amine. *Langmuir* 2006,22,8581–8586.
- [33] Wang, Y.; Teng, X.; Wang, J.-S.; Yang, H. Solvent-free atom transfer radical polymerization in the synthesis of Fe₂O₃@polystyrene core-shell nanoparticles. *Nano Lett.* 2003,3,789–793.
- [34] Kim, S.; Nealey, P. F.; Bates, F. S. Directed assembly of lamellae forming block copolymer thin films near the order–disorder transition. *Nano Lett.* 2014,14,148–152.
- [35] Mehdizadeh Taheri, S.; Fischer, S.; Foerster, S. Routes to nanoparticle-polymer superlattices. *Polymers* 2011,3,662–673.
- [36] Akcora, P.; Liu, H.; Kumar, S. K.; Moll, J.; Li, Y.; Benicewicz, B. C.; Schadler, L. S.; Acehan, D.; Panagiotopoulos, A. Z.; Pryamitsyn, V.; et al. Anisotropic self-assembly of spherical polymer-grafted nanoparticles. *Nat. Mater.* 2009,8,354–359.
- [37] Yang, Y. A.; Wu, H.; Williams, K. R.; Cao, Y. C. Synthesis of CdSe and CdTe nanocrystals without precursor injection. *Angew. Chem.* 2005,117,6870–6873.
- [38] Park, J.; An, K.; Hwang, Y.; Park, J. G.; Noh, H. J.; Kim, J. Y.; Park, J. H.; Hwang, N. M.; Hyeon, T. Ultra-large-scale syntheses of monodisperse nanocrystals. *Nat. Mater.* 2004,3,891–895.
- [39] Hines, M. A.; Scholes, G. D. Colloidal PbS nanocrystals with size-tunable near-infrared emission: Observation of post-synthesis self-narrowing of the particle size distribution. *Adv. Mater.* 2003,15,1844–1849.

REFERENCES

- [40] Ehlert, S.; Lunkenbein, T.; Breu, J.; Foerster, S. Facile large-scale synthetic route to monodisperse ZnO nanocrystals. *Colloids Surf., A.* 2014,444,76–80.

Supporting Information

Materials and Methods

Chemicals. Cyclohexane (Aldrich) and tetrahydrofuran (THF, Aldrich) were purified by distillation from a sodium-potassium alloy and from the benzophenone-potassium adduct. Isoprene (Aldrich) was purified successively by distillation from CaH_2 (Aldrich) and di-n-butyl magnesium (Aldrich). Ethylene oxide (AirLiquide) was purified by distillation from CaH_2 and n-butyl lithium (Aldrich). All other chemicals were used as received, which include sodium oleate (TCI Europe, >97.0%), sec-butyl lithium (1.4 M in cyclohexane; Aldrich), tetrahydrofuran (THF, Sigma-Aldrich, 99.9%), cadmium acetate dihydrate (Sigma-Aldrich, 98%), octadecene (Sigma-Aldrich, tech.), bis(trimethylsilyl) sulfide (TMS, Aldrich), methanol (AppliChem, tech.), silver nitrate (Sigma-Aldrich, $\leq 99\%$), selenium (Aldrich), triethylamine (Sigma-Aldrich, $\leq 99\%$), acetone (AppliChem, tech.), iron chloride hexahydrate (Sigma-Aldrich, >98%), hexane (Sigma-Aldrich, 95%), oleic acid (Alfa Aesar, 90%), 1,1' carbonyldiimidazole (CDI, Sigma-Aldrich, reagent grade), chloroform (Aldrich, anhydrous, amylene stabilized), pentaethylenhexamine (PEHA, Sigma-Aldrich, tech.), tetrabutyl ammonium hydroxide (TBAH, Alfa Aesar, 1M in methanol), ethanol (AppliChem, tech.), triethylamine (Aldrich, 99%), lead(II)-nitrate (Aldrich, 99%), zinc chloride (Aldrich, 99%), styrene (Aldrich, 99%).

Nanocrystal synthesis. Cadmium selenide nanocrystals were synthesized *via* the thermal decomposition of cadmium oleate.^[1] In a typical synthesis 1.6g (2.5 mmol) of cadmium oleate were dissolved in 35 ml octadecene and added to 45ml of selenium (0.1M) in octadecene solution. The mixture was degased by 100 °C under vacuum for 1h and subsequent heated to 240 °C under a nitrogen atmosphere. According to the requirements the solution was kept at this temperature for 1 to 30 minutes and then cooled to room temperature. The nanocrystals were purified by at least 3 precipitation dissolving cycles with ethanol/ methanol and THF. Silver nanocrystals were synthesized *via* the reduction of silver oleate.^[2] In a typical synthesis 1g of

REFERENCES

silver oleate were mixed with 20 ml of triethylamine and heated to 80 °C for 3h. The nanocrystals were purified by precipitation with acetone and dissolving in THF two times. Iron-oxide nanoparticles were synthesized by thermal decomposition of an iron oleate complex according to the procedure of Park et al.^[3] The iron oleate complex was synthesized from a reaction mixture of iron(III)chloride and sodium oleate at 70 °C. The viscous and brownish iron-oleate compound (31.89 g) was dissolved in octadecene and as a stabilizing agent oleic acid (5.04 g) was added to the solution. The reaction mixture was heated under reflux at a rate of 2 °C/min up to 110 °C in vacuum, and after that in a nitrogen atmosphere with the same heating rate up to 317 °C. The reaction mixture was stirred under reflux at 317 °C for 20 min. After the solution was cooled down at RT, 50% THF was added to the nanoparticle-solution to avoid the formation of separated phases. The work up was carried out by precipitation of the nanoparticles in acetone. The particles could be easily redispersed in toluene or THF. The lead sulfide nanocrystals were synthesized as reported by Hines.^[4] In a typical synthesis 0.3g of lead oleate were dissolved in 200 ml of octadecene and degased at 100 °C under vacuum for 1h. The solution was heated to 150 °C under nitrogen atmosphere and 20 ml of a TMS octadecen solution was injected subsequently the mixture was cooled to 90 °C and kept there for 1h. The nanocrystals were purified by two precipitation dissolving cycles with methanol and THF. Zinc oxide nanocrystals were synthesized by hydrolysis of zinc oleate in organic solvent.^[5] In a typical synthesis 16 ml of TBAH solution (1M) were added to 15 g zinc oleate in 300 ml THF and kept at 50 °C for 16h. The nanocrystals were purified by at least 3 precipitation dissolving cycles with methanol and THF.

Polymer synthesis. Polystyrene (PS) was synthesized by living anionic polymerization in THF using high vacuum techniques and argon as inert atmosphere. The polymerization of styrene was initiated with sec-butyl lithium at -70 °C. The polymerization was terminated either with ethylene oxide to obtain a hydroxyl end group or with CO₂ to obtain a carboxylic acid end group. The mixture was stirred for at least 12 hours at room temperature and terminated with degassed acetic acid. The polymer was precipitated in

cold (-20°C) methanol. Polyisoprene (PI) was synthesized *via* living anionic polymerization in cyclohexane using high vacuum techniques and dry nitrogen as inert atmosphere. The polymerization of isoprene was initiated with sec-butyl lithium at 30°C . After complete conversion of isoprene a small amount of THF was condensed into the reactor. Then ethylene oxide in an at least 10-fold excess over the initiator concentration was added to the solution to cap the living PI chain ends. The mixture was stirred for at least 12 hours at 40°C and terminated with degassed acetic acid. The polymer was precipitated in cold (-20°C) methanol. The narrow distributed, hydroxyl functionalized polymer was further functionalized by a following two-step reaction to attach a multidentate amine group to the polymer. In the first step, the hydroxyl group was activated with 1,1'-carbonyldiimidazole (CDI) in chloroform. Therefore the polymer solution in chloroform was added drop-wise to a CDI (25-fold excess) solution in chloroform. After stirring the reaction for 24 hours at room temperature, the solution was extracted three times with water to remove residual CDI and dried under vacuum. In the next step, pentaethylenehexamine (PEHA, 25-fold excess) was dissolved in chloroform and the CDI activated polymer solution in chloroform was added drop-wise to the amine solution. After a reaction time of 24 hours the solution was extracted three times with water and dried under vacuum.

Characterisation. The grafting density D was calculated with the formula:

$$D = \frac{4 * r_n^3 * \rho_n * N_A * (100 - X_n)}{3 * d_n^2 * M_p * X_n}$$

Were r_n and d_n are the nanocrystal radius respectively the diameter, ρ_n is the material density in bulk, N_A is the Avogadro constant, M_p is the molecular mass of the polymer and X_n is the weight fraction of the nanocrystals in percent derived from the TGA measurements. This formula is for spherical particles, under the assumptions that the density of the particles is similar to the density of the bulk material and that no free polymer is present.

Figure 8 shows the ability of the TGA method to characterize the coated nanocrystals regarding the amount of ligand on the surface.

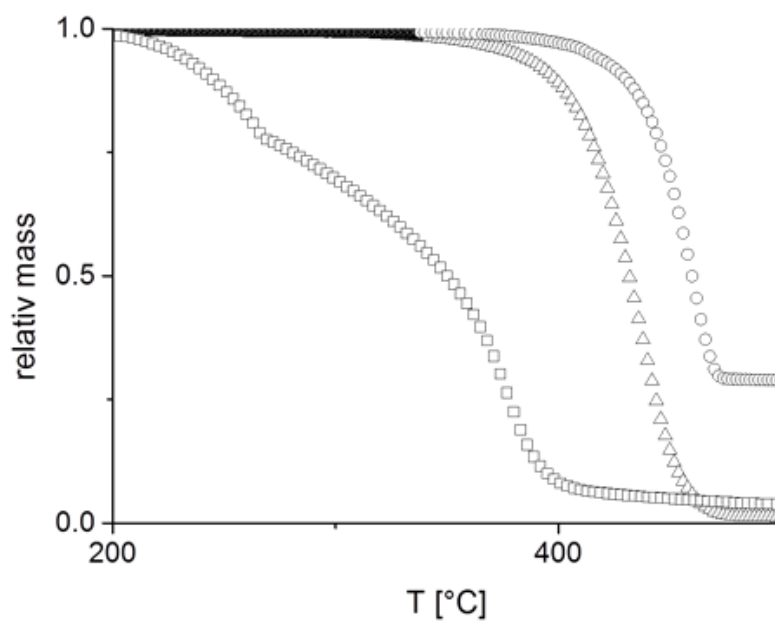


Figure 8: TGA measurements of technical oleic acid (squares), polystyrene (9kPS, triangles) and ZnO nanocrystals coated with 9kPS (circles).

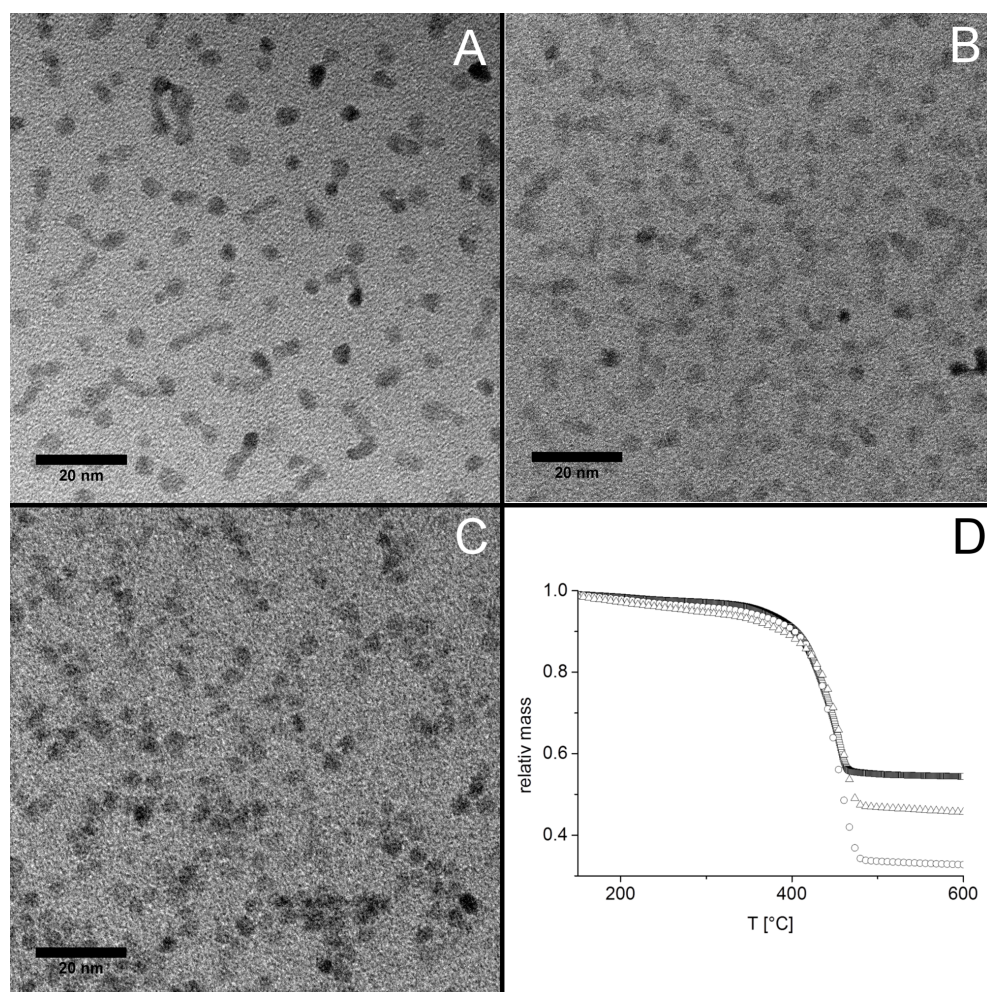


Figure 9: TEM images of polystyrene (2700 g/mol) coated ZnO nanocrystals (4 nm) with different grafting densities A: $1,35 \text{ nm}^{-2}$, B: $0,98 \text{ nm}^{-2}$, C: $0,68 \text{ nm}^{-2}$ and the TGA measurements (D) for the three composites (A: circles, B: triangles, C: squares).

REFERENCES

Figure 9 show another example for the controlled aggregation followed by TGA measurements. The derived grafting density for the coated nanocrystals decreases significant with increasing aggregation.

References

- [1] Yang, Y. A.; Wu, H.; Williams, K. R.; Cao, Y. C. Synthesis of CdSe and CdTe nanocrystals without precursor injection. *Angew. Chem.* 2005,117,6870–6873.
- [2] Yamamoto, M.; Kashiwagi, Y.; Nakamoto, M. Size-controlled synthesis of monodispersed silver nanoparticles capped by long-chain alkyl carboxylates from silver carboxylate and tertiary amine. *Langmuir* 2006,22,8581–8586.
- [3] Park, J.; An, K.; Hwang Y.; Park J. G.; Noh H. J.; Kim J. Y.; Park J. H.; Hwang N. M.; Hyeon, T. Ultra-large-scale syntheses of monodisperse nanocrystals. *Nat. Mater.* 2004,3,891–895.
- [4] Hines, M. A.; Scholes. G. D. Colloidal pbs nanocrystals with size-tunable near-infrared emission: Observation of post-synthesis self-narrowing of the particle size distribution. *Adv. Mater.* 2003,15,1844–1849.
- [5] Ehlert, S.; Lunkenbein, T.; Breu J.; Foerster, S. Facile large-scale synthetic route to monodisperse ZnO nanocrystals. *Colloids Surf., A.* 2014,444,76–80.

6 A General Route to Optically Transparent, Highly Filled Polymer Nanocomposites

Sascha Ehlert, Corinna Stegelmeier, Daniela Pirner, Stephan Förster*
Physical Chemistry I, University of Bayreuth, 95440 Bayreuth, Germany

submitted: 2014

Polymer nanocomposites are currently of immense interest in fundamental research as well as in a large variety of industrial applications. Nanocomposites offer potentially new or largely enhanced material properties, but nanoparticle agglomeration mostly prevents these enhancements and deteriorates many useful properties. This is particularly true for optical applications that take advantage of the optical properties of inorganic nanoparticles which are combined with transparent polymers for ease of processing and protection,^[1] but fail due to agglomeration which causes turbidity and strongly reduces optical transmission.

We report a general route to non-aggregated highly filled, optically transparent polymer nanocomposites. The method is based on a spherical polymer brush coating of the nanoparticles which provides thermodynamic miscibility of nanoparticles and polymer matrix over the complete range of nanoparticle volume fractions. This prevents nanoparticle aggregation in the polymer matrix that causes turbidity. Depending on the extinction coefficient of the nanoparticles, optically transparent nanocomposites for nanoparticle weight fractions up to 45wt% can be reached. This is demonstrated for a large variety of chemically different nanoparticle/polymer combinations.

Since the first reports of polymer-Au nanocomposites for optical applications,^[2, 3] nanocomposites consisting of inorganic metal or semiconducting nanoparticles and transparent polymer matrices have been investigated towards applications involving selective light absorption in the UV/Vis- range, photoluminescence, and extreme refractive index polymeric materials.

For nanocomposites used as UV-photo-protective materials, high transparency in the visible range and steep absorption in the near UV-range ($\lambda < 400$ nm) are required. The most promising inorganic materials are ZnO and TiO₂ nanoparticles, which have bulk band-gap energies of around 3 eV. TiO₂-PMMA and ZnO-PMMA nanocomposites have been reported.^[4, 5, 6] For effective UV absorption nanoparticle contents of up to 35 wt% have to be used. Due to nanoparticle aggregation, the transparency of highly filled nanocomposites could only be realized by using micrometer thin films. Larger film thicknesses resulted in strongly increased opaqueness/translucence.

For photoluminescent materials, semiconductor-polymer nanocomposites are attractive, since semiconductor nanoparticles show wavelength-tunable light emission due to the quantum size effect. Semiconductor nanocrystals can cover a large range of light emission wavelengths (400 - 1400 nm) and due to their higher photostability and narrow emission band width they are better suited for many opto-electronic applications than organic dyes. These unique properties of semiconductor nanoparticles together with the excellent processability of polymers offer a range of applications. Studies on photoluminescent nanocomposites involved CdSe-poly(lauryl methacrylate),^[7] CdSe-PS,^[8] CdS/SiO₂-PMMA,^[9] CdTe-PS, CdTe-PMMA,^[10] and recently core/shell quantum dots of CdSe/CdS incorporated in a poly(butylmethacrylate) matrix,^[11] mostly in the form of thin films.

Compared to inorganic solids, optical applications of polymers are often limited due to the relatively narrow range of the refractive index (RI) which is typically only in the range between 1.3 and 1.7. The introduction of inorganic nanoparticles into a polymer matrix can result in polymeric materials with larger variations in the RI, which finds potential applications in lenses, optical filters, reflectors, optical waveguides, optical adhesives, solar cells, or antireflection films.^[12] For high-RI materials, PbS was the mostly studied inorganic additive whereas for low-RI materials Au nanoparticles have been incorporated.^[13, 14, 15, 16]

A general requirement for inorganic nanoparticles to be used for transparent polymer nanocomposites is a small size. Rayleigh's law can be used to estimate the intensity loss of light passing through a composite by scattering

$$I = I_0 \exp - \left[\frac{3\phi l R^3}{4\lambda^4} \left(\frac{n_{NP}}{n_P} - 1 \right) \right] \quad (1)$$

where I is the intensity of the transmitted and I_0 of the incident light, ϕ is the volume fraction of the particles, l is the optical path length, R is the radius of the spherical particles, λ is the wavelength of the light, n_{NP} is the refractive index of the nanoparticles, and n_P is the refractive index of the polymer matrix. It can be seen from Equation 1 that the light loss by scattering steeply increases with particle size. Generally, 40 nm is considered as an upper limit for nanoparticle diameters to avoid intensity loss of transmitted light due to Rayleigh scattering. The transparency/opacity is also dependent on the difference of the refractive index between nanoparticles and the polymer matrix. When the RI of nanoparticles and polymer matrix is similar, transparency can also be achieved with bigger nanoparticles. Agglomeration of nanoparticles will cause a considerable increase of opacity. To meet the challenge of preparing optically transparent nanocomposites, these are either prepared by directly incorporating the nanoparticles into a polymer matrix by physic-chemical methods,^[17, 18, 19, 20, 21, 22] by chemical methods based on *in-situ* polymerization,^[4, 5, 23] or sol/gel routes.^[24] The latter involves trapping the nanoparticles in the dispersed state, thereby avoiding aggregation and achieving a more homogeneous dispersion of nanoparticles in the polymer matrix.

In the present study we consider nanoparticle polymer combinations relevant for applications, including PbS-nanoparticles for high-refractive index nanocomposites, Ag- and Au-nanoparticles for low-refractive index and plasmonic nanocomposites, CdSe-, ZnO- and PbS- for photoluminescent nanocomposites, and Fe₂O₃ for magnetic nanocomposites. These are integrated into the most common optically transparent polymers such as PMMA and PS,

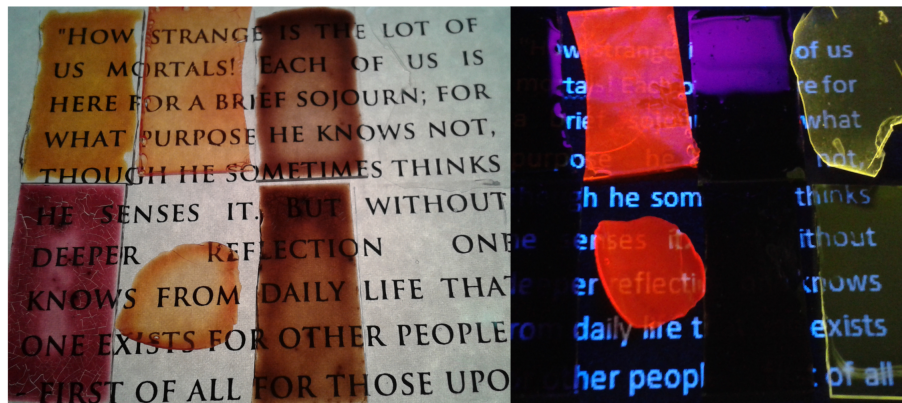


Figure 1: Photographs of transparent nanocomposites films ($150\mu\text{m}$) on glass. Upper row: Ag-PMMA ($100\mu\text{m}$, 2wt%), CdSe-PMMA ($200\mu\text{m}$, 10wt%), PbS-PI (10wt%) and free standing ZnO-PMMA ($250\mu\text{m}$, 10wt%). Lower row: Au-PS ($100\mu\text{m}$, 2wt%), free standing CdSe-PS ($100\mu\text{m}$, 29%), Fe₂O₃-P2VP (5wt%) and ZnO-PS ($150\mu\text{m}$, 45wt%). Left: day light, Right: UV-light illumination of the semiconductor nanocomposites.

but also into PI and P2VP which are optically transparent as well, but have different mechanical or chemical properties to demonstrate the broad applicability of the method.

For our study the nanoparticles were stabilized with a polymer brush of the same polymer as the matrix polymer to afford complete thermodynamic miscibility and thus to avoid nanoparticle agglomeration. For complete miscibility up to the highest volume fractions of nanoparticles the grafting density of the polymer brush must be sufficiently high to overcome attractive interparticle forces. Since for this work high grafting densities are required and many different nanoparticle-polymer combinations are considered, we used the ligand exchange method for the end-attachment of the polymer chains.^[25] This method employs functional groups on the polymer chain ends to coordinatively bind to the nanoparticle surface. With a set of a few polymers with coordination groups and several nanoparticles it is possible to create a broad range of nanocomposites.

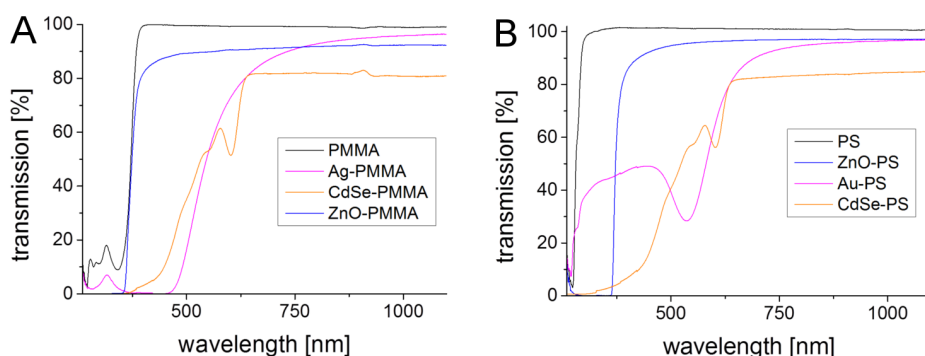


Figure 2: UV-vis spectra for nanocomposites with A) PMMA and B) PS matrices and different nanoparticles (Ag, CdSe, ZnO) showing $>80\%$ transparency at high loading ratios in the wavelength range above the absorptions edge (ZnO, CdSe) or the plasmon resonance (Ag).

Figure 1 shows a variety of different nanocomposites as 100 -250 μm thick films prepared *via* solvent casting on glass slides (Ag-PMMA, CdSe-PMMA, PbS-PI, Au-PS, Fe_2O_3 -P2VP, ZnO-PS, or as free-standing films (ZnO-PMMA, CdSe-PS). All are optically transparent at filling ratios of up to 45wt% of nanoparticles. For the Au- and Ag-nanocomposites with their strong plasmon absorption we kept the weight fractions at lower values (2wt%) to keep the visible optical transparency. The CdSe- and ZnO-semiconductor nanocomposites show the characteristic fluorescence upon UV-illumination. The UV/Vis spectra in Figure 2 show for all nanocomposites transmissions of $>80\%$ except for the wavelength range at which the nanoparticles absorb light.

In Figure 3 TEM images of these nanocomposites are shown. We observe well-dispersed nanoparticles, where the inter particle distance is due to the thickness of the polymer brush and the amount of free matrix polymer. The ZnO-PMMA composite is transparent although the nanoparticles are aggregated to some degree, because the mean diameter of the aggregates is still below 25 nm. In Figure 3G and H we show TEM-images of microtomed thin sections of bulk nanocomposites also proving the absence of aggregation.

The miscibility of nanoparticles and polymer matrix not only provides transparent nanocomposites for optical applications, but also increases the mechanical properties of the nanocomposites. As an example, nanoindentation measurements show a considerable improvement of the elastic modulus for the ZnO/PMMA nanocomposites, increasing from 10 GPa for pure PMMA over 23 GPa for the 5% reaching 35 GPa for the 10% nanocomposite (see Supporting Information), demonstrating the improved scratch resistance of these materials.

In conclusion, we report a general route to non-aggregated highly filled, optically transparent polymer nanocomposites for a large variety of different nanoparticle/polymer matrix combinations including Ag, Au, CdSe, ZnO, Fe₂O₃, PbS in poly(methylmethacrylate) (PMMA), polyisoprene (PI), polystyrene (PS), and poly-2-vinylpyridine (P2VP) as examples. The incorporation of nanoparticles not only enables optical applications, but also improves mechanical properties like scratch resistance.

Experimental Section

Nanoparticle synthesis. The gold nanoparticles were synthesized by the method of Yu *via* reduction of chloroauric acid by oleylamine.^[26] Cadmium selenide nanocrystals were synthesized by the method of Cao *via* thermal decomposition of cadmium oleate.^[27] Silver nanocrystals were synthesized after Nakamoto *via* reduction of silver oleate.^[28] Iron oxide nanocrystals were synthesized after Hyeon *via* thermal decomposition of iron oleate.^[29] The lead sulfide nanocrystals were synthesized as reported by Hines.^[30] Zinc oxide nanocrystals were synthesized by hydrolysis of zinc oleate in organic solvent as reported by our group.^[31]

Polymer synthesis. Polystyrene (PS) was synthesized by living anionic polymerization with *sec*-butyl lithium as initiator at -70°C in THF. The polymerization was terminated either with ethylene oxide to obtain a hydroxyl end group or with CO₂ to obtain a carboxylic acid end group. The hydroxyl end group was subsequently activated by 1,1-carbonyldiimidazole

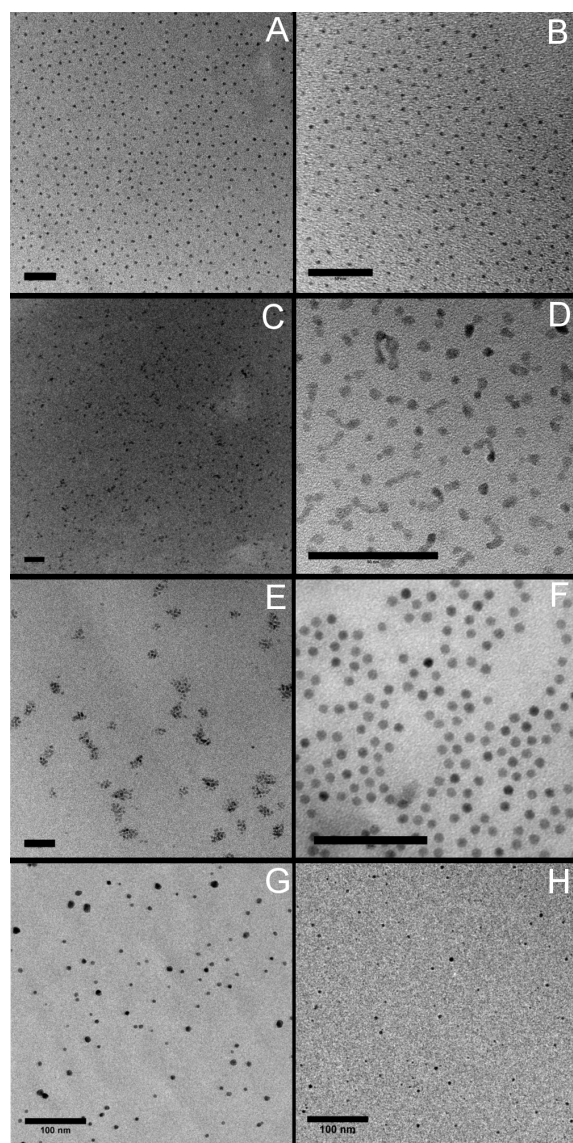


Figure 3: TEM images of solvent cast nanocomposites A - F. A is a PbS-PI composite (7nm, 10%), C and E are PMMA composites with CdSe-NP (4nm, 10%), ZnO-NP (4nm, 22nm aggregates, 10%). B and D are PS composites with CdSe-NP (3nm, 29%), ZnO-NP (4nm, 45%). F is a Fe₂O₃-P2VP composite (6nm, 10%). Scale bars 50nm. G and H are TEM-images of thin microtomed sections of 10wt% Au-PS (G) and 2.5wt% Ag-PMMA (H) nanocomposites. No aggregation of nanoparticles is observed (scale bar 100nm).

(CDI) and reacted with pentaethylenehexamine (PEHA) or diethylenetetraamine (DETA) to create a multivalent amine function.

Polyisoprene (PI) was synthesized by living anionic polymerization in cyclohexane. The polymerization was initiated with *sec*-butyl lithium at 30 °C and terminated with ethylene oxide to obtain hydroxyl terminated PI. The hydroxyl end group was subsequently activated by CDI and reacted with PEHA or DETA to create a multivalent amine function.

Poly-2-vinylpyridine (P2VP) was synthesized by living anionic polymerization in THF at -70 °C with *sec*-butyl lithium as initiator. The polymerization was terminated with ethylene oxide to obtain a hydroxyl end group. This end group was subsequently activated by CDI and reacted with PEHA to create a multivalent amine function.

Polymer grafted nanoparticle. The polymer brush on the nanoparticle surface was prepared by the ligand exchange method developed in our group *via* multiple precipitation dissolution cycles.^[25]

Nanocomposite preparation. The nanocomposites were prepared by mixing the brush grafted nanoparticle in the desired concentration with the matrix polymer in solution.

Characterization. The nanocomposites were characterized by transmission electron microscopy (TEM), thermo gravimetric analysis (TGA) and UV-vis spectroscopy. TEM images were obtained on a Zeiss 922 Omega microscope. The TGA measurements were performed with a Mettler Toledo TGA1 with alumina pans, under nitrogen flow and a heating rate of 20K/min. The UV/Vis spectra were measured using an Agilent 8453. The films for photos and UV-vis measurements were solvent cast on glass slides. The samples for TEM were either cast on Cu-grids from diluted solution or put on the Cu-grid after cutting the films with a microtome. For the TGA measurements parts of the films were used.

Supporting Information

Supporting Information is available from the Wiley Online Library or from the author.

Acknowledgements

The authors would like to thank the DFG collaborative research center SFB480, project B9, for financial support.

References

- [1] S. Li, M. M. Lin, M. S. Toprak, D. K. Kim, M. Muhammed, *Nano Reviews* 2010, 1, 5214.
- [2] W. Caseri, *Chem. Eng. Comm.* 2009, 196, 549.
- [3] W. Caseri, *Macromol. Rapid. Comm.* 2000, 21, 705.
- [4] J. Zhang, S. Luo, L. Gui, *J. Mater. Sci.* 1997, 32, 1469.
- [5] A. H. Yuwono, B. Liu, J. Xue, J. Wang, H. I. Elim, W. Ji, Y. Li, T. J. White, *J. Mater. Chem.* 2004, 14, 2978.
- [6] C. H. Hung, W. T. Whang, *J. Mater. Sci.* 2005, 15, 267.
- [7] J. Lee, V. C. Sundar, J. R. Heine, M. G. Bawendi, K. F. Jensen, *Adv. Mater.* 2000, 12, 1102.
- [8] L. Erskine, T. Emrick, A. P. Alivisatos, J. M. J. Fréchet, *Polym. Prep.* 2000, 41, 593.
- [9] S. C. Farmer, T. E. Patten, *Chem. Mater.* 2001, 13, 3920.
- [10] H. Zhang, Z. Cui, Y. Wang, K. Zhang, X. Ji, C. Lü, B. Yang, M. Gao, *Adv. Mater.* 2003, 15, 777.
- [11] G. G. Yordanov, G. D. Gicheva, C. D. Dushkin, *Mater. Chem. Phys.* 2009, 113, 507.

REFERENCES

- [12] H. Althues, J. Henle, S. Kaskel, *Chem. Soc. Rev.* 2007, 36, 1454.
- [13] M. Weibel, W. Caseri, U. W. Suter, H. Kiess, E. Wehrli, *Polym. Adv. Technol.* 1991, 2, 75.
- [14] L. Zimmermann, M. Weibel, W. Caseri, U. W. Suter, *J. Mater. Res.* 1993, 7, 1742.
- [15] C. Lü, C. Guan, Y. Liu, Y. Cheng, B. Yang, *Chem. Mater.* 2005, 17, 2448.
- [16] L. Zimmermann, M. Weibel, W. Caseri, U. W. Suter, P. Walter, *Polym. Adv. Technol.* 1993, 4, 1.
- [17] J. Zheng, R. W. Siegel, C. G. Toney, *J. Polym. Sci. Polym. Phys.* 2003, 41, 1033.
- [18] V. Khrenov, M. Klapper, M. Koch, K. Mullen, *Macromol. Chem. Phys.* 2005, 206, 95.
- [19] M. Xiong, G. Gu, B. You, L. Wu, *J. Appl. Polym. Sci.* 2003, 90, 1923.
- [20] D. Sun, N. Miyatake, H. J. Sue, *Nanotechnology* 2007, 18, 215606.
- [21] N. S. Allen, M. Edge, A. Ortega, G. Sandoval, C. M. Liauw, J. Verran, J. Stratton, R. B. McIntyre, *Polym. Degrad. Stab.* 2004, 85, 927.
- [22] S. H. Stelzig, M. Klapper, K. Müllen, *Adv. Mater.* 2008, 20, 929.
- [23] C. H. Hung, W. T. Whang, *J. Mater. Sci.* 2005, 15, 267.
- [24] J. Noack, L. Schmidt, H.-J. Glaesel, M. Bauer, E. Kemnitz, *Nanoscale* 2011, 3, 4774.
- [25] S. Ehlert, S. Mehdizadeh Taheri, D. Pirner, M. Drechsler, H.-W. Schmidt, S. Förster, *ACS Nano* 2014, 8, 6114.
- [26] H. Yu, M. Chen, P. M. Rice, S. X. Wang, R. L. White, S. Sun, *Nano. Lett.* 2005, 5, 379.

REFERENCES

- [27] Y. A. Yang, H. Wu, K. R. Williams, Y. C. Cao, *Angew. Chem.* 2005, 117, 6870.
- [28] M. Yamamoto, Y. Kashiwagi, M. Nakamoto, *Langmuir* 2006, 22, 8581.
- [29] J. Park, K. An, Y. Hwang, J. G. Park, H. J. Noh, J. Y. Kim, J. H. Park, N. M. Hwang, T. Hyeon, *Nat. Mater.* 2004, 3, 891.
- [30] M. A. Hines, G. D. Scholes, *Adv. Mater.* 2003, 15, 1844.
- [31] S. Ehlert, T. Lunkenbein, J. Breu, S. Foerster, *Colloids Surf., A.* 2014, 444, 76.

Supporting Information

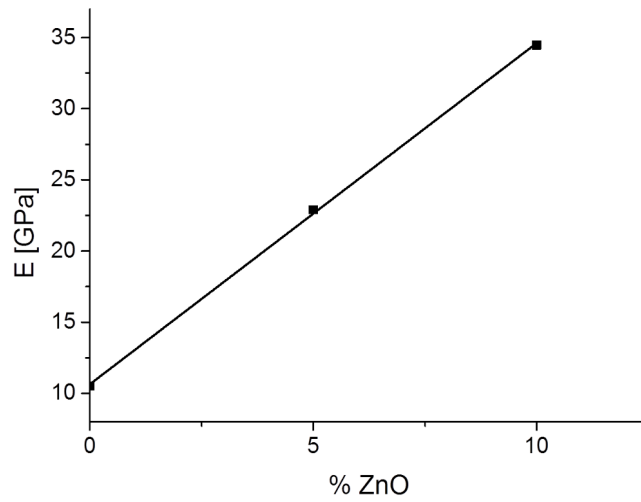


Figure 4: Elastic modulus measured by nanoindentation of a ZnO/PMMA nanocomposite.

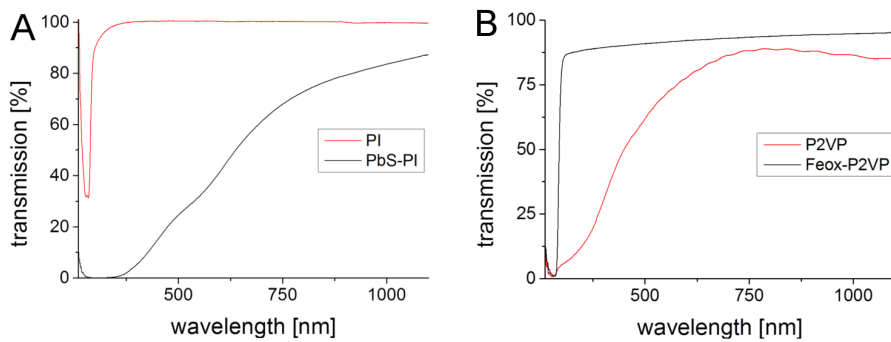


Figure 5: UV-vis spectra of PbS-PI (A) and iron oxide-P2VP (B) nanocomposites with high transmission.

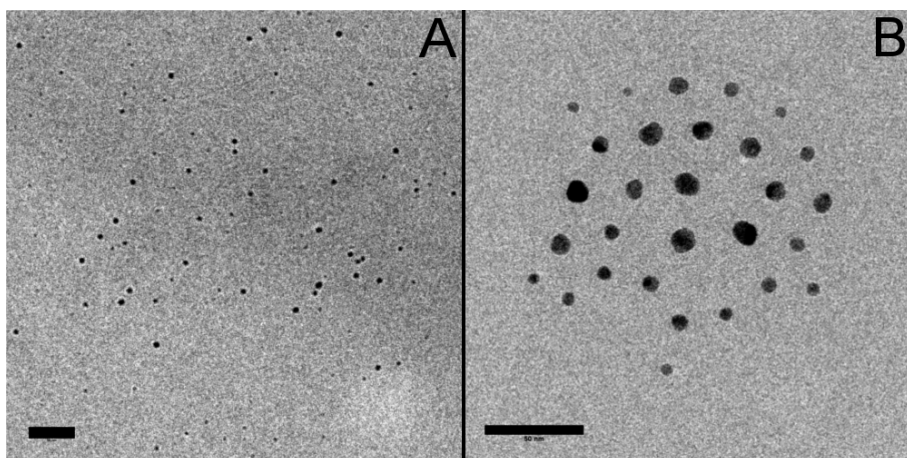


Figure 6: TEM-images of solvent cast Ag-PMMA (A, 15nm, 2%) and Au-PS (B, 15nm, 10%) nanocomposites.

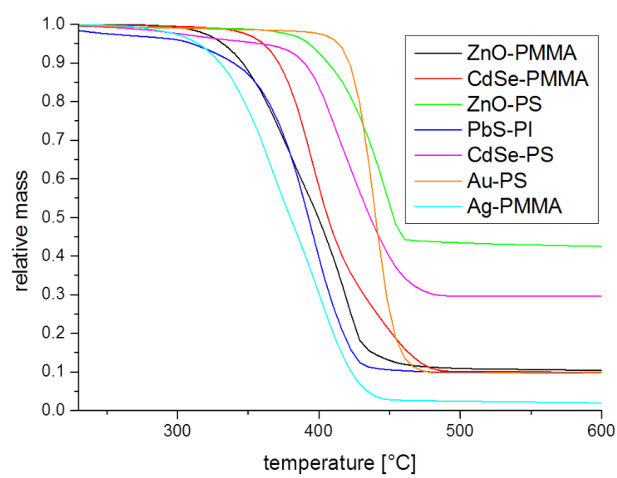


Figure 7: TGA measurements of the nanocomposites.

7 Summary

In this thesis a general approach to obtain fully miscible nanocomposites is developed, based on the attachment of polymer brush layers on nanoparticle surfaces. The development of this approach involved the synthesis of high quality nanoparticles, the attachment of polymer brush layers onto the nanoparticle surface using a novel ligand exchange method, and the preparation of polymer nanocomposites.

To show the versatility of this approach, first a large range of high quality nanoparticles relevant for a variety of different applications was synthesized. These comprise magnetic Fe_2O_3 -, semiconducting CdSe-, CdSe/ZnS/ZnSe-, PbS-, and metallic Au- and Ag-nanoparticles. For the synthesis of high quality samples in the size range of 3 - 20 nm with high crystallinity, narrow size distribution and well-defined shapes, published preparation procedures were optimized. In case of semiconducting ZnO-nanoparticles a completely new synthetic route was developed. It utilizes the hydrolyzation of zinc oleate in organic solvents. This leads to a good control over the nanoparticle growth to yield narrow size distribution and provides excellent steric stabilization in organic solvents. The use of zinc stearates and the robustness of the synthesis allow upscaling to produce 5 g of narrow disperse nanoparticles in one batch. The surface modification of the different nanoparticles was achieved by a novel ligand exchange procedure. It exchanges the original ligands which stabilized the nanoparticles during and after their synthesis (e.g. oleate or oleyl amine) by polymer ligands having one or more surface-binding moieties at their chain end. The attachment of these ligand polymers to the nanoparticle surface via their chain-ends lead to the formation of a dense polymer brush layer around the nanoparticles. The ligand exchange procedure involves a sequence of precipitation- and dissolution cycles. The first cycles remove the original ligand and bind the polymer ligand, while the following cycles remove the unbound polymer ligands. The exchange is driven by a higher binding-affinity and a large stoichiometric excess of the polymer ligands. The advantage of the ligand exchange method compared to established grafting-from and grafting-to methods are the good control over the grafting

density resulting in a control of nanoparticle aggregation/stabilization, and the possibility to reach very high grafting densities of > 1 chain/nm², the possibility to control the brush thickness, and the interparticle distance over a range of 5 - 25 nm with high precision. The versatility of the ligand exchange procedure allows to coat nanoparticles with polymer layers for a large variety of nanoparticle/polymer combinations (e.g. polystyrene, polymethylmethacrylate, polyisoprene, polyethylene, polyvinylpyridine). It was shown that for upscaling of the procedure also commercially available copolymers could be used as polymer ligands. The low chain-segment density of polymer brushes at their periphery reduce the loss of conformational entropy of polymer matrix chains upon mixing, thereby providing full thermodynamic miscibility of the coated nanoparticles with the polymer matrix in a polymer nanocomposite.

Using this method, highly transparent polymer polystyrene, polymethacrylate, polyisoprene and polyvinylpyridine nanocomposites could be prepared, containing up to 40 wt% nanoparticles. The incorporation low amounts of nanoparticles (2 - 5 wt%) already leads to a 3-fold increase of the modulus and a highly increased scratch resistance.

With the ligand exchange method it is possible to prepare nanoparticles with lower grafting densities to control the aggregation of the nanoparticles in a polymer matrix. Whereas at high grafting densities single nanoparticles are well dispersed and homogeneously distributed in the polymer matrix, at lower grafting densities they start to form multiplets, eventually growing into linear chains and networks. This represents a route to a controlled percolation of nanoparticles in a polymer matrix to provide electrically or thermally conducting paths to increase the efficiency of electro-optic devices such as hybrid solar cells or the thermal conductivity of polymers.

8 Zusammenfassung

In dieser Arbeit wird ein universeller Ansatz entwickelt, um voll mischbare Nanokomposite herzustellen. Dieser Ansatz basiert auf einer bürstenförmigen Polymerschicht auf der Partikeloberfläche. Für die Entwicklung dieser Methode müssen zunächst qualitativ hochwertige Nanopartikel synthetisiert werden, welche anschließend mittels eines Ligandenaustauschverfahrens mit der Polymerschicht versehen werden. Die so präparierten Nanopartikel werden mit einem Matrixpolymer zu einem Nanokomposit verarbeitet.

Um die Vielseitigkeit dieser Methode zu zeigen, wurde eine Reihe qualitativ hochwertiger Nanopartikel mit Relevanz für eine Vielzahl von Anwendungen synthetisiert. Diese Nanopartikel umfassen magnetische Fe_2O_3 -, halbleitende CdSe-, CdSe/ZnS/ZnSe-, PbS- und metallische Au- und Ag-Nanopartikel. Für die Synthese dieser Nanopartikel in einem Größenbereich von 3 - 20 nm, mit einer hohen Kristallinität, einer engen Größenverteilung sowie gut definierter Form wurden bekannte Präparationsmethoden optimiert. Eine Synthese für halbleitende ZnO-Nanopartikel wurde neu entwickelt. Bei dieser Methode wird die Hydrolyse von Zinkoleat in einem organischem Lösungsmittel verwendet, dies erlaubt eine gute Kontrolle über das Wachstum der Partikel und führt damit zu einer engen Größenverteilung. Diese sehr robuste Synthese kann mit unterschiedlichen Edukten (z.B. Zinkstearat, NaOH, KOH) durchgeführt werden und liefert bis zu 5 g eng verteilte gut stabilisierte Nanopartikel.

Die Oberflächenmodifikation der Nanopartikel mit einer Polymerschicht wurde mit einem neu entwickelten Ligandenaustauschverfahren durchgeführt. In diesem Verfahren werden die ursprünglichen Liganden, welche die Nanopartikel während der Synthese stabilisieren (z.B. Oleat oder Oleylamin), gegen Polymerliganden ausgetauscht. Die Polymerliganden tragen eine oder mehrere Haftgruppen an einem Kettenende. Die über diese Gruppen mit einem Kettenende an die Nanopartikel gebundenen Polymerketten bilden eine dichte bürstenförmige Schicht um die Nanopartikel. Das Verfahren besteht aus einer Sequenz aus Fällungs- und Lösungsschritten. Die ersten Zyklen dienen der Entfernung des Ursprungsliganden und der Bindung des Polymerliganden,

während die folgenden Zyklen den Überschuss an Polymerligand entfernen. Die treibende Kraft hinter dem Austausch ist die höhere Affinität und der stöchiometrische Überschuss des Polymerliganden. Die Vorteile des Verfahrens gegenüber den üblichen Methoden (z.B. "grafting-to" und "grafting-from") sind die gute Kontrolle sowie die Höhe der Belegungsdichte (> 1 Kette pro nm^2). Daraus resultiert eine Kontrolle über die Stabilität bzw. die Aggregation der Partikel sowie über die Dicke der Polymerschicht und den damit verbunden Interpartikelabstände in einem Bereich von 5 bis 20 nm. Die Vielseitigkeit des Verfahrens erlaubt es unterschiedliche Nanopartikel mit einer Vielzahl an Polymeren zu beschichten (z.B. Polystyrol, Polymethylmethacrylat, Polyisopren, Polyethylen, Polyvinylpyridin). Auch kommerziell erhältliche Polymere können mit diesem Verfahren verarbeitet werden und ermöglichen so ein "Upscaling". Bei einer Mischung der beschichteten Nanopartikel mit einem Matrixpolymer führt die niedrigere Dichte der bürsten-förmigen Polymerschicht an ihrer Peripherie zu einem geringeren Verlust von konformativer Freiheit der Matrixpolymerketten. Dies führt dazu, dass die Nanopartikel thermodynamisch mit einer Polymermatrix zu einem Nanokomposit mischbar sind.

Mit Hilfe dieses Verfahrens lassen sich hoch transparente Nanokomposite aus Polystyrol, Polymethylmethacrylat, Polyisopren und Polyvinylpyridin mit diversen Nanopartikeln herstellen. Die Transparenz bleibt erhalten bis zu einem Nanopartikelanteil von 40 Gew.-%. Schon bei einem niedrigen Nanopartikel Gehalt (2 - 5 Gew.-%) erhöht sich der elastische Modul des Nanokomposites um das 3-fache und auch die Kratzfestigkeit ist stark erhöht.

Die Kontrolle über die Belegungsdichte mit diesem Verfahren ermöglicht es, Nanopartikel mit einer niedrigeren Belegungsdichte herzustellen. Diese lassen sich anschließend in einer Polymermatrix verteilen und sind je nach Belegungsdichte einzeln und homogen verteilt oder bilden mit sinkender Belegungsdichte zunächst Multipletts, Ketten bis hin zu Netzwerken von Nanopartikeln. Hiermit lassen sich z.B. Perkolationsnetzwerke in einer Polymermatrix bilden, welche die elektrische oder thermische Leitfähigkeit erhöhen.

9 Danksagung

An dieser Stelle möchte ich mich bei allen bedanken, deren Unterstützung die Anfertigung dieser Arbeit ermöglicht hat. Im Einzelnen gilt mein Dank:

Prof. Dr. Stephan Förster für die Bereitstellung des interessanten Themas, die Möglichkeit des Umgebungswechsels und für die erfolgreichen wissenschaftlichen Diskussionen sowie die Freiheiten bei der Gestaltung meiner Forschung.

Elisabeth Düngfelder für die Erleichterung des ganzen Bürokrats und die netten Unterhaltungen zwischendurch.

Jennifer Hennessy ebenfalls für die Erleichterung des Bürokrats sowie für den ganzen Spaß sowohl in als auch außerhalb der Uni.

Dr. Stephan Hauschild für die Hilfe bei technischen und Computerproblemen sowie allen andern Problemen.

Karlheiz Lauterbach für die Hilfe bei fast allen anderen Problemen und die vielen tollen Geschichten.

Den in Hamburg gebliebenen für die schöne Zeit dort: Dr. Stephanie Domes, Dr. Jasmin Nitsche und Dr. Julian Thiele.

Wie auch meinem Klüngel (Wa jungens echt jetzt!!!) ohne die das Studium wohl recht langweilig geworden wäre: Christian Schmidtke, Alexander Stark.

Sowie allen anderen Leuten aus PC1, der Karg- und Retsch-Gruppe:
(alphabetisch sortiert und ohne Wertung)

Alexander Exner, Astrid Rauh, Carolin Fürst, Christian Stelling, Christoph Angermann, Corinna Stegelmeier, Daniela Pirner, Denise Barelmann-Kahlbohm, Eddie Hofmann, Fabian Nutz, Dr. Jan Schröder, Katja von Nessen, Kirsten

Volk, Kristina Wagner, Lina Mayr, Maria Michaelis, Maria Ritter, Prof. Dr. Markus Retsch, Dr. Martin Dulle, Dr. Martin Trebbin, Mathias Schlenk, Matthias Bieligmeyer, Prof. Dr. Matthias Karg, Dr. Mikheil Doroshenko, Miriam Mauer, Nonio Wolter, Pia Ruckdeschel, Ralph Neubauer, Dr. Sara Mehdizahdeh Taheri, Sebastian Höhn, Sebastian With, Dr. Simone Wagner, Susanne Seibt, Tobias Güttler, Töbi Honold und Dr. Xuelian Chen.

Insbesondere:

Den Kellerkindern für den gelegentlichen "Feierabend" Drink: Susi, Maria und Miri.

Meinen Büromitbewohnern für die schöne Zeit und den Spass den wir hatten: Caro, Denise, Sara.

Meiner WG für die WG-Erfahrung und die vielen Unternehmungen ausserhalb der UNI: Denise, Jan, Sara, Sebastian.

Ein besonder Dank gilt meiner Kletter-Gruppe für das Vertrauen und die Sicherheit: Caro, Kirsten, Sebastian.

Und zu guter letzt natürlich ein riesen Dank an meine Eltern und meinen Bruder, die mich immer Unterstützt haben.

(Eidesstattliche) Versicherungen und Erklärungen

(§5 Nr.4 PromO)

Hiermit erkläre ich, dass keine Tatsachen vorliegen, die mich nach den gesetzlichen Bestimmungen über die Führung akademischer Grade zur Führung eines Doktorgrades unwürdig erscheinen lassen.

(§8 S.2 Nr.5 PromO)

Hiermit erkläre ich mich damit einverstanden, dass die elektronische Fassung meiner Dissertation unter Wahrung meiner Urheberrechte und des Datenschutzes einer gesonderten Überprüfung hinsichtlich der eigenständigen Anfertigung der Dissertation unterzogen werden kann.

(§8 S.2 Nr.7 PromO)

Hiermit erkläre ich eidesstattlich, dass ich die Dissertation selbstständig verfasst und keine anderen als die von mir angegebenen Quellen und Hilfsmittel benutzt habe.

(§8 S.2 Nr.8 PromO)

Ich habe die Dissertation nicht bereits zur Erlangung eines akademischen Grades anderweitig eingereicht und habe auch nicht bereits diese oder eine gleichartige Doktorprüfung endgültig nicht bestanden.

(§8 S.2 Nr.9 PromO)

Hiermit erkläre ich, dass ich keine Hilfe von gewerblichen Promotionsberatern bzw.-vermittlern in Anspruch genommen habe und auch künftig nicht nehmen werde.

.....

Ort, Datum, Unterschrift